



**Fredilson da Veiga Melo**

Biochemistry, B. Sc.

**Isolation and identification of bioactive secondary metabolites from *Salinispora arenicola* obtained from ocean sediments from the Madeira Archipelago**

Dissertation for degree of Master in

Biochemistry

Supervisor: Dr. Susana P. Gaudêncio

Assistant Researcher, REQUIMTE, LAQV, Chemistry  
Department and UCIBIO, Life Science Department –  
FCT/UNL

Co-supervisor: Dr. Florbela Pereira

Post-Doc Researcher, REQUIMTE, LAQV, Chemistry  
Department – FCT/UNL



**Fredilson da Veiga Melo**

Biochemistry, B. Sc.

**Isolation and identification of bioactive secondary metabolites  
from *Salinispora arenicola* obtained from ocean sediments  
from the Madeira Archipelago**

Dissertation for degree of Master in

Biochemistry

Supervisor: Dr. Susana P. Gaudêncio

Assistant Researcher, REQUIMTE, LAQV, Chemistry Department  
and UCIBIO, Life Science Department – FCT/UNL

Co-supervisor: Dr. Florbela Pereira

Post-Doc Researcher, REQUIMTE, LAQV,  
Chemistry Department – FCT/UNL

**December 2016**



Copyright © Fredilson da Veiga Melo, Faculdade de Ciências e Tecnologia, Universidade Nova de Lisboa

The Faculty of Science and Technology and Universidade Nova de Lisboa have the right, forever and without geographical limits, to file and publish this dissertation through printed copies reproduced in paper or digital form, or by any other means known or Be invented, and to disclose it through scientific repositories and to allow its copying and distribution for non-commercial educational or research purposes, provided the author and publisher are credited.



## **Acknowledgments**

To my mom for allowing me to pursue my dream. This is not a repayment, but a token of appreciation for the trust you put on me.

To my landlords who have become a second family.

To Dr Susana Gaudêncio and Dr Florbela Pereira for taking me in their lab, and for being very understanding and patient. It has truly been a one of a kind experience in learning about both science and my capabilities. Thank you.

To Professor Dr. P. Castilho from Madeira University and M. Freitas from Estação de Biologia Marinha, Funchal, Portugal, for logistic support during the sample collection expedition, and to Professor W. Fenical, Dr P. R. Jensen and Christopher Kauffman from Scripps Institution of Oceanography, CA, USA for their help during the sample collection.

To Professor Dr Ilda Santos-Sanches (DCV, FCT-UNL) and her lab for their help with the antimicrobial bioassays, to Dr. Rosário Mato for kindly providing VRE EF82 strain.

To Dr. Isabel Cunha (CIIMAR) for the antifouling assays.

To Professor Dr. Teresa Barros (FCT-UNL) and her lab for all the help with the optical rotation assay.

To Ana Teresa and to Professor Dr. Eurico Cabrita from the RMN facilities for all their assistance and support. The NMR spectrometers are part of The National NMR Facility, supported by Fundação para a Ciência e a Tecnologia (RECI/BBB-BQB/0230/2012).

To all the people in the 202 lab. A special thanks to Marisa Paulino for showing me around the lab, teaching me the ropes and being an overall awesome friend, and to Tiago Dias for his amazing work on his thesis and the guidance during the project, and to all the co-workers I worked alongside in the “Tesouros Oceânicos” project.

To all my friends and family for supporting me during my academic trajectory, and especially during these two years which have proved to be the most important academically so far.

Funding from FCT/MEC, through grants PTDC/QUIQUI/119116/2010, IF/00700/2014, SFRH/BPD/108237/2015, UID/QUI/ 50006/2013 (LAQV) and UID/Multi/04378/2013 (UCIBIO) and co-financed by the ERDF under the PT2020 partnership agreement POCI-01-0145-FEDER-007265 and POCI-01- 0145-FEDER-007728, respectively. The EU 7<sup>th</sup> Framework Programme (FP7/2007–2013) under grant agreement PCOFUND-GA-2009-246542 and 269138-NanoGuard.

To you all thank you.

Obrigado.





## Resumo

Recentemente tem-se verificado um aumento de microrganismos patogénicos resistentes a antibióticos, doenças infecciosas e o aparecimento de novas ameaças à saúde humana e à economia. A incapacidade dos fármacos inspirados em produtos naturais terrestres para resolver estas questões levou os cientistas a olhar para *habitats* inexplorados à procura de novos fármacos. O meio ambiente marinho estabeleceu-se como um tesouro notavelmente rico de novos compostos bioativos com uma vasta gama de propriedades biológicas, incluindo anti-microbiana, anti-fúngica, anti-cancerígena, anti-inflamatória e citotóxica. No curto espaço de tempo em que o ambiente marinho tem vindo a ser explorado, a sua bioprospecção resultou na aprovação de sete fármacos, encontrando-se actualmente 23 compostos em ensaios clínicos e centenas no *pipeline* pré-clínico.

Neste trabalho, utilizou-se uma abordagem guiada por ensaios biológicos para o estudo de metabolitos secundários bioativos da estirpe *Salinispora arenicola* PTM-99 recolhida a partir de sedimentos oceânicos ao largo da costa do arquipélago da Madeira. Técnicas cromatográficas, tais como cromatografia *flash* e Cromatografia Líquida de Alto Desempenho (HPLC), foram utilizadas para fazer o isolamento e purificação de metabolitos secundários. Cerca de 52 compostos foram isolados de uma cultura resultante de 7 dias de incubação e 82 compostos foram isolados de uma cultura de 14 dias de incubação (contando os compostos da fracção F8-F9). A cultura de 7 dias foi testada quanto à actividade antibacteriana contra as estirpes de bactérias patogénicas *Enterococcus faecium* VRE EF82 resistente à vancomicina e *Staphylococcus aureus* resistente à meticilina MRSA COL, tendo 20 compostos revelado actividade. Os compostos exibiram actividade antibacteriana numa gama de MIC 250 a 62,5 µg /ml.

Os compostos bioativos e outros relevantes foram estruturalmente analisados através de métodos espectroscópicos incluindo Ressonância Magnética Nuclear unidimensional e bidimensional, ultravioleta, infra-vermelho e o método não-espectroscópico de rotação óptica específica. Verificou-se que a maioria dos compostos isolados contém núcleo de lactama, núcleo de piperazina e/ou estrutura aromática. Duas diceptopiperazinas conhecidas são descritas pela primeira vez no género *Salinispora*. Dois macrólidos encontram-se correntemente a ser elucidados estruturalmente.

**Palavra-chave:** *Salinispora arenicola*, metabolitos secundários, dicetopiperazina, actinobactérias, actividade antibacteriana, RMN



## Abstract

Recently there has been an increase in pathogenic microorganisms resistant to antibiotics, infectious diseases and the appearance of new threats to human health and the economy. The inability of terrestrial natural product-based drugs to solve these problems has led scientists to look at unexplored habitats in search of new drugs. The marine environment has established itself as a remarkably rich treasure of new bioactive compounds with a wide range of biological properties, including antimicrobial, anti-fungal, anti-cancer, anti-inflammatory and cytotoxic. In the short time the marine environment has been explored, its bioprospecting has resulted in the approval of seven drugs, with currently 23 compounds in clinical trials and hundreds in the pre-clinical pipeline.

In this work, a bioassay-guided approach was used to study the bioactive secondary metabolites of the *Salinispora arenicola* strain PTM-99 collected from oceanic sediments off the coast of the Madeira archipelago. Chromatographic techniques, such as flash chromatography and High Performance Liquid Chromatography (HPLC), were used for the isolation and purification of secondary metabolites. About 52 compounds were isolated from a resulting culture of 7 days of incubation and 82 were isolated from a culture of 14 days of incubation (counting the F8-F9 fraction compounds). The 7-day-old culture was tested for antibacterial activity against pathogenic bacteria *Enterococcus faecium* VRE EF82 resistant to vancomycin and *Staphylococcus aureus* resistant to methicillin MRSA COL, having 20 compounds revealed activity. The compounds exhibited antibacterial activity in the range of MIC 250 to 62.5 µg/ml.

Bioactive and other relevant compounds were structurally analyzed through spectroscopic methods including one-dimensional and two-dimensional Nuclear Magnetic Resonance experiments, ultra-violet, Infra-red and the non-spectroscopic method specific optical rotation. It was found that most of the compounds isolated contain lactam core, piperazine core and/or aromatic backbone. Two known diketopiperazines are reported for the first time from the *Salinispora* genus. Two macrolides are currently being structurally elucidated.

**Keywords:** *Salinispora arenicola*, secondary metabolites, diketopiperazine, actinomycetes, antimicrobial activity, NMR



## Table of contents

Resumo.....	v
Abstract.....	vii
1. INTRODUCTION .....	3
1.1. Bioprospecting .....	3
1.2. Natural products: secondary metabolites .....	3
1.3. Marine environment.....	4
1.4. Marine secondary metabolites: pharmaceuticals .....	5
1.4.1. Case study: Salinosporamide A .....	8
1.4.2. Marine secondary metabolites: antimicrobial .....	8
1.5. Marine secondary metabolites: antifoulants.....	10
1.5.1. Microfouling .....	10
1.5.2. Macrofouling.....	10
1.5.3. Butyrylcholinesterase: a valid target for antifouling agents development.....	11
1.6. Marine natural products: the example of diketopiperazines .....	11
1.6.1. Biosynthetic pathways .....	12
1.6.2. Biological activities.....	12
1.7. Actinomycetes.....	14
1.7.1. Bioactivity and ecology .....	14
1.7.2. Ecologic role of actinomycetes .....	15
1.7.3. The Salinispora genus .....	15
1.8. Aim of the thesis .....	20
2. MATERIALS AND METHODS.....	23
2.1. Bacterial cell culture: materials and growth conditions.....	23
2.2. Extraction and fractionation of the crude.....	23
2.2.1. Ethyl acetate extraction .....	23
2.2.2. Fractionation by flash-chromatography .....	23
2.3. Isolation of secondary metabolites by HPLC.....	24
2.4. Bioassay .....	25
2.4.1. Antimicrobial activity .....	25
2.4.2. Anti-fouling activity.....	27
2.5. Structure elucidation .....	27
2.5.1. NMR .....	27
2.5.2. Infra-red .....	27

2.5.3.	Optical rotation .....	27
2.5.4.	Structure elucidation data.....	28
3.	RESULTS AND DISCUSSION .....	31
3.1.	Fractionation of the crude extract .....	31
3.2.	Isolation of compounds by HPLC and bioassays.....	32
3.2.1.	Fraction F2 .....	32
3.2.2.	Fraction F4-F7 .....	35
3.2.3.	Fraction F8-F9 .....	38
3.2.3.	Antifouling assay .....	40
3.3.	Structure elucidation .....	41
3.3.1.	PTM-99-(F2)-F27 and PTM-99-(F2)-F31 .....	41
3.3.2.	PTM-99-(F4-F7)-F30.....	52
3.3.3.	PTM-99-(F4-F7)-F34.....	56
4.	CONCLUSIONS AND FUTURE WORK .....	61
5.	REFERENCES .....	65
6.	ANNEX.....	77

## List of figures

Figure 1.1. Original collected sources (A) and predicted source organisms (B) of marine natural product-derived drugs on clinical pipeline.....	4
Figure 1.2. Chemical structures of marine secondary metabolites commercially available.....	7
Figure 1.3. Chemical structure of the drug candidate salinosporamide A (NPI-0052, Nereus Pharmaceuticals).....	8
Figure 1.4. Selected chemical structure of marine-derived natural products with antimicrobial activity.....	10
Figure 1.5. Chemical structures of selected diketopiperazines from marine origin.....	13
Figure 1.6. Selected novel and unique metabolites from rare marine actinomycetes.....	15
Figure 1.7. A <i>Salinispora</i> strain streaked on agar.....	16
Figure 1.8. Geographic distribution of reported <i>Salinispora</i> genus.....	17
Figure 1.9. Selected structure of compounds produced by <i>Salinispora</i> strains.....	19
Figure 2.1. Template of 96-well microtiter plate illustrating the disposition of samples and controls for the antibacterial test. ....	26
Figure 3.1. Fractions of the strain <i>S. arenicola</i> PTM-99 obtained by flash chromatography of the crude. Fraction F1 to F9, from the left to the right.. ....	31
Figure 3.2. Chromatogram with 3D field (190 – 300 nm) of the crude fraction F2.. ....	33
Figure 3.3. UV profile of compounds isolated from fraction F2.. ....	34
Figure 3.4. Chromatogram with 3D field (190 – 300 nm) of the crude fraction F4-F7.....	35
Figure 3.5. UV profile of compounds isolated from fraction F4-F7.....	36
Figure 3.6. Chromatogram with 3D field (190 – 300 nm) of the crude fraction F8-F9.....	38
Figure 3.7. UV profile of compounds isolated from fraction F8-F9.....	39
Figure 3.8. UV profile of compound PTM-99-(F2)-F27. ....	41
Figure 3.9. <sup>1</sup> H NMR and HMBC spectra of compounds PTM-99-(F2)-F27 (A) and PTM-99-(F2)-F31 (B).....	42
Figure 3.10. NMR data and proposed alkene astructure for the corresponding section. ....	43
Figure 3.11. Symmetrical alkene chain.....	44
Figure 3.12. The carbon at 125.52 ppm closes the alkene chain forming a macrocyclic ring. ....	45
Figure 3.13. CH group at 68.88 ppm forms the bridge connecting two ends of a cyclic structure.....	45
Figure 3.14. Macrocyclic ring composed of quaternary carbons of ester and amide groups proposed for compound PTM-99-(F2)-F27.....	46
Figure 3.15. Two-dimentional NMR data for proton signal 1.32 illustrating the partitioning of the signal into left ( <i>l</i> ) and right ( <i>r</i> ) side.....	46
Figure 3.16. 2-Ethyl-1-butyl substitute. ....	47
Figure 3.17. CH group at 68.88 ppm forms the bridge connecting two ends of a cyclic structure.....	47
Figure 3.18. Macrocyclic ring composed of quaternary carbons of ester and amide groups proposed for compound PTM-99-(F2)-F31.....	48
Figure 3.19. IR spectrum of compound PTM-99-(F2)-F27.....	49
Figure 3.20. UV profile of compound PTM-99-(F4-F7)-F30.....	52
Figure 3.21. NMR data highlighting the lactam core of the diketopiperazine.....	53
Figure 3.22. Proposed structure for the compound PTM-99-(F4-F7)-F30. ....	53
Figure 3.23. Initially proposed structures for the compound PTM-99-(F4-F7)-F30. ....	55
Figure 3.24. IR spectrum of compound PTM-99-(F4-F7)-F30.....	55
Figure 3.25. Proposed structure for the compound PTM-99-(F4-F7)-F34. ....	56

Figure 6.1. Chromatogram profile of F2 from 14D culture, with 3D field.....	77
Figure 6.2. <sup>1</sup> H NMR of the compound PTM-99-(F2)-F27.....	77
Figure 6.3. <sup>13</sup> C NMR of the compound PTM-99-(F2)-F27.....	78
Figure 6.4. COSY of the compound PTM-99-(F2)-F27.....	78
Figure 6.5. HSQC-DEPT of the compound PTM-99-(F2)-F27.....	79
Figure 6.6. HMBC of the compound PTM-99-(F2)-F27.....	79
Figure 6.7. TOCSY of the compound PTM-99-(F2)-F27.....	79
Figure 6.8. <sup>1</sup> H NMR of the compound PTM-99-(F2)-F31.....	80
Figure 6.9. <sup>13</sup> C NMR of the compound PTM-99-(F2)-F31.....	80
Figure 6.10. COSY of the compound PTM-99-(F2)-F31.....	81
Figure 6.11. HSQC-DEPT of the compound PTM-99-(F2)-F31.....	81
Figure 6.12. HMBC of the compound PTM-99-(F2)-F31.....	82
Figure 6.13. TOCSY of the compound PTM-99-(F2)-F31.....	82
Figure 6.14. <sup>1</sup> H NMR of the compound PTM-99-F4-F7-F30.....	83
Figure 6.15. <sup>13</sup> C NMR of the compound PTM-99-F4-F7-F30.....	83
Figure 6.16. COSY of the compound PTM-99-(F4-F7)-F30.....	84
Figure 6.17. HSQC-DEPT of the compound PTM-99-(F4-F7)-F30.....	84
Figure 6.18. HMBC of the compound PTM-99-(F4-F7)-F30.....	84
Figure 6.19. TOCSY of the compound PTM-99-(F4-F7)-F30.....	85
Figure 6.20. <sup>1</sup> H NMR of the compound PTM-99-(F4-F7)-F34.....	85
Figure 6.21. <sup>13</sup> C NMR of the compound PTM-99-(F4-F7)-F34.....	86
Figure 6.22. COSY of the compound PTM-99-(F4-F7)-F34.....	86
Figure 6.23. HSQC-DEPT of the compound PTM-99-(F4-F7)-F34.....	87
Figure 6.24. HMBC of the compound PTM-99-(F4-F7)-F34.....	87
Figure 6.25. TOCSY of the compound PTM-99-(F4-F7)-F34.....	87

Disclaimer: all images of structures used in the 1. INTRODUCTION section of this thesis were retrieved from the ChemSpider database (<http://www.chemspider.com/>), unless stated otherwise.



## List of tables

Table 1.1. FDA-approved marine derived drugs. Modified from Marine Pharmacology: Clinical Development (data from April 2016).....	6
Table 1.2. Selected marine secondary metabolites with antimicrobial activity.....	9
Table 1.3. Examples of secondary metabolites isolated from marine actinomycetes.....	14
Table 1.4. Secondary metabolites from the <i>Salinispora</i> genus.....	18
Table 2.1. Composition of A1 medium.....	23
Table 2.2. Composition of the mobile phase for each fraction. ....	24
Table 2.3. HPLC elution conditions for fraction F2. ....	24
Table 2.4. HPLC elution conditions for fraction F4-F7.....	25
Table 2.5. HPLC elution conditions for fraction F8-F9.....	25
Table 2.6. Composition of the BHI growth medium. ....	26
Table 3.1. Mass of fractions derived from crude fractionation.....	31
Table 3.2. Mass yield and antimicrobial activity (MIC) of compounds isolated from fraction F2, from a 7 days culture. ....	34
Table 3.3. Yield and antimicrobial activity (MIC) of compounds isolated from fraction F4-F7, from a 7 days culture. ....	36
Table 3.4. Yield and antimicrobial activity (MIC) of compounds isolated from fraction F8-F9, from a 7 days culture. ....	39
Table 3.5. NMR data for compound PTM-99-(F2)-F27.....	50
Table 3.6. NMR data for compound PTM-99-(F2)-F31.....	51
Table 3.7. NMR data for compound PTM-99-(F4-F7)-F30. ....	54
Table 3.8. NMR data for compound PTM-99-(F4-F7)-F34. ....	56



## Abbreviations

<b><sup>13</sup>C</b>	Nuclear magnetic resonance of <sup>13</sup> C
<b><sup>1</sup>H</b>	Nuclear magnetic resonance of <sup>1</sup> H
<b>1D</b>	One-dimensional
<b>2D</b>	Two-dimensional
<b>7D</b>	7 days culture
<b>14D</b>	14 days culture
<b>ACN</b>	Acetonitrile
<b>BHI</b>	Brain-Heart Infusion medium
<b>COSY</b>	Correlation spectroscopy
<b>DEPT 90</b>	Distortionless Enhancement by Polarization Transfer 90
<b>DEPT 135</b>	Distortionless Enhancement by Polarization Transfer 135
<b>DMSO</b>	Dimethyl sulfoxide
<b>FDA</b>	Food and drug administration
<b>FT-IR</b>	Fourier transform Infrared
<b>HMBC</b>	Heteronuclear Multiple-Bond Correlation
<b>HPLC</b>	High performance liquid chromatography
<b>HSQC</b>	Heteronuclear Single Quantum Correlation
<b>IC<sub>50</sub></b>	Half maximal inhibitory concentration
<b>LC</b>	Liquid chromatography
<b>MIC</b>	Minimum inhibitory concentration
<b>MRSA</b>	Methicillin-resistant <i>Staphylococcus aureus</i>
<b>NMR</b>	Nuclear magnetic resonance
<b>NOESY</b>	Nuclear overhauser enhancement spectroscopy
<b>NRPS</b>	Nonribosomal peptide synthetases
<b>OD<sub>600</sub></b>	Optical density at 600 nm
<b>PI</b>	Proteasome inhibitor
<b>SCUBA</b>	Self-contained underwater breathing apparatus
<b>TOCSY</b>	Total Correlated Spectroscopy
<b>USA</b>	United States of America
<b>UV</b>	Ultra violet
<b>VRE</b>	Vancomycin-resistant <i>Enterococcus faecium</i>



# *Introduction 1*

## 1. INTRODUCTION

### 1.1. Bioprospecting

Nature has been the major source, and inspiration, of products used in the daily life. From medicine (e.g. chemicals and genes) to mechanical engineering (e.g. transportation and construction) through nutraceuticals (e.g. nutrients and dietary supplements) and cosmetics, there is a systematic search for products from Nature with a commercial purpose, which is designated bioprospecting, or biodiversity prospecting (Newman *et al.*, 1999; Artuso, 2000). Within the wide range of beneficial properties of natural products, their use as antibiotics and drugs has received the most attention (Cragg and Newman, 2013; Martins *et al.*, 2014; Demain and Sanchez, 2009). Current biodiscovery efforts employ genome mining and genetic approaches, alongside the more traditional bioassay-guided approaches (Jensen *et al.*, 2015).

### 1.2. Natural products: secondary metabolites

Natural products are defined as any substance produced by living organisms. In the bioprospecting context, they are commonly referred to as secondary metabolites (Cannell, 1998). While primary metabolites are indispensable building blocks keeping the producing organism alive and functional, secondary metabolites are usually produced at a later stage (idiophase), usually the end of the life cycle of the organism, derived from the primary metabolism (Ruiz *et al.*, 2010), as a response to abiotic (e.g. nutrient limitation) or biotic stress (e.g. predator) (Assmann *et al.*, 2000; Manzo *et al.*, 2011; Penesyanyan *et al.*, 2011). The dependence of the biosynthesis of secondary metabolites upon the ever changing environmental elicitors and the subsequent enzymatic modifications of the secondary metabolite down the biosynthetic pathways contribute for a vast degree of diversity among those metabolites (Rao and Ravishankar, 2002; Ferrari, 2010).

Four primary metabolic pathways are responsible for providing the precursors for the most part of the produced secondary metabolites; 1) Acetate pathway (precursor: acetyl coenzyme A), 2) Methylerythritol phosphate pathway (precursor: methylerythritol 4-phosphate), 3) Mevalonate pathway (precursor: mevalonic acid) and 4) Shikimate pathway (precursor: shikimic acid) (Dewick, 2001). The products of these pathways may also combine to originate secondary metabolites. This hybridization of pathways plays a key role in the buildup of structural diversity (Shen *et al.*, 2001), combined with natural enzyme-mediated reactions of oxidation, methylation, cyclisation, halogenation, reduction, elimination and rearrangement of the pathways (Staniek *et al.*, 2013). Consequently, secondary metabolites are more diverse structurally and functionally compared to primary metabolites (Firn and Jones, 2003; Fischbach and Clardy, 2007). It is noteworthy the fact that only bacteria possess all four pathways, as shown in the above mentioned references (Dewick, 2001; Shen *et al.*, 2001; Staniek *et al.*, 2013; Firn and Jones, 2003; Fischbach and Clardy, 2007).

The secondary metabolites garnering most attention are those capable of producing an effect upon living organisms or living tissues, the so-called bioactive secondary metabolites. At present time, roughly 60% of available pharmaceutical drugs are natural product-based (Cragg *et al.*, 2009; Lam, 2007; Carter, 2011), with one-quarter being derived from microbes (Patridge *et al.*, 2016).

It is a known fact that bacteria engage in both warfare and communication using secondary metabolites, which essentially shapes the microbial community and its surrounding environment. So, understanding those interactions promoted by bioactive compounds, such as antibiotics, is an essential drive in biodiscovery efforts (Long and Azam, 2001; Rypien *et al.*, 2010; Slattery *et al.*, 2001). Such interactions are particularly interesting in the marine environment, as the poor exploration of this habitat coupled with its overwhelming complexity, comparing to other habitats, constitutes a rich new trove for bioprospecting and biodiscovery (Jensen *et al.*, 2015; Imhoff *et al.*, 2011).

### 1.3. Marine environment

Although, geographically, the terrestrial habitat has been the most exhaustively explored due to the ease of access to the resources, especially plants, recent advances in the technologies of self-contained underwater breathing apparatus (SCUBA) and underwater vehicles, has made it possible to explore the depths of the oceans as never before for new sources of natural products (Dias *et al.*, 2012; Russo *et al.*, 2015). The oceans, covering approximately 71% of Earth, are teeming with life in the most unexpected environment, harboring an estimated 50-80% of all life on the planet, with half of the animal phyla having no terrestrial counterpart (Whitehead, 1999; Millero, 2013; Palumbi and Palumbi, 2015; Margulis and Chapman, 2009).

Since Bergaman and Feeney kick-started the scientific research into marine natural products, 60 years ago (Huang *et al.*, 2010), the exploration of the marine habitat has yielded many unique and remarkable new compounds in the last few decades, with properties ranging from pigments and fragrances to cosmetics and drugs (Guidi and Landi, 2014; Martins *et al.*, 2014; Cragg and Newman, 2013). So far, over 30,000 secondary metabolites have been isolated from marine sources (Habbu *et al.*, 2016). Although these compounds have been reported as isolated from sponges, corals, ascidians, algae and microorganisms (Davidson, 1995; Fenical and Jensen, 1993), recent studies have been pointing out microorganism associated with the supposed source macroorganism as the real origin of most of the isolated compounds (Hu *et al.*, 2011, Newman and Gragg, 2014; Newman and Giddings, 2013). One example of such case is bryostatin 1, an antitumor agent currently facing phase I of clinical trials. Bryostatin 1 was originally isolated from the bryozoan animal (Pettit *et al.*, 1982), and later from the bacterial symbiont "*Candidatus Endobugula sertula*". The strong evidences supporting this affirmation are the fact that the biosynthetic genes for the metabolite are present in the bacteria but not in the animal, and an observed decrease in the production of the metabolite accompanying the decrease of bacterial symbiont following an antibiotic treatment (Sudek *et al.*, 2007). The core evidence for this shift in what is thought to be the producer of the compounds lies with the similarity between the chemical structure of compounds isolated from macroorganisms and microorganisms. Figure 1.1 shows the collected source and the predicted source of marine natural products derived or inspired drugs currently available in the market.

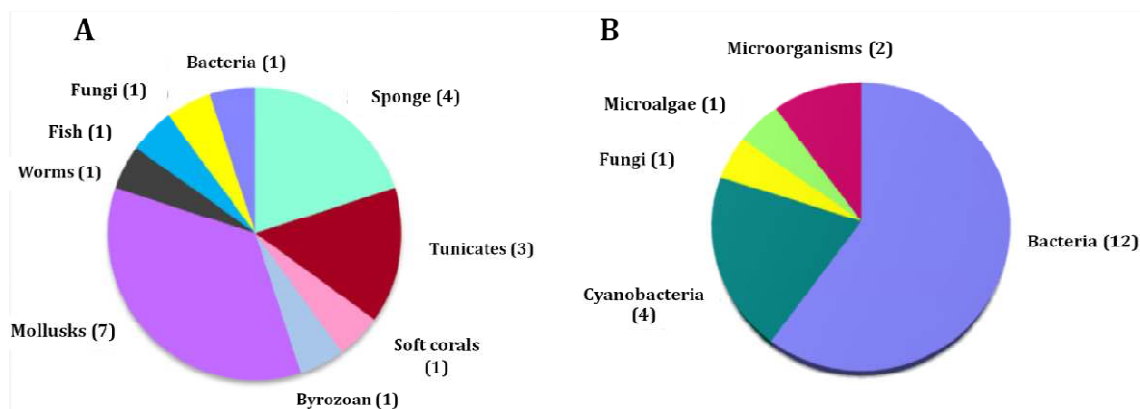


**Figure 1.1. Original collected sources (A) and predicted source organisms (B) of marine natural product-derived drugs on clinical pipeline.** Adapted from Gerwick and Moore, 2012.

It is postulated that the complex ecological system of the oceans is a process in the making, spanning 3.5 billion years, driving the evolution of the microbial community. Factors such as pressure, light availability, temperature, predators, salinity and nutrient availability vary greatly in the oceans, conditioning the microbial community into specific habitats with different niches (Ray, 1988; Du, 2006; Dionisi, 2012; De Carvalho and Fernandes, 2010). The microorganisms are found in association, with inert or biotic surfaces, or as free-living in the ocean water or sediments. As result, the marine microbial community presents a wider range of physiological and chemical capabilities compared to its terrestrial counterpart (Jayanth *et al.*, 2002).

The adaptation of the marine microorganisms has established them as a source of structurally unique and biologically active natural products (Huang *et al.*, 2010), with interesting properties such as antimicrobial, anti-fungal, anti-cancer, anti-inflammatory, and other pharmacological activities (Faulkner, 2001; Gul and Hamann, 2005; Mayer and Hamann, 2005), and the progress made in water oriented technologies such as Remotely Operated Vehicles (ROVs) and Autonomous Underwater Vehicles (AUVs), has allowed the exploration of the most diverse and extreme marine habitats (Russo *et al.* 2015). However, the evolutionary drive has made the common laboratory-based approach of secondary metabolite production a very difficult task (Taylor, 2007, Webster and Taylor, 2012). It is estimated that the uncultured marine microorganisms account for an astonishing 99.1%, lagging behind the terrestrial microorganisms in 0.9 percentage point, in a phenomenon which is designated ominously “the great plate count anomaly” (Stafsnes, 2013). This hindrance comes from the fact that it is difficult to mimic the optimal conditions that form the elicitor leading to the production of secondary metabolites, or the secondary metabolites of interest (Bertrand *et al.* 2014). Bioinformatics analyses have shown that a considerable number of metabolites are not produced under laboratory conditions, leaving the biosynthetic potential of these microorganisms relatively untapped (Gomez-Escribano and Bibb, 2013). Consequently, new strategies such as genome mining – combination of bioinformatics, molecular genetics and natural product analytical chemistry to obtain the product of an identified gene cluster, has been developed (Challis, 2008; Nett *et al.*, 2009). Therefore, it proves necessary to collect the microorganism directly from the source, be it water, sediments or host macroorganisms.

#### **1.4. Marine secondary metabolites: pharmaceuticals**

In the span of 40 years since the approval of the first marine-derived drug by the Food and Drug Administration (FDA, USA), the subject of marine natural products has established itself as a key player in the area of drug development, with thousands of compounds being characterized annually giving origin to drugs either directly or indirectly through lead structures inspiring synthetic drugs (Molinski *et al.*, 2009). As of mid-2016, there are six Food and Drug Administration (FDA, USA)-approved drugs from marine origin (Table 1.1, Figure 1.2). Not surprisingly, more than half of the approved drugs target different types of cancer: cytarabine (Cytosar-U<sup>®</sup>, 1969) targets leukemia, eribulin mesylate (Halaven<sup>®</sup>, 2010) aims at metastatic breast cancer, trabectedin (Yondelis<sup>®</sup>, 2015) is promising against soft tissue sarcoma and ovarian cancer, and brentuximab vedotin (Adcetris<sup>®</sup>, 2011) is efficient against anaplastic large t-cell systemic malignant lymphoma and Hodgkin’s disease. As for the remaining drugs, ziconotide (Prialt<sup>®</sup>, 2004) targets severe chronic pain and omega-3-acid ethyl esters (Lovaza<sup>®</sup>, 2004) targets hipertriglyceridemia (Mayer *et al.* 2016; Marine Pharmacology: Clinical Development, 2016).



**Table 1.1. FDA-approved marine derived drugs.** Modified from Marine Pharmacology: Clinical Development (data from April 2016).

<b>Compound Name</b>	<b>Trademark (FDA Approved Year)</b>	<b>Marine Organism</b>	<b>Chemical Class</b>	<b>Molecular Target</b>	<b>Disease Area</b>
<b>Trabectedin (ET-743)</b>	Yondelis® (2015)	Tunicate	Alkaloid	Minor groove of DNA	Cancer
<b>Brentuximab vedotin (SGN-35)</b>	Adcetris® (2011)	Mollusk/cyanobacterium	ADC(MMAE)	CD30 & microtubules	Cancer
<b>Eribulin Mesylate (E7389)</b>	Halaven® (2010)	Sponge	Macrolide	Microtubules	Cancer
<b>Omega-3-acid ethyl esters</b>	Lovaza® (2004)	Fish	Omega-3 fatty acids	Trygliceride-synthesizing enzymes	Hypertri- - glyceridemia
<b>Ziconotide</b>	Prialt® (2004)	Cone snail	Peptide	DNA polmerase	Pain
<b>Cytarabine (Ara-C)</b>	Cytosar-U® (1969)	Sponge	Nucleoside	DNA polymerase	Cancer

**ADC (MMAE):** Antibody Drug Conjugate (Monomethylauristatin E)

Aside from the approved drugs, there are currently dozens of marine derived compounds in the clinical pipeline, with three of them already undergoing Phase III (plinabulin (n.a.), plitidepsin (Aplidin) and tetrodotoxin (Tectin), being the first two for cancer treatment and the later for chronic pain), and another five of them are in Phase II being one of them evaluated for treatment of schizophrenia, Alzheimer's disease and other central nervous system diseases. The remaining drugs in the clinical pipeline, target different types of cancer (Pharmacology: Clinical Development, 2016; Sawadogo *et al.*, 2013). Cancer is a very hot topic in drug discovery as it is the second largest cause of death worldwide. The use of natural products in cancer treatment has proved to be remarkable and very promising (Sawadogo *et al.*, 2013; Russo *et al.*, 2011). Hundreds of compounds with promising bioactivity, including antibacterial, antidiabetic, antifungal, anti-inflammatory, antiprotozoal, antituberculosis, and antiviral, in addition to activities affecting the nervous system, are currently in the preclinical pipeline (Mayer *et al.*, 2013).

Among the approved drugs, only zirconolite and trabectedin are commercialized in their original chemical structure, while the remaining five are synthetically manufactured with inspiration from marine lead chemical structures (Gerwick and Moore, 2012). It is estimated that for each five million extracts screened, one compound reaches the marketplace, out of the only five compounds that make it to the clinical phase (Cragg *et al.*, 2012). It is estimated that several new compounds will hit the marketplace in the near future as the marine biota keeps on revealing novel compounds with unique structures (Mayer *et al.*, 2010; Boobathy *et al.*, 2009; Gram *et al.*, 2010).

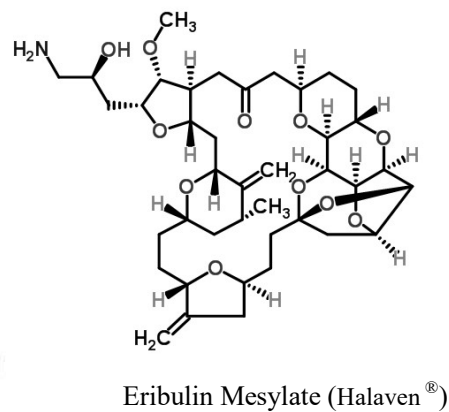
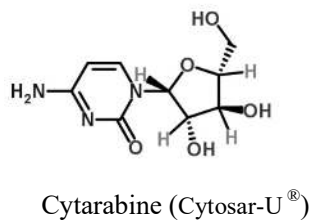
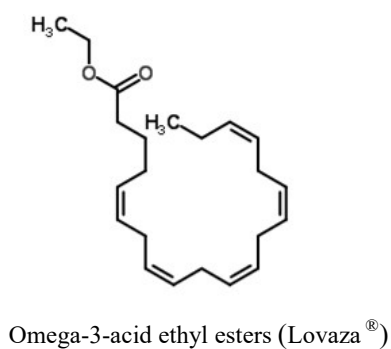
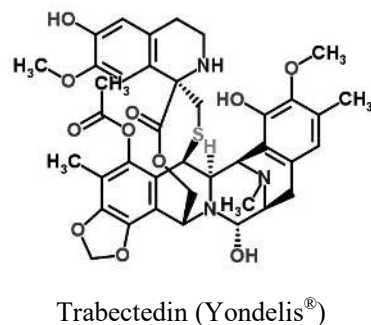
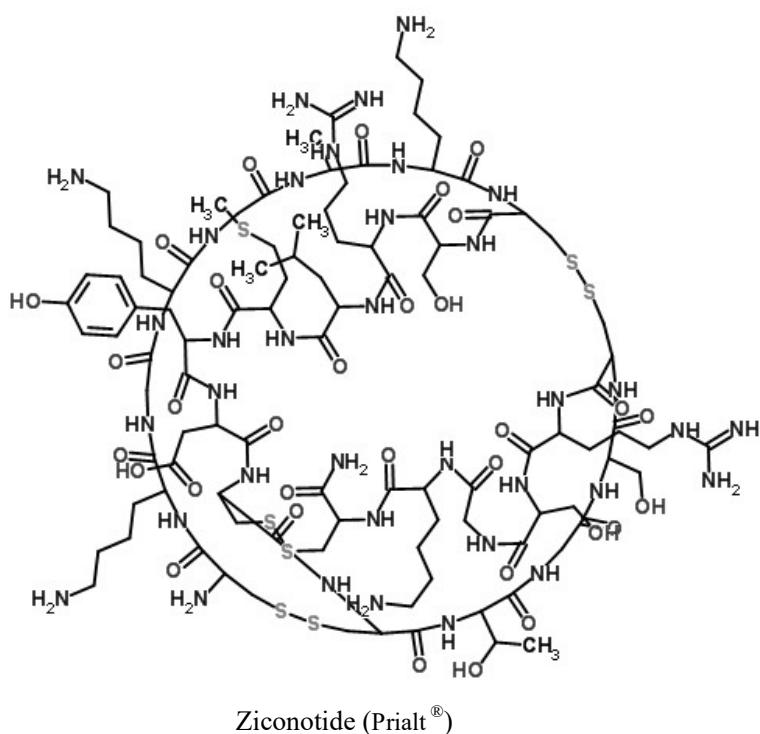
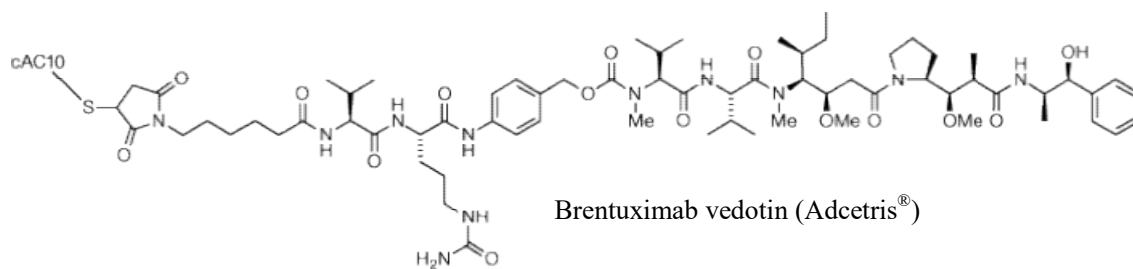
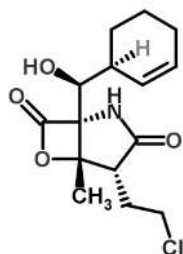


Figure 1.2. Chemical structures of marine secondary metabolites commercially available.

#### 1.4.1. Case study: Salinosporamide A

A fairly recent success story in the field of marine actinomycetes biodiscovery comes from the rare proteasome inhibitor (PI) salinosporamide A (Marizomib) (Figure 1.3), isolated from a lab-cultured marine obligate actinobacterium *Salinispora tropica*. Salinosporamide A is characterized by a  $\gamma$ -lactam- $\beta$ -lactone pharmacophore which strongly inhibits the full range of activities of the 20S proteasome by binding to its catalytic  $\beta$ -subunit site S1, and makes this process irreversible through its chloroethyl group (Gulder and Moore, 2010), consequently inhibiting the cell's primary route of regulated proteolysis. Furthermore, salinosporamide A is also efficient against bortezomib (Velcade®)-resistant multiple myeloma cells. Currently undergoing phase I of clinical trials, the data obtained so far evidence exciting clinical benefits for the treatment of multiple myeloma in relapsed and relapsed/refractory patients (Gerwick and Moore, 2012, Potts *et al.*, 2011).



Salinosporamide A  
(Marizomib)

**Figure 1.3. Chemical structure of the drug candidate salinosporamide A (NPI-0052, Nereus Pharmaceuticals).**

Studies of the biosynthetic pathway through chemical synthesis and metabolic engineering led to the production of novel analogues which displayed very interesting and potent bioactivity, as is the case of fluorosalinosporamide, potent but slowly reversible and salinosporamide X7 which is more potent *in vivo* (Eustaquio and Moore, 2008; Nett *et al.*, 2009). The use of a seawater-based fermentation process and the implementation of artificial regulation of the biosynthetic pathway are proof-of-concept milestones in marine drugs development, being salinosporamide A reference example as its production has improved of 100 fold to 450 mg/L (Gerwick and Moore, 2012; Fenical *et al.*, 2009).

It is known that *S. tropica* itself possesses 20S proteasome machinery, so it is only logical that the question about how the bacterium copes with its self-made PI arises. Analysis of the whole genome sequence of the bacterium, revealed the existence of a redundant  $\beta$ -subunit, *sall*, peripheral to the pathway regulatory gene *sal*, whose protein product has a 30-fold resistance to salinosporamide A, and also a cross resistance to bortezomib (the first therapeutic proteasome inhibitor tested in humans). This altered substrate specificity is thought to be due to an A49V mutation in the Sall protein. (Gerwick and Moore, 2012, Kale *et al.*, 2011, Franke *et al.*, 2011)

#### 1.4.2. Marine secondary metabolites: antimicrobial

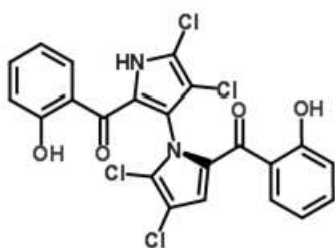
Recent years have seen an increase in pathogenic microorganisms resistant to antibiotics, culminating with the appearance of the so-called superbugs. The biofilm, a complex organized bacterial community usually surrounded by a matrix of extracellular polymeric substances (EPS), account for 80% of microbial infections (Singh *et al.*, 2016; Motlagh *et al.*, 2016). This phenomenon has prompted a search for new sources of bioactive products with antibiotic properties. Among the considered sources, marine environment has presented itself as “particularly promising”. Although,

only recently being more deeply explored, the marine compounds characterized so far have shown a wide and highly potent range of biological activity, including antimicrobial. Therefore, it is believed that the solution to the world's antibiotic crisis may lie in the oceans (Donia and Hamann, 2003). In the past few years, several compounds possessing anti-bacterial activity have been identified. Table 1.2 and Figure 1.4 summarize some of those with the greatest potential.

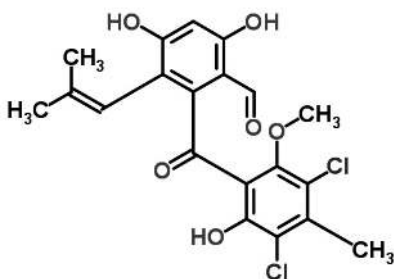
**Table 1.2. Selected marine secondary metabolites with antimicrobial activity (Donia and Hamann, 2003; Habbu *et al.*, 2016).**

Compound Name	Marine Organism	Antimicrobial test	MIC/IC <sub>50</sub>
<b>Bromosphaerone</b>	Algae	<i>Staphylococcus aureus</i>	0.047 µg/ml
<b>Cribrastatin 3</b>	Sponge	<i>Neisseria gonorrhoeae</i> penicillin-resistant <i>Neisseria gonorrhoeae</i> (clinical isolate)	0.09 µg/ml 0.39 µg/ml
<b>Marinopyrroles A and B</b>	Bacteria	meticillin-resistant <i>Staphylococcus aureus</i>	0.61 and 1.1 µmol/L respectively (MIC90)
<b>Jorumycin</b>	Mollusk	various Gram positive bacteria (eg, <i>Bacillus subtilis</i> , <i>S. aureus</i> )	0.050 µg/ml (inhibition zone of 16 mm)
<b>Pestalone</b>	Fungus	meticillin-resistant <i>Staphylococcus aureus</i> vancomycin-resistant <i>Enterococcus faecium</i>	0.037 µg/ml 0.078 µg/ml
<b>Squalamine</b>	Fish	<i>Staphylococcus aureus</i>	1.0 µg/ml
<b>Phenanthroviridone</b>	Actinomycete	<i>Staphylococcus aureus</i>	0.25 µg/ml

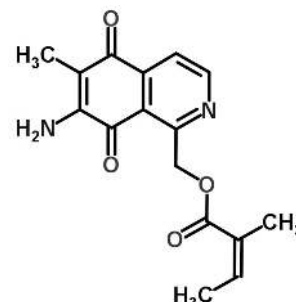
A point worthy of note is the co-culture of a marine fungus with a unicellular marine bacterium to yield pestalone. This mixed fermentation could be a potential method for the discovery of novel antibiotics (Donia and Hamann, 2003).



Marinopyrrole A  
(Bacteria)



Pestalone  
(Fungus)



Cribrastatin 3  
(Sponge)

**Figure 1.4. Selected chemical structure of marine-derived natural products with antimicrobial activity.**

## 1.5. Marine secondary metabolites: antifoulants

A very common occurrence in aquatic environment is the encrustation of microorganisms and macroorganisms to surfaces and of the first to the surfaces of the latter. This process is designated as biofouling. Although this unwanted attachment is essential for the colonizing organisms, it represents an engineering, health and economic hindrance to humans. Submerged man-made surfaces, such as oil and gas platforms, ship hull, aquaculture systems, drinking water systems, power plants and medical equipment, are rapidly inhabited by biofilm forming microorganisms and, given the conditions, subsequently by macroorganisms (Davey and O'toole, 2000; Huggett *et al.*, 2009). Biofouling poses a direct threat to human health by their proliferation on hospitals on medical apparatus such as catheters (Trautner and Darouiche, 2004), pacemakers (Marrie *et al.*, 1982; Santos *et al.*, 2011), cardioverter defibrillators (Symeon and Dimitris, 2011) heart valves and vascular prostheses (Amirante and Miró, 2008). The estimated additional hospital costs associated with cardiac devices alone ranges from 30 to €140 million per year (Kuehn *et al.*, 2010). The shipping industry is one of the most affected economic areas. An additional rise in the fuel consumption, estimated in \$56 million per year for, and \$1 billion over 15 years, is linked to hydrodynamic drag caused by hull biofouling (Schultz *et al.*, 2011). Power plants are another hot-spot area of biofouling with an estimated \$15 billion annual expenditure to control the problem on vital parts cooled by seawater. Furthermore, there are environmental costs derived from an increase in the emission of greenhouse gases and introduction of alien species by fouled hulls (Vimala, 2016). Therefore, finding efficient antifouling agents presents itself as a pressing matter. The solutions presented so far have involved toxic substances, such as organotin compounds incorporated into paint, which have been shown to cause adverse effects in the marine life (e.g. mussel larvae mortality and oyster shell malformation) (Alzieu, 2000), leading to their subsequent banning by the International Maritime Organization (IMO) and Marine Environmental Protection Committee (MEPC) in 2003 (Kotake, 2012; Sonak *et al.*, 2009). This restriction has led to a shift on the focus of the search for antifouling solutions, with the efforts concentrating now on environmentally friendly antifoulants (Dobresov, 2006; Magin *et al.*, 2010).

### 1.5.1. Microfouling

For the biofouling to occur, the necessary conditions must be met. For the initial phase of biofouling, which is designated microfouling, usually, these conditions are provided by dissolved organic matter which accumulates on the submerged surfaces forming a conditioning film, in what is known as molecular fouling or biochemical conditioning. This occurs in a matter of seconds to minutes after submerging the surface. Afterwards, in minutes to hours, fouling microorganisms (microfoulers), mainly bacteria and diatoms, move on to attach to the surface, forming a biofilm (Qian and Xu, 2012; Abarzua and Jakubowski, 1995; De Beer *et al.*, 1994; Stoodley *et al.*, 1994). The organization of the microbial community is managed through quorum sensing. This cell-density dependent mechanism regulates communication, through molecular compounds, and, subsequently, access to nutrients and stress resistance (Reading and Sperandio, 2005; Dobretsov, 2009).

### 1.5.2. Macrofouling

The biofouling process starts with the unwanted accumulation of microorganisms on man-made surfaces and culminates with the colonization by macroorganisms, or macrofouling. In the macrofouling level, larva and spore attach to the surface in a span of days, and take weeks to years to grow (Qian and Xu, 2012; Abarzua and Jakubowski, 1995; De Beer *et al.*, 1994; Stoodley *et al.*, 1994). The macrofouler organisms include algae and invertebrates, classified as soft foulers or shell free, and barnacles and tube worms, belonging to the class of hard foulers or shelled organisms. The microfoulers are the basis of biofouling, but macrofoulers are the main responsible for the damages observed on submerged man-made surfaces. This damage is due, for example, to the calcium carbonate skeletal structures of shelled microorganisms, which upon tightly holding them to ship hulls, result in increased hydrodynamic drag (Qian *et al.*, 2007; Kirschner *et al.*, 2012; Salta, 2012).

Biofouling occurs both on man-made structures and on marine species. Sessile or slow moving organisms such as sponges, sea weeds and corals are the main victims, constantly facing the threat of being overgrown by biofouling organisms (Worm *et al.*, 2003). Not surprisingly, there is a wide variety of species that have developed diverse strategies for preventing biofouling or removing already established biofoulers (antifouling) (Dafforn, 2011). The strategies range from symbiotic relationships, physical defense to highly potent chemical arsenal (Burns and Ilan, 2003; Burns *et al.*, 2003). The observation of these natural antifouling processes has motivated scientists to extract and examine marine natural products for the production of novel antifouling agents (Salta, 2012). Current approaches to antifouling solutions include incorporation of antifouling agents into paints, biological mimicking through bio-inspired surface modifications (*e.g.* antifouling surface topographies) and bio-materials (*e.g.* surfaces with self-renewing properties) (Palumbi and Palumbi, 2015; Liu and Jiang, 2012; Nir and Rechtes, 2016).

### 1.5.3. Butyrylcholinesterase: a valid target for antifouling agents development

The cholinesterase (ChE) is an enzymatic family specialized in hydrolyses of choline-based esters. This family includes the acetylcholinesterase (AChE), or true cholinesterase, and pseudocholinesterase (PChE) to which the butyrylcholinesterase (BuChE) belongs to (Lane *et al.*, 2005; Johnson and Moore, 2012a). The AChE plays a major role in neurotransmission as it is responsible for terminating cholinergic synapses by degrading acetylcholine (ACh) (Girard *et al.*, 2007). The inhibition of AChE causes disruption of several biological functions, including respiration, feeding and behavior (Cunha *et al.*, 2007). BuChE also seems to play a role in this disruption process, although auxiliary, at a much smaller rate than AChE; the preferential substrate of BuChE is butyrylcholine (Pezzemanti *et al.*, 2011). Furthermore, BuChE has a toxicologically important role by acting as a scavenger of anticholinergic compounds, such as organophosphorus poisons (OP), (Masson and Lockridge, 2010; Johnson and Moore, 2012) and a protective role towards AChE, since this latter has lower activity with the increase of substrate concentration and its inhibition increases the concentration of ACh at the synaptic cleft (Lane *et al.*, 2005). Furthermore, BuChE is widely distributed throughout the tissues of the organism (Cunha *et al.*, 2007). Lastly, it has been shown that BuChE's activity increases with the progress of dementia, such as Alzheimer's disease (AD), contrary to AChE's activity (Pagnin *et al.*, 2016). These characteristics have made those cholinesterases the main targets in the development of anticholinergic agents (Johnson and Moore, 2012b).

Studies have found that ACh plays a major role in the settlement of macro-fouling organisms. In 2003, Faimali and co-workers (Faimali *et al.*, 2003) reported that the total inhibition of AChE resulted in no settlement of *Balanus amphitrite cyprids* barnacles. In 2011, Young and co-workers reported the induction and attachment of the blue-lipped mussel *Perna canaliculus*. These and other studies (Dobretsov and Qian, 2003; Almeida *et al.*, 2015) have established ChEs as valid targets in the development of anti-fouling agents.

### 1.6. Marine natural products: the example of diketopiperazines

Diketopiperazines (DKPs) are an emerging class of small molecules garnering most attention due to their potent range of bioactivity and the structure readily-prone to modifications. Among other sources, they are isolated from marine organisms (Bowling *et al.*, 2007; Lebar *et al.*, 2007; Folmer *et al.*, 2007). The class of DPKs is composed of three regioisomers: 2,3-diketopiperazines (2,3-DKPs), 2,5-diketopiperazines (2,5-DKPs) and 2,6-diketopiperazines (2,6-DKPs). These three isomers share a common piperazine core but differ in the distribution of the carbonyl group in the piperazine ring. They are chirally enriched organic molecules generally biosynthesized from amino acids, and synthetically obtained as product of condensation of two  $\alpha$ -amino acids, or result of "degradation of polypeptides in food and beverages" (2,5-DKPs), derivative of iminodiacetic acids (2,6-DKPs) or ethylenediamine (2,3-DKPs) (Dinsmore and Beshore, 2002). Of the three types of molecules, 2,5-

DKP has received the most attention. 2,5-DPKs have double lactam core, are conformationally rigid, and their subunit can be free or associated with other products (Huang *et al.*, 2014; Mollica *et al.*, 2014). The structural composition of these molecules renders them easy to synthesize and modify through combinatorial chemistry (Mollica *et al.*, 2014), making them valuable drug candidates.

### 1.6.1. Biosynthetic pathways

Although many diketopiperazines have been characterized so far, the molecules are derived from only three biosynthetic pathways: a nonribosomal pathway, a nonribosomal pathway-derived pathway, and a nonribosomal-independent pathway. In the nonribosomal pathway, the enzymatic complex NRP synthase (NRPS) catalyses the formation of the diketopiperazine; the nonribosomal pathway-derived pathway corresponds to DKP derivatives generated as side-products of the former pathway; (Bowling *et al.*, 2007; Lebar *et al.*, 2007; Folmer *et al.*, 2007) and, finally, the nonribosomal-independent pathway which produces the antifungal antibiotic nystatin in *Streptomyces noursei* (Brautaset *et al.*, 2000).

### 1.6.2. Biological activities

Some DPKs have been found to possess remarkable anti-cancer activity, with a prominent example being the plinabulin, derived from phenylahistin, and chemically optimized, rendering it semi-synthetic. This drug candidate, currently in phase II of clinical trial, exerts its action against microtubules having a “colchicines-like tubulin depolymerisation activity” (Mollica *et al.*, 2014). A very prominent feature that has come to light concerning the anti-cancer activity of DPKs lies with their lipophylicity: higher lipophylicity correlates with higher anti-cancer activity. For example, it has been observed that prenylation of DPKs enhances greatly their growth inhibitory activity against cancer cells, *in vitro* (Mollica *et al.*, 2014). Aside from anti-cancer activity, DPKs have also exhibited anti-bacterial (Deepa *et al.*, 2015), antifungal, antifouling (Liao *et al.*, 2015), antiviral, cytotoxic and plant-growth regulatory activities (Martins and Carvalho, 2007; Huang *et al.*, 2010). The fungus *Leptosphaeria* sp. isolates leptosin G, G1, G2 and H have shown to be potent cytotoxic agents against P388 lymphocytic leukemia (Huang *et al.*, 2010). The metabolite (-)-phenylahistin exhibits activity against P388 cells, effecting by causing their arrest; powerful cytotoxic activity has also been observed (Bladt *et al.*, 2013; Kanoh *et al.*, 1999). The *Salinispora arenicola* has been found to produce cyclomarins (A-C) with potent anti-inflammatory activity. The structurally related peptides cyclomarazines A and B were also isolated from *S. arenicola*, and displayed moderate antimicrobial activity against methicillin-resistant *Staphylococcus aureus* (MRSA) and vancomycin resistant *Enterococcus faecium* VRE strains, with values of 18 and 13 µg/ml, respectively (Schultz *et al.*, 2008). The sponge *Geodia baretii* has proven to be a trove of antifouling compounds, furnishing the promising antifouling agent baretin, already tested as a paint incorporate, and bromobenzisoxazolone baretin acting at molecular level inhibiting the settlement of barnacle larvae (Huang *et al.*, 2010). The compounds cyclo(1-Phe-(4R)-hydroxy-1-Pro), from *Pseudoalteromonas luteoviolacea*, and cyclo(1-(4-hydroxy-Pro)-d-Leu), from bacterium A108, act as plant-growth activity stimulators. Golmaenone, from *Aspergillus* sp., has shown to be a promising sunscreen protector agent, presenting a value of 90 mm for ultraviolet-A (UVA; 320-390). The structure of the compounds mentioned above, is presented in Figure 1.5.

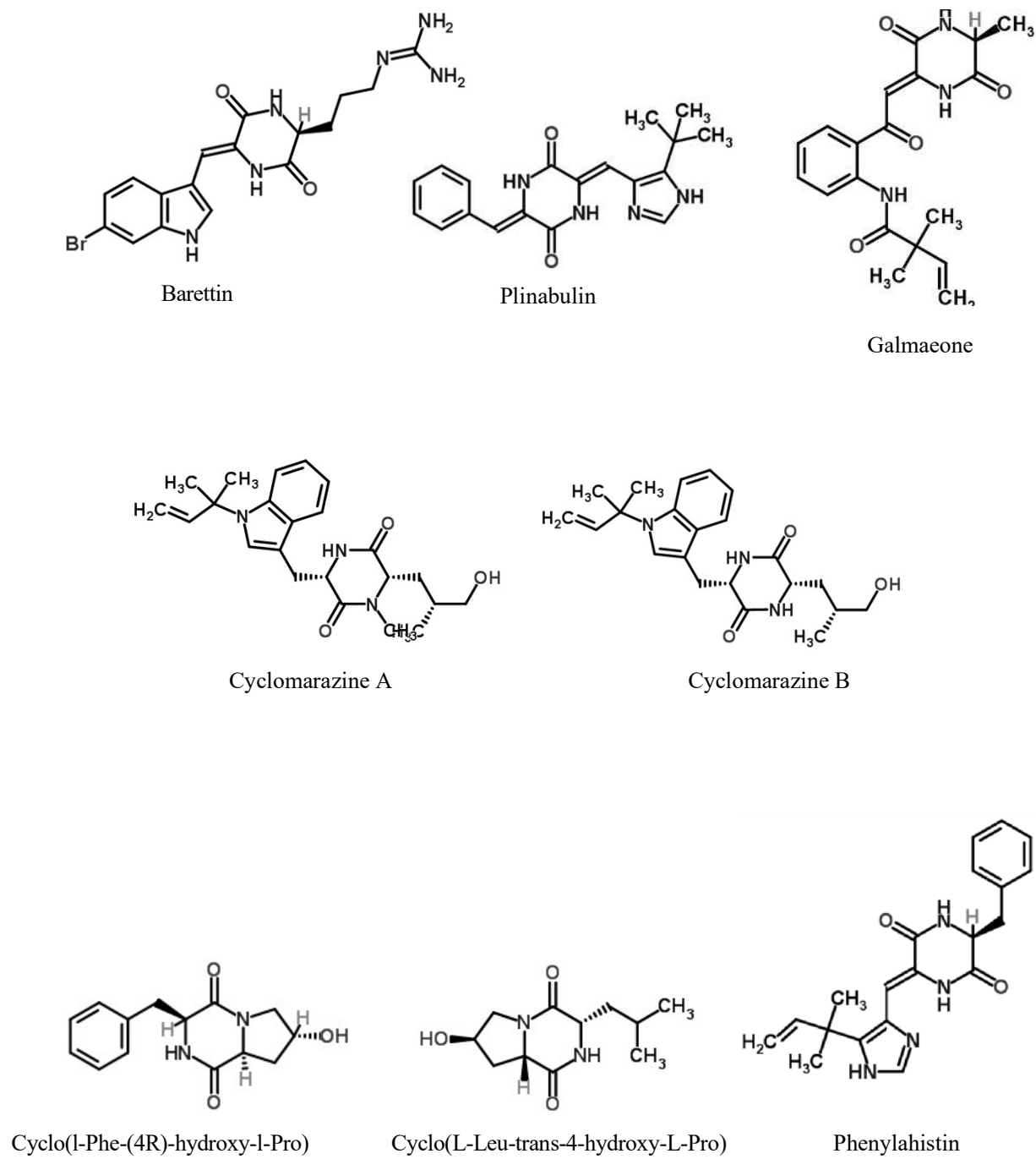


Figure 1.5. Chemical structures of selected diketopiperazines from marine origin.



## 1.7. Actinomycetes

### 1.7.1. Bioactivity and ecology

Actinomycetes are an ongoing source of clinically relevant metabolites, with an established share of roughly 75% of all natural products used as anti-infective agents, of which more than 50% are produced by the genus *Streptomyces* (Gomez-Escribano and Bibb, 2013; Gomez-Escribano *et al.*, 2016; Subramani and Aalbersberg, 2012). These gram-positive, rich in G+C content, inhabitants of both the terrestrial and marine environment, commonly associated with sponges in the latter (Simister *et al.*, 2012; Abdelmohsen *et al.*, 2014; Russo *et al.*, 2015; Fenical and Jensen, 2006), produce more than 40% of all microbe-derived natural products (Bérdy, 2012). However, analysis of sequences of bacteria from this group has revealed that the genetic potential for production of natural products far surpasses the observed from laboratory fermentations (Challis, 2014).

Terrestrial actinomycetes have been thoroughly studied and are regarded as remarkable producers of a wide range of bioactive and economically relevant metabolites; however, their marine counterparts remain relatively untapped. Although many terrestrial spore-forming actinomycetes are washed into the sea, studies of marine isolates suggest their produced metabolites often differ structurally from those produced by the terrestrial ones, due to evolutionary divergence (Jensen *et al.*, 2005; Han, 2012). Furthermore, bacteria harvested from ocean sediments and studied by culture-independent approaches, including members of the genera *Streptomyces* and the obligate marine bacteria *Salinispora* and *Marinispora*, have hinted at a marine origin for the marine actinomycetes (Bredholdt *et al.*, 2007; Subramani and Aalbersberg, 2012; Ward and Bora 2006). These bacteria have been shown to produce unique compounds with unparalleled bioactivity (Table 1.3), belonging to a wide range of compound classes such as peptides, tetracyclines, macrolides, polyenes and  $\beta$ -lactams. Rare actinomycetes have received special attention as their metabolites tend to be structurally complex, highly potent and low in toxicity (Subramani and Aalbersberg, 2012) (Figure 1.6).

**Table 1.3. Examples of secondary metabolites isolated from marine actinomycetes.** Adapted from Subramani and Aalbersberg, 2012.

Compound Name	Bacterium	Biological activity
Salinosporamide A	<i>Salinispora tropica</i>	Anti-cancer; antimalarial
2-Allyloxyphenol	<i>Streptomyces</i> sp.	Antimicrobial; food preservative; oral disinfectant
Marinomycins A-D	<i>Marinispora</i>	Antimicrobial; anti-cancer
Butenolides	<i>Streptoverticillium luteoverticillatum</i>	Antitumor
Lodopyridone	<i>Saccharomonospora</i> sp.	Antitumor
Arenimycin	<i>Salinispora arenicola</i>	Antimicrobial

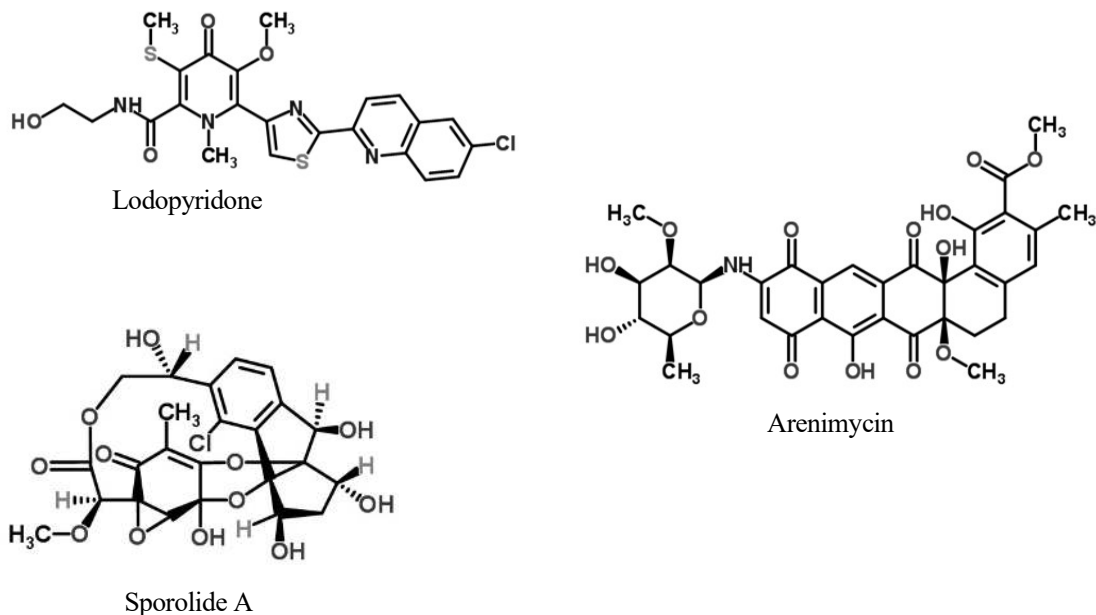


Figure 1.6. Selected novel and unique metabolites from rare marine actinomycetes.

### 1.7.2. Ecologic role of actinomycetes

The capabilities of marine actinomycetes extend beyond antibiotic production. The ecological functions encompass probing of environmental and substrate conditions by its availability (Ramesh and Mathivanan 2009), degradation and turnover of materials, such as cellulose by *Streptomyces* sp., and hydrolysis of chitin agar by more than a hundred studied actinomycetes (Subramani and Aalbersberg, 2012). Proteolytic, amylolytic, lipolytic and phosphate-solubilising activities have also been reported (Sivakumar *et al.*, 2007). Actinomycetes have also been implicated in the degradation of alginate, laminarin, oil and other hydrocarbonates, and wood submerged in seawater (Sivakumar *et al.*, 2007; Subramani and Aalbersberg, 2012). Finally, they are also involved in “mineralization of organic matter, improvement of physical parameters and environmental protection” (Subramani and Aalbersberg, 2012).

### 1.7.3. The *Salinispora* genus

The *Salinispora* genus is composed of the obligate marine species *Salinispora arenicola*, *Salinispora pacifica* and *Salinispora tropica* (Maldonado *et al.*, 2005; Ahmed *et al.*, 2013). The three closely related species share about 99% 16S rRNA gene sequence identity (Ahmed *et al.*, 2013). *S. arenicola* is the eldest among the three *Salinispora* species (Jensen *et al.*, 2015). These aerobic, Gram-positive spore-forming bacteria are visually characterized by their ubiquitous bright orange or pink pigmentation (Figure 1.7); however, the pigmentation can change to dark brown and black during sporulation. The spores are non-motile and borne singly or in clusters, and are carried by branched substrate hyphae formed by these bacteria. As characteristic of actinomycetes, they present high G+C content, ranging from 70 to 73 mol%. The bacteria present good growth in temperatures ranging from 10 to 30 °C, and pH 7-12, with colonies usually appearing between 3 to 6 weeks, depending on growth media (Maldonado *et al.*, 2005). The species *S. arenicola* shows an optimum growth temperature in the region of 20-28°C, seawater requirement in the range of 25-50%, with sodium enriched medium as valid alternative. The species was first collected off the coast of Bahamas (Maldonado *et al.*, 2005).

The *Salinispora* genus is the first obligate marine bacteria reported in the order *Actinomycetales*, as it requires sodium salt or seawater based media, for growth, and fail to grow in medium where seawater is replaced for deionised (DI) water (Maldonado *et al.* 2005a; Russo *et al.*, 2015; Mincer *et al.*, 2005; Tsueng *et al.*, 2008). It belongs to the group of rare actinomycetes, *i.e.* non-streptomycete, contributing, alongside others from its category, with only 25% against the *Streptomyces*' 75% of all actinomycetales compounds (Subramani and Aalbersberg, 2012). However, these orange-pigmented bacteria (Jensen *et al.*, 2015) have attained high reputation after the anti-cancer drug candidate salinosporamide A was isolated from *S. tropica* by Fenical and co-workers. The genus was also first reported by Fenical two decades ago (Jensen *et al.*, 2015).

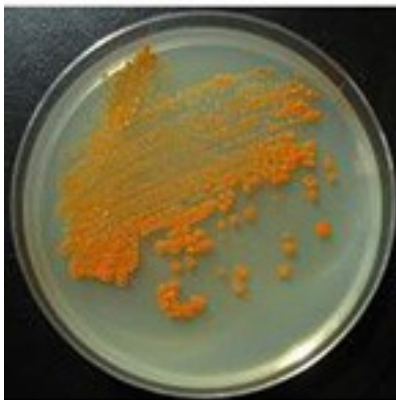


**Figure 1.7.** A *Salinispora* strain streaked on agar. Modified from Murphy *et al.*, 2010.

Due to their seawater or salt-based media requirement for growth, along with their morphological and chemotaxonomic characteristics, the *Salinispora* species were proposed to represent a species within the genus *Micromonospora*. However, subsequent studies showed that they belonged to a new genus, for which the name *Salinispora* was proposed (Jensen *et al.*, 2015).

It has been shown that these bacteria require the  $\text{Na}^+$  ion for the maintenance of osmotic environment and protection of cell integrity (Das *et al.*, 2006), and the salt plays a crucial role in modelling the pattern of bacterial growth and natural compounds production (Bose *et al.*, 2015; Tsueng *et al.*, 2008). For example, it has been shown that replacing the undefined commercial synthetic salt Instant Ocean, which is composed of sodium and chloride, for a similar but defined sodium-chloride-based formulation yields a higher production of salinosporamide A, while a sodium-sulphate-based salt formulation has a salinosporamide A profile production similar to that obtained when Instant Ocean is used (Tsueng *et al.*, 2008). Potassium and lithium-sulphate-based salt formulation have also been shown to support growth of a *Salinispora tropica* and *Salinispora pacifica* strain and its production of salinosporamide A (Tsueng *et al.*, 2008; Tsueng and Lam, 2010), while a *Salinispora arenicola* strain presents slow growth in lithium-based formulation (Tsueng and Lam, 2008). These examples illustrate the importance of salinity in secondary metabolites production, especially in the case of the *Salinispora* genus, whose isolation passes necessarily by employing seawater or salt-based selective methods (Qiu *et al.*, 2008; Khanna *et al.*, 2011; Maldonado *et al.*, 2005a).

*Salinispora* strains have been reported in association with macroorganisms such as ascidians, seaweeds, and, more often, sponges (Vidgen *et al.*, 2012; Jensen *et al.*, 2007; Kim *et al.*, 2005; Jensen *et al.*, 2015). They have been harvested and cultured from depths up to 1100 m, and detected in a culture independent manner from depths as great as 5669 m (Mincer *et al.*, 2005; Prieto-Davó, 2013). Globally, the genus is abundant and presents a widespread distribution in the tropical and sub-tropical oceanic region, with *S. arenicola* reported from all sites the genus has been harvested from, while the

*S. tropica* has been restricted only to the Caribbean, and the *S. pacifica* follows the pattern of distribution of *S. arenicola*, however with a couple of restrictions (Figure 1.8) (Freet *et al.*, 2012).

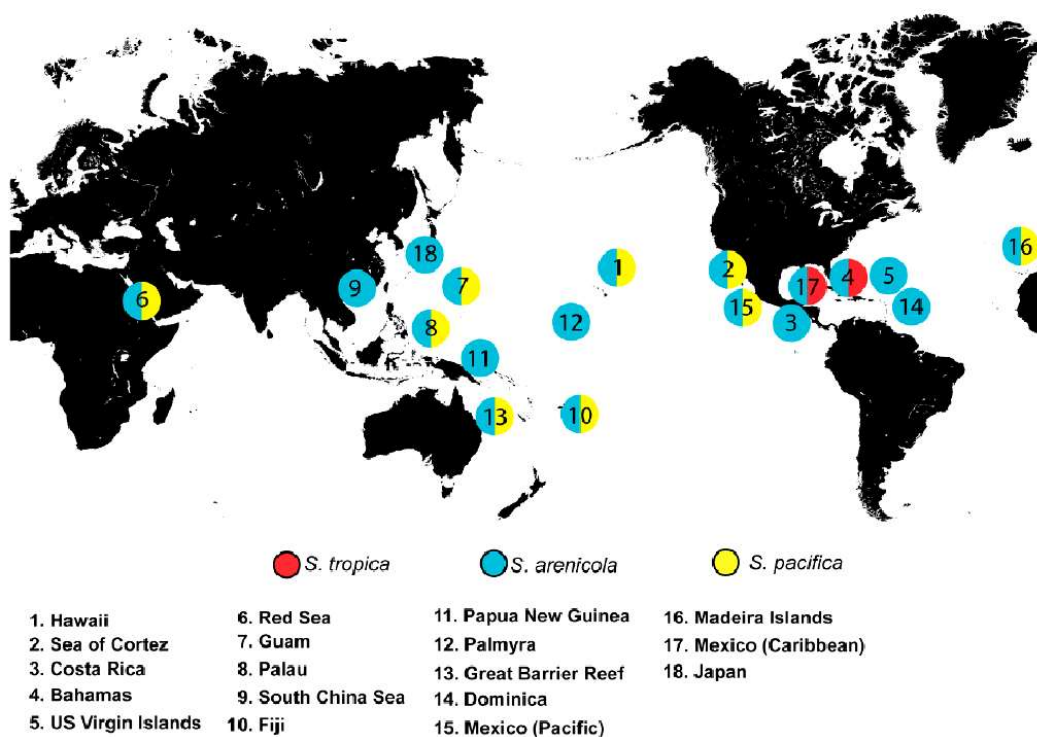


**Figure 1.8. Geographic distribution of reported *Salinispora* genus.** The strain of *S. arenicola* studied in this thesis was collected off the coast of the Madeira Archipelago (16). Image from Jensen *et al.*, 2015.

### 1.7.3.1. Bioactive compounds produced by *Salinisporas*

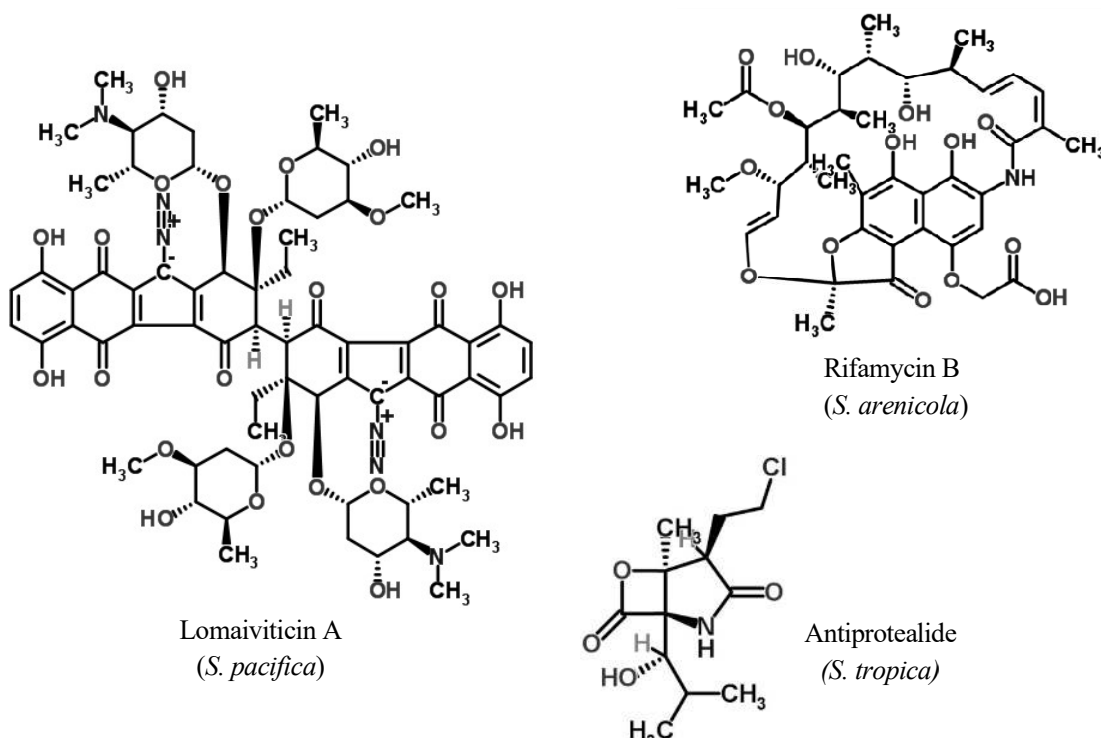
The *Salinispora* genus is a prolific source of novel and unique secondary metabolites and enzymes, with many being pharmaceutically and economically relevant. So far, no less than 10 kinds of novel structurally unique novel compounds have been isolated from its strains (Jensen *et al.*, 2007; Ziemert *et al.*, 2014). In fact, a hefty 10% of the genome of the species is devoted to secondary metabolism (Udvary *et al.*, 2007). The observed cosmopolitan distribution of *Salinispora* species in the marine environment alongside the observed genomic island location of a majority of their secondary metabolite biosynthetic gene clusters (Penn *et al.*, 2009) may be due to this range of powerful metabolite arsenal, allowing the strains to strive, compete and prevail under stressful conditions. The observed bioactivities from the metabolites produced by strains of the *Salinispora* species range from antibacterial (*e.g.* rifamycins), passing by anti-cancer (*e.g.* Salinosporamide A) to antimalarial (*e.g.* Salinosporamide A) (Kim *et al.*, 2006; Felling *et al.*, 2003; Fenical and Jensen, 2006). Table 1.4 summarizes the compounds from this genus. Figure 1.9 shows the structure of the selected compounds.

Table 1.4. Secondary metabolites from the *Salinispora* genus. Adapted from Jensen *et al.*, 2015.

Compound	Species <sup>a</sup>	Biosynthetic origin	Novelty	Activity (target)
salinosporamide A	<i>S. tropica</i>	PKS-NRPS	new	proteasome
sporolide A	<i>S. tropica</i>	ePKS	new	reverse transcriptase <sup>d</sup>
salinilactam	<i>S. tropica</i>	type I PKS	new	ND
sioxanthin	<i>S. tropica</i>	terpene	new	ND
antiprotealide	<i>S. tropica</i>	PKS-NRPS	new	proteasome
pacificanone A	<i>S. pacifica</i>	type I PKS	new	ND
salinipyronone A	<i>S. pacifica</i>	type I PKS	new	ND
cyanosporoside A	<i>S. pacifica</i>	PKSe	new	ND
lomaiviticin A	<i>S. pacifica</i>	type II PKS	new	cytotoxic (DNA)
enterocin	<i>S. pacifica</i>	type II PKS	known	antibiotic
saliniketol A <sup>b</sup>	<i>S. arenicola</i>	type I PKS	new	ornithine decarboxylase
arenicolide A	<i>S. arenicola</i>	type I PKS	new	ND
saliniquinone	<i>S. arenicola</i>	type II PKS	new	cytotoxic
cyclomarin A	<i>S. arenicola</i>	NRPS	known	anti-inflammatory
cyclomarazine <sup>c</sup>	<i>S. arenicola</i>	NRPS	new	ND
arenimycin	<i>S. arenicola</i>	NRPS	new	antibiotic
arenamide A	<i>S. arenicola</i>	type II PKS	new	anti-inflammatory (NFκB)
staurosporines	<i>S. arenicola</i>	alkaloid	known	protein kinase
isopimara-8,15-dien-19-ol	<i>S. arenicola</i>	terpene	new	ND
rifamycin B	<i>S. arenicola</i>	type I PKS	known	RNA polymerase
mevinolin	<i>S. arenicola</i>	PKS	known	HMG-CoA reductase
desferioxamine B	<i>St, Sa, and Sp</i>	NRPS	known	iron chelator
Lymphostin	<i>St, Sa, and Sp</i>	NRPS-PKS	known	Immunosuppressant

<sup>a</sup> Original report of compound detection from *Salinispora* spp. <sup>b</sup> Rifamycin synthase intermediate.

<sup>c</sup> Cyclomarin synthetase intermediate. <sup>d</sup> Predicted, e = enediyne, ND = not determined.



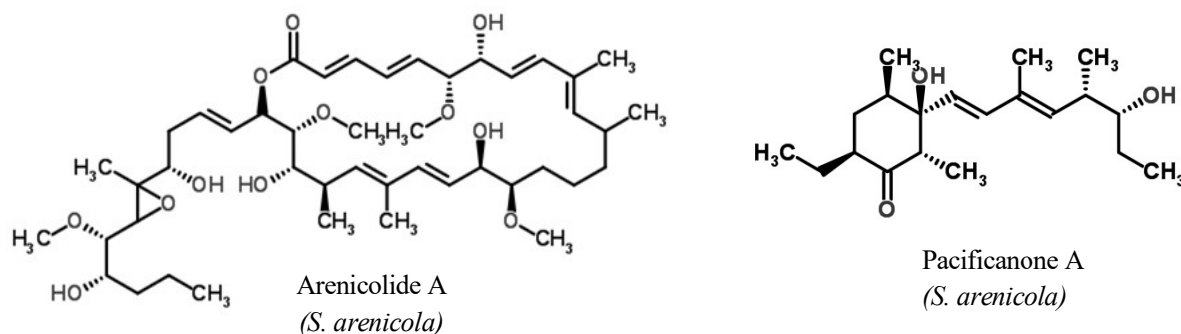


**Figure 1.9.** Selected structure of compounds produced by *Salinispora* strains.

Lomaiviticin A, together with its sister lomaiviticin B, was of the first compound from the *Salinispora* genus to be described, although at the time the *Salinispora* species was designated *Micromonospora lomaivitiensis* due to a misconception in taxonomic attribution. This compound possesses potent antibiotic activity against Gram-positive bacteria *S. aureus* and *E. faecium* with MIC values ranging from 6 to 25 ng/spot. The compound also exhibits powerful cell cytotoxicity against cancer cell lines with IC<sub>50</sub> values ranging from 0.01 to 98 ng/ml. The mechanism of cytotoxicity has been found to be carried out through cleavage of double-stranded DNA (He *et al.*, 2001). Arenicolide A-C are macrolide polyketides of planar structure isolated for the *S. arenicola* strain CN-005. Arenicolide A showed moderate cytotoxicity against HCT-116 cell line, with an IC<sub>50</sub> value of 30 µg/ml, but showed no activity against the bacterial pathogens MRSA and VREF (Williams *et al.*, 2007). Antiprotealide was isolated from *S. tropica*, but was initially reported as a product of synthesis by hybridizing the cyclohexenyl ring of salinosporamide A with the isopropyl functional group of ofomuralide. This compound is a proteasome inhibitor with an IC<sub>50</sub> value of 38.2 nM against Purified Yeast 20S Proteasome β 5-Subunit and cytotoxicity with IC<sub>50</sub> of 0.856 µM (McGlinchey *et al.*, 2008). The rifamycin family includes rifamycin B, O, SV and W. It has been shown that these compounds are produced in a time and salinity dependent manner during the growth cycle of *S. arenicola* (Jensen *et al.*, 2015). Rifamycins are a group of antibiotics active against gram-positive bacteria (Kim *et al.*, 2006). Salinilactam is polyene macrolactam isolated from *S. tropica* strain CNB-440 (Udwary *et al.*, 2007). Sioxanthin, technically named (2'*S*)-1'-(β-D-glucopyranosyloxy)-3',4'-didehydro-1',2'-dihydro-φ,ψ-caroten-2'-ol, is a C-40 carotenoid responsible for the orange pigmentation characteristic of the *Salinispora* sp. cultures. Its glycosylated end puts it in a very select structural group of only nine carotenoids, since glycosylation is rare among actinomycete carotenoids; and since the other end of the molecule contains an aryl group, the overall compound contains a polar and a non-polar head groups. Investigation of the genome by gene sequence homology suggests that the compound is produced by all members of the *Salinispora* sp. The biological function of this carotenoid is still under investigation, but it is postulated that, like other carotenoids, it may play a role in the prevention of oxidative stress due to its central conjugated chain, and as a structural molecule where the glycosyl moiety contributes for the proper folding of the thylakoid membrane (Richter *et al.*, 2015). Arenamides A and B were, and are to date, isolated only from *S. arenicola* strain CNT-088. The compounds were found to inhibit NFκB in transfected 293/NFκB-Luc human embryonic kidney cells by blocking TNF (tumor necrosis factor)-induced activation with IC<sub>50</sub> values of 3.7 and 1.7 µM, in a dose and time-dependent manner, respectively; and present moderate cytotoxicity against HCT-116 human colon carcinoma with IC<sub>50</sub> values of 13.2 and 19.2 µg/ml, respectively. The compounds presented only mild activity against MRSA and VREF (Asolkar *et al.*, 2010).

## 1.8. Aim of the thesis

The work presented in this thesis is part of an ongoing project “Tesouros Oceânicos- Sedimentos oceânicos do arquipélago da Madeira: nova fonte de compostos inovativos e bioativos” ref.-PTDC/QUI-QUI/119116/2010 in Dr. Susana Gaudêncio’s lab at Faculty of Science and Technology of the New University of Lisbon (FCT-UNL). The ongoing project is exploring the poorly untapped Portuguese marine environment (Prieto-Davó *et al.*, 2016). The main goal of this work was to search for novel marine bioactive compounds produced by the actinomycete strain *Salinispora arenicola* PTM-099, and the evaluation of their biological activities. We have applied a bioassay-guided approach to look for potential bioactive agents and rely on spectroscopic methods for determining the structure of the isolated compounds. The working steps are as follows:

- Isolating secondary metabolites from laboratory-grown cultures of *S. arenicola* strain PTM-99 by chromatographic methods
- Screening evaluation of bioactive secondary metabolites produced by the previously selected bioactive *S. arenicola* strain PTM-99 :
  - antimicrobial assay
  - antifouling assay (target-based and phenotype-based)
- Structurally elucidating the bioactive metabolites through spectroscopic and non-spectroscopic methods
- Obtaining lead-like agents with bioactive and innovative proprieties for industrial applications.

## ***Materials and methods 2***





## 2. MATERIALS AND METHODS

### 2.1. Bacterial cell culture: materials and growth conditions

The *Salinispora arenicola* strain used in this work was previously collected from marine sediments off the coast of the Madeira Archipelago as part of the project “Tesouros Oceânicos- Sedimentos oceânicos do arquipélago da Madeira: nova fonte de compostos inovativos e bioativos” ref.-PTDC/QUI-QUI/119116/2010, in July 2012. The *S. arenicola* species was identified through the dereplication using the 16s rRNA gene sequencing method (GenBank accession number: KT446218) (Prieto-Davó *et al.*, 2016) and afterwards cryopreserved in A1 medium (Table 2.1) and 10% glycerol, at -80°C.

**Table 2.1. Composition of A1 medium.**

Component	Quantity (1L)
Peptone (Bacto)	2 g
Yeast extract (Bacto)	4 g
Starch (Difco)	10 g
Water	250 ml
Filtered seawater	750 ml

A frozen stock of bacterial cells was thawed from its cryogenic preservation and transferred to a 50 ml A1 medium for growth, in a 100 ml Erlenmeyer flask covered with cotton and aluminum foil. The culture was dark-incubated at 25°C, with shaking at 200 rpm for 7-14 days. The culture was subsequently transferred to fifteen 2 L Erlenmeyer flasks for a total of 15 L of culture and incubated under the conditions described above. The A1 medium was prepared using natural seawater filtered and autoclaved.

### 2.2. Extraction and fractionation of the crude

#### 2.2.1. Ethyl acetate extraction

The crude extract was obtained by liquid-liquid partitioning using equal volumes of EtOAc (LABCHEM) and culture. The extract was subsequently dried-up using a rotary evaporator and finally traces of solvent were removed under vacuum. The resulting crude was weighted for yield record and definition of fractionation conditions.

#### 2.2.2. Fractionation by flash-chromatography

The crude was fractionated using an adaptation of Still *et al.* (1978) preparative chromatography method. A 5 cm<sup>3</sup> volume of silica gel (Merk) was used as the stationary phase in a 30 mm diameter column, and the eluent combinations isooctane (Prolabo, 99.5%)/EtOAc and MeOH (Prolabo, 100%)/EtOAc, resulting in nine fractions. The eluent mixes are shown in the Table 2.2.

**Table 2.2. Composition of the mobile phase for each fraction.**

<b>Fraction</b>	<b>Eluent mix 400 ml (%)</b>
<b>F1</b>	100:0 isooctane/EtOAc
<b>F2</b>	80:20 isooctane/EtOAc
<b>F3</b>	60:40 isooctane/EtOAc
<b>F4</b>	40:60 isooctane/EtOAc
<b>F5</b>	20:80 isooctane/EtOAc
<b>F6</b>	0:100 isooctane/EtOAc
<b>F7</b>	10:90 MeOH/EtOAc
<b>F8</b>	50:50 MeOH/EtOAc
<b>F9</b>	100:0 MeOH/EtOAc

The crude extract was dissolved, loaded onto the column, and then eluted with the eluent mixes described above. The polarity of the eluent increases with the numeric designation of the fraction. The fractions were dried in a rotary evaporator, subsequently resuspended and transferred to tared vials, and finally the remainder of the solvent was evaporated in a vacuum line. The fractions were stored in the dark at room temperature until further experiments.

### 2.3. Isolation of secondary metabolites by HPLC

The fractions presenting relevant bioactivity were selected for isolation. The isolation process was initiated by performing the optimization of the High-Performance Liquid Chromatography (HPLC) program. A phase of trial and error was performed to test the eluents for their capacity to separate the components of the fractions and the optimum gradient concentration. In this work, water and acetonitrile formed the gradient in the separation process.

The compounds of the fractions were purified by reversed phase HPLC equipped with UV-Vis photodiode array detection (LC/UV-Vis-DAD) (DIONEX Ultimate 3000), scanning 190 to 300 nm. The separation was performed on a 250 mm x 10 mm, 5  $\mu$ m, 100 Å, C<sub>18</sub> column (Phenomenex), using as eluent water and acetonitrile on a binary gradient system, running at a flow rate of 1.5 ml/min. The gradient profile was defined for each fraction. The samples were dissolved in MeOH or THF (1mg/1 $\mu$ l) (Carlo Erba Reagents, 99.9%), centrifuged for 5 min and injected in the loop. The optimized conditions are presented in the Tables 2.3, 2.4 and 2.5.

**Table 2.3. HPLC elution conditions for fraction F2.**

<b>Time (min)</b>	<b>% ACN</b>	<b><math>\lambda</math> (nm) UV</b>
<b>0</b>	45	
<b>25</b>	45	210
<b>26</b>	75	235
<b>70</b>	75	245
<b>71</b>	100	275
<b>150</b>	100	

**Table 2.4. HPLC elution conditions for fraction F4-F7.**

Time (min)	% ACN	$\lambda$ (nm) UV
0	10	
20	45	210
140	45	234
141	100	250
170	100	275

**Table 2.5. HPLC elution conditions for fraction F8-F9.**

Time (min)	% ACN	$\lambda$ (nm) UV
0	10	
20	70	210
110	70	234
111	100	250
120	100	275

## 2.4. Bioassay

### 2.4.1. Antimicrobial activity

The purified compounds were tested for antibacterial activity through the determination of the minimum inhibitory concentration (MIC) using a modified version of the serial dilution assay method according to the Clinical and Laboratory Standards Institute (Dias, 2013). The experiment was performed using as targets the clinically relevant human pathogenic bacteria vancomycin-resistant *Enterococcus faecium* VRE EF82 (Mato *et al.*, 2009) and methicilin-resistant *Staphylococcus aureus* MRSA COL (Gill *et al.*, 2005). The purified compounds were solubilized in dimethyl sulfoxide (DMSO) to a concentration of 10 mg/ml. The samples were stored at room temperature and protected from light until use.

The pathogenic gram-positive bacterial strains were thawed from their cryopreservation (-80°C), transferred aseptically to solid Brain Heart Infusion (BHI) medium (Table 2.6) and incubated overnight at 37°C. Isolated colonies of the overnight cultures were used to inoculate a 5 ml liquid BHI medium and incubated overnight at 37°C with shaking at 180 rpm. The culture was measured in the morning for optical density at 600 nm (OD<sub>600</sub>), in an Ultraspect 3100 Pro Amersham Biosciences, to assess its absorbance, being the intended value from 0.04 to 0.06. The concentration for the intended absorbance was adjusted by dilution when necessary.

**Table 2.6. Composition of the BHI growth medium.**

Component	Quantity (1L)
BHI (DIFCO)	37 g
Agar	15 g
Water	1000 ml

Aliquots of 195  $\mu$ l of culture were added to the row A of a 96-wells microtiter plate. To the first 10 wells of row A was added 5  $\mu$ l of purified compound, and to the remaining two wells of the row were added 5  $\mu$ l of DMSO and 5  $\mu$ l of vancomycin (1mg/ml), respectively, as controls. An aliquot of 100  $\mu$ l of culture and 100  $\mu$ l of BHI were added to the last wells of row G, respectively, for use also as control. The serial dilution was performed by aliquoting 100  $\mu$ l of the mixture of row A, up until well 10, to the row B, mixed, and from this another 100  $\mu$ l of the mixture was aliquoted to the next row, and so forth until row F. On row G, 100  $\mu$ l of culture was added to well 11 and 100  $\mu$ l of BHI was added to well 12; these two aliquots were used as controls. The display of the samples in the assay is illustrated in Figure 2.1.

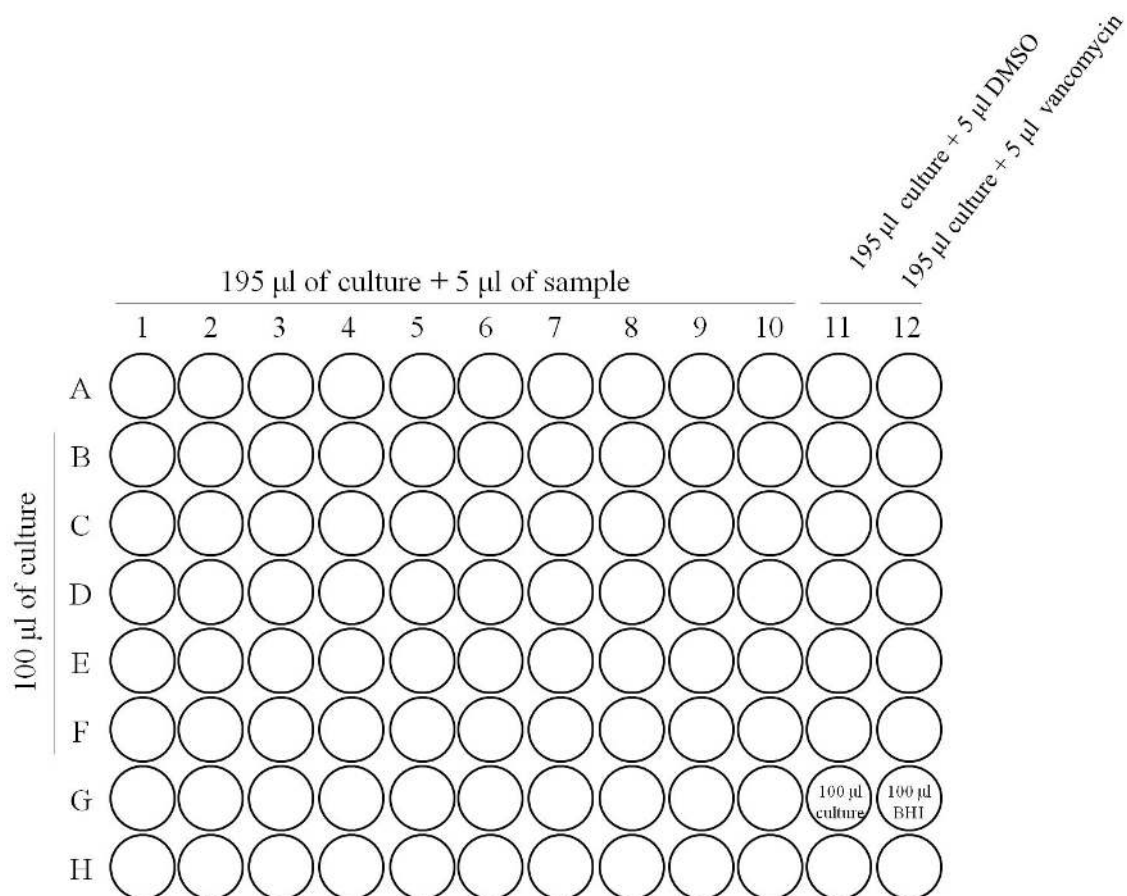


**Figure 2.1. Template of 96-well microtiter plate illustrating the disposition of samples and controls for the antibacterial test.**

In this way, a serial dilution was achieved and the obtained concentration was the following: 250, 125, 62.5, 31.25, 15.63, 7.81, 3.91, 1.95, 0.98 e 0.49  $\mu\text{g/ml}$ , from A to F row, respectively.

The microtiter plates were incubated overnight at 37°C without shaking. Following a period of incubation of 18 to 24 hours, the bioactivity was evaluated by assessing the turbidity of the cultures in each well, comparing to the blanks in wells 11 and 12 of row G.

#### **2.4.2. Anti-fouling activity**

The anti-fouling activity was performed both as target-based and phenotype-based. As target-based, the enzyme butyrylcholinesterase was used as target; as a phenotype-based, mussel larva of the species *mytilus galloprovincialis* was evaluated. This assay was performed by Dr Isabel Cunha at CIIMAR (Centro Interdisciplinar de Investigação Marinha e Ambiental), in Porto. The experimental procedure for this experiment is described in Almeida *et al.*, 2015.

#### **2.5. Structure elucidation**

The structure of the purified compounds was elucidated by the combination of a multitude of spectroscopic methods, including Nuclear Magnetic Resonance Spectroscopy (NMR), Infra-red Spectroscopy (IR) and non-spectroscopic methods such as Optical rotation (OR).

##### **2.5.1. NMR**

The spectra were acquired on a Bruker Advance 400 MHz, with the samples dissolved in deuterated chloroform ( $\text{CDCl}_3$ ; Cambridge Isotope Labs, 99.8%). The spectra were recorded for one-dimensional (1D) experiments with the nuclei  $^1\text{H}$  (at 400.13 MHz) and  $^{13}\text{C}$  (at 100.61 MHz), with Distortionless Enhancement by Polarization Transfer 90 (DEPT 90) and Distortionless Enhancement by Polarization Transfer 135 (DEPT 135), and for two-dimensional (2D) experiments Correlated Spectroscopy (COSY), Heteronuclear Single Quantum Correlation (HSQC), edited HSQC, Heteronuclear Magnetic Resonance (HMBC), and Total Correlated Spectroscopy (TOCSY).

##### **2.5.2. Infra-red**

The spectra were acquired on a Perkin Elmer Spectrum Two, with the samples dissolved in chloroform ( $\text{CHCl}_3$ ; Carlo Erba Reagents, 99%). The spectra were recorded in sodium chloride ( $\text{NaCl}$ ) cells.

##### **2.5.3. Optical rotation**

The optical activity of the purified compounds was assed using Bellingham+Stanley, model ADP410 Polarimeter, equipped with a sodium lamp. The samples were measured on a cell with 2 ml volume of capacity and 5 dm of optical path length. The experiment was carried out at room temperature.

#### 2.5.4. Structure elucidation data

Content removed due to confidentiality

**PTM-99-(F4-F7)-F30:** orange-colored powder with a mass of 6.16 mg;  $UV_{\max}$ : 194.2 nm;  $R_T$ : 60.4 min;  $[\alpha]^{26}_D = -123.37$  (0.308g/100 ml;  $CHCl_3$ );  $^1H$  NMR (400 MHz,  $CDCl_3$ )  $\delta$  ppm = 0.96 (3H, d,  $J = 6.60$  Hz, H13), 1.01 (3H, d,  $J = 6.60$  Hz, H12), 1.53 (1H, ddd,  $J = 14.43, 9.48, 4.95$  Hz, H10), 1.76 (1H, m, H11), 1.91 (1H, m, H8), 2.04 (2H, m, H8, H10), 2.13 (1H, m, H9a), 2.36 (1H, dtd,  $J = 12.90, 6.69, 2.93$ , H9b), 3.57 (2H, m, H7), 4.02 (1H, dd,  $J = 9.17, 2.45$ , H5), 4.13 (1H, t,  $J = 8.01$ , H2), 6.01 (1H, br. s, H3);  $^{13}C$  NMR (101 MHz,  $CDCl_3$ )  $\delta$  ppm = 21.17 (C13), 22.72 (C8), 23.27 (C12), 24.68 (C11), 28.09 (C9), 38.57 (C10), 45.49 (C7), 53.38 (C5), 58.96 (C2), 166.13 (C4), 170.23 (C1); FT-IR: 3259.25, 2956.43, 2872.57, 1675.26, 1637.99, 1470.28, 1433.01, 1302.56  $cm^{-1}$ .

**PTM-99-(F4-F7)-F34:** orange-colored oil with a mass of 4.38 mg;  $UV_{\max}$ : 210, 242.2, 298 nm;  $R_T$ : 70.1 min;  $[\alpha]^{26}_D = -45.66$  (0.219g/100 ml; MeOH);  $^1H$  NMR (400 MHz,  $CDCl_3$ )  $\delta$  ppm = 1.93 (1H, dd,  $J = 16.87, 7.34$  Hz, H4), 2.02 (2H, m, H4, H5), 2.34 (1H, m, H5), 2.80 (1H, dd,  $J = 14.31, 10.64$  Hz, H10), 3.57 (1H, m, H3, H10), 3.66 (1H, m, H3), 4.09 (1H, t,  $J = 7.27$  Hz, H6), 4.28 (1H, dd,  $J = 10.96, 9.28$  Hz, H9), 7.24 (2H,  $J = 6.97$  Hz, H3', H5'), 7.30 (1H, d,  $J = 7.09$  Hz, H4'), 7.35 (2H, d,  $J = 7.46$  Hz, H2', H6');  $^{13}C$  NMR (101 MHz,  $CDCl_3$ )  $\delta$  ppm = 22.52 (C4), 28.33 (C3), 36.77 (C10), 45.45 (C5), 56.18 (C9), 59.12 (C6), 127.55 (C4'), 129.10 (C3', C5'), 129.26 (C2', C6'), 135.87 (C1'), 165.05 (C1), 169.44 (C7); FT-IR: 3235.96, 3030.97, 2970.41, 2886.55, 1665.94, 1502.89, 1437.66, 1344.49, 1228.02, 1116.21, 1004.40, 752.82, 701.57, 664.30, 482.61  $cm^{-1}$ .

## ***Results and discussion 3***





### 3. RESULTS AND DISCUSSION

#### 3.1. Fractionation of the crude extract

Two *Salinispora arenicola* PTM-99 cultures were prepared: a 7 days (7D) culture and a 14 days (14D) culture. The 2<sup>nd</sup> culture was prepared to obtain higher amount of compounds for structure elucidation. However, due to the slow growth of the bacteria, it took 14 days for the bacteria to grow to a proper density for extraction. Here will be reported data from both cultures since they were used for different experiments.

The extraction of metabolites from the 7D culture yielded a dry mass of crude of 397.01 mg and the 14D culture yielded 894.65 mg of crude. The extraction was followed by fractionation of the crude.

The step of fractionation is of considerable importance as it helps eliminating salts, lipids and other contaminants that may interfere in the bioassay, by both masking the activity or providing false positive. In Dr. Gaudêncio's lab the fractionation method of choice is flash chromatography and results in 9 fractions (Figure 3.1). The procedure is an adaptation of Still *et al.* (1978)'s method. For the mass of crude of 14D, which falls in the range of 900 mg mass, a 30 mm column is used and the crude is eluted with 400 ml of eluent. The fractions are eluted in an increasing polarity of the eluent, resulting in the fraction 9 (F9) being the most polar in contrast to the fraction 1 (F1) which is least polar (Table 3.1). In fact, after dried, the fractions with lower polarity presented an oily consistency.

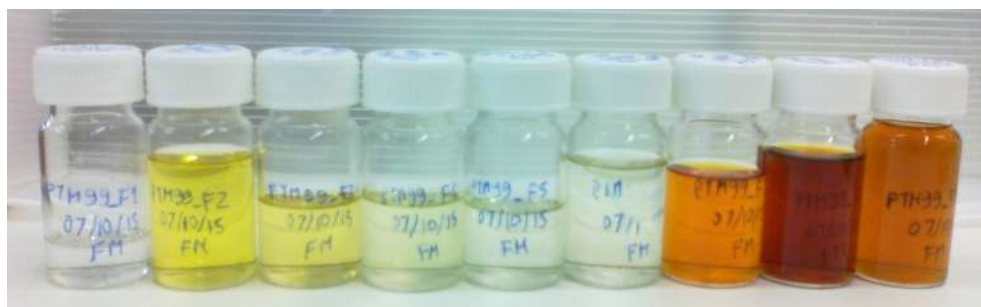


**Figure 3.1.** Fractions of the strain *S. arenicola* PTM-99 obtained by flash chromatography of the crude. Fraction F1 to F9, from the left to the right. The samples may be light-sensitive.

**Table 3.1.** Mass of fractions derived from crude fractionation of the 14D culture.

Fraction	Mass (mg)
F1	20.70
F2	53.44
F3	29.62
F4	23.68
F5	24.73
F6	23.59
F7	87.88
F8	208.78
F9	186.32

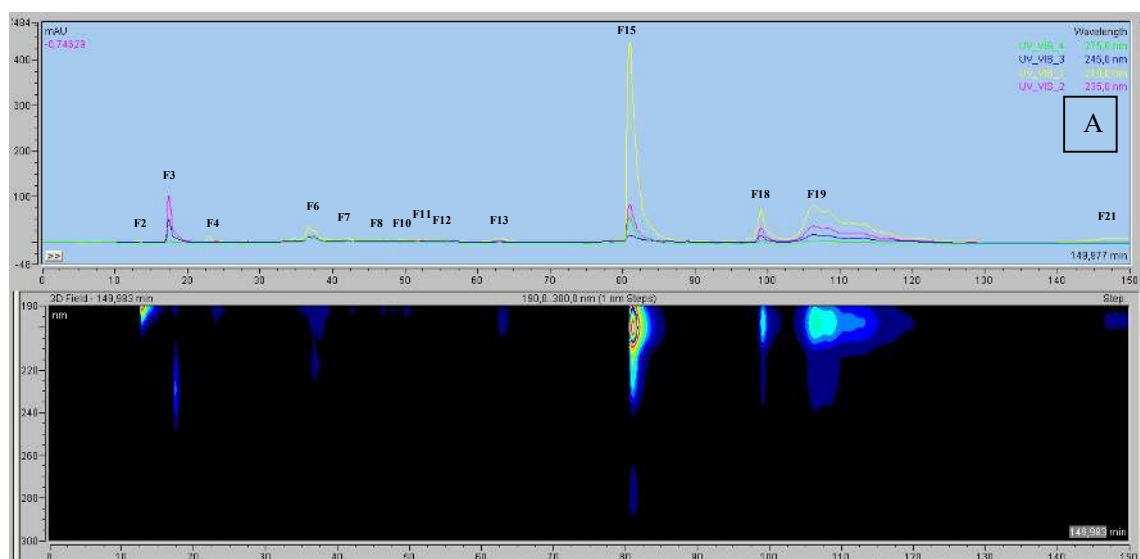
### 3.2. Isolation of compounds by HPLC and bioassays

The fractions were selected for purification according to the results of antimicrobial and antifouling assays, determined previously to this work. The fractions which displayed antimicrobial activity were the fractions F2 (31.25 µg/ml against MRSA; 62.50 µg/ml against VRE), F4 (250 µg/ml against both MRSA and VRE), F7 and F8 (both 125 µg/ml against VRE). In a first phase of optimization (7D), due to low mass yield, similarity between UV profiles of some fractions and interesting activity against butyrylcholinesterase, it was decided that the fractions from F4 to F7 should be mixed together, as well as fractions F8 and F9 with one another. The fraction F2 was dissolved in tetrahydrofuran (THF), and the fractions F4-F7 and F8-F9 were dissolved in MeOH. This setup was maintained in the next isolation (14D) (see Tables 2.3, 2.4 and 2.5).

#### 3.2.1. Fraction F2

From the 7D culture, 15 compounds were isolated; and from the 14D culture, 26 compounds were isolated.

The comparative analysis of the chromatogram revealed an overall increase in the production, in the 14D culture, of the compounds tested for antimicrobial activity; however there was also an increase in the production of compounds, which were not observed in the culture 7A (Figure 3.2).



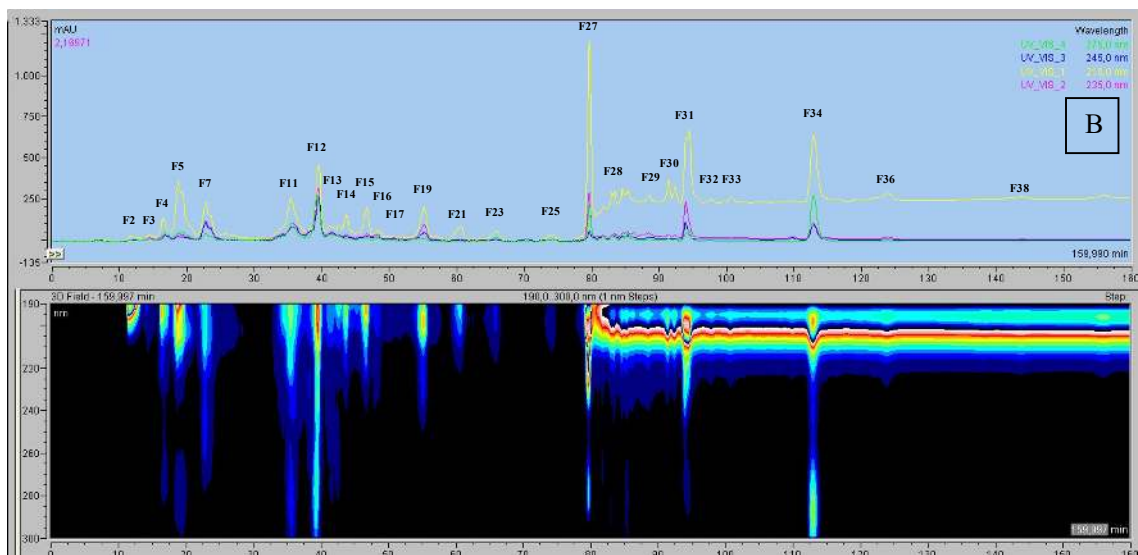


**Figure 3.2. Chromatogram with 3D field (190 – 300 nm) of the crude fraction F2.** A - fraction F2 from a 7D culture; B - fraction F2 from a 14D culture.

The analysis of the UV profile of the isolated compounds led to the finding that the compounds F13, F15, F17, F18 and F21 of the 7D culture may belong to the same family due to the similar UV absorption. The same analysis to the compounds F4, F14, F16, F19, F25, F27, F28, F29, F30, F31, F33, F36 and F38 of the 14D culture, also puts these compounds in the same family (Figure 3.3). In fact, this family constitutes the major class of compounds isolated during this project. The characteristic UV spectra resemble those of peptides, with the two peaks at approximately 220 and 280 nm being characteristic of peptide bond and aromatic group, respectively. Furthermore, the spectra also resemble those of the lactam core (cyclic amide) present in the amino acid synthesis-derived class diketopiperazines and the esterification-derived lactone core (cyclic ester) of macrolides. Finally, the peak at approximately 190 nm is characteristic of diketopiperazines (UNODC, 2013; Rahimi *et al.*, 2016), although this statement is very controversial since this region is known to be one where several other molecules can absorb. However, the results of structural elucidation indicate the occurrence of both diketopiperazine and macrolide classes.

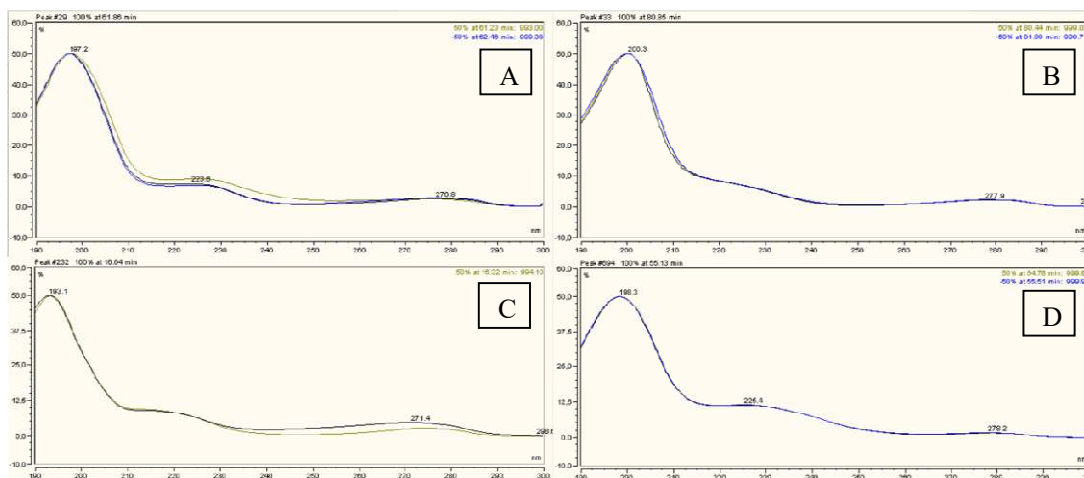


**Figure 3.3.** UV profile of compounds isolated from fraction F2. The compounds presented three peaks from 190 and 280 nm, characteristic of peptides. A and B correspond to the compounds F13 and F15 of the 7D culture; C and D correspond to the compounds F4 and F19 of the 14D culture.

The tested compounds did not present any relevant antimicrobial activity. Nevertheless, it is worth pointing out the MIC of 62.5  $\mu\text{g/ml}$  against VRE EF82 of compounds F2 and F15; F15 was also the only one presenting any activity against MRSA COL (MIC 250  $\mu\text{g/ml}$ ) (Table 3.2). Therefore, the decision about the structural elucidation step was based primarily on the UV spectra and the mass availability for the NMR experiments. The compounds F27 of the 14D culture, which is the equivalent of F15 of the 7D culture, and the compound F31 of the 14D culture, proceeded to the structural elucidation phase. Furthermore, since the results for 7D culture were low, it was decided that the 14D culture should not be tested and that the bioassay focus should be shifted towards the antifouling assay against butyrylcholinesterase.

**Table 3.2.** Mass yield and antimicrobial activity (MIC) of compounds isolated from fraction F2, from a 7 days culture.

Compound	R <sub>T</sub> (min)	Mass (mg)	MRSA COL ( $\mu\text{g/ml}$ )	VRE EF82 ( $\mu\text{g/ml}$ )
F2	12.9	0.66	n.a.	62.5
F3	17.2	0.57	n.a.	125
F4	22.8	0.59	n.a.	n.a.
F6	33	0.69	n.a.	125
F7	40.8	0.36	n.a.	250
F8	44.6	0.4	n.a.	n.a.
F10	49.2	0.27	n.a.	n.a.
F11	51.3	0.53	n.a.	n.a.
F12	54.3	0.51	n.a.	250
F13	59.7	0.46	n.a.	n.a.
F15	77.2	3.02	250	62.5
F18	97.6	3.77	n.a.	250
F19	102.9	10.84	n.a.	250
F21	133.1	14.46	n.a.	n.a.

n.a. – not active; “-” – not tested

### 3.2.2. Fraction F4-F7

From the 7D culture, 19 compounds were isolated; and from the 14D culture, 30 compounds were isolated (Figure 3.4).

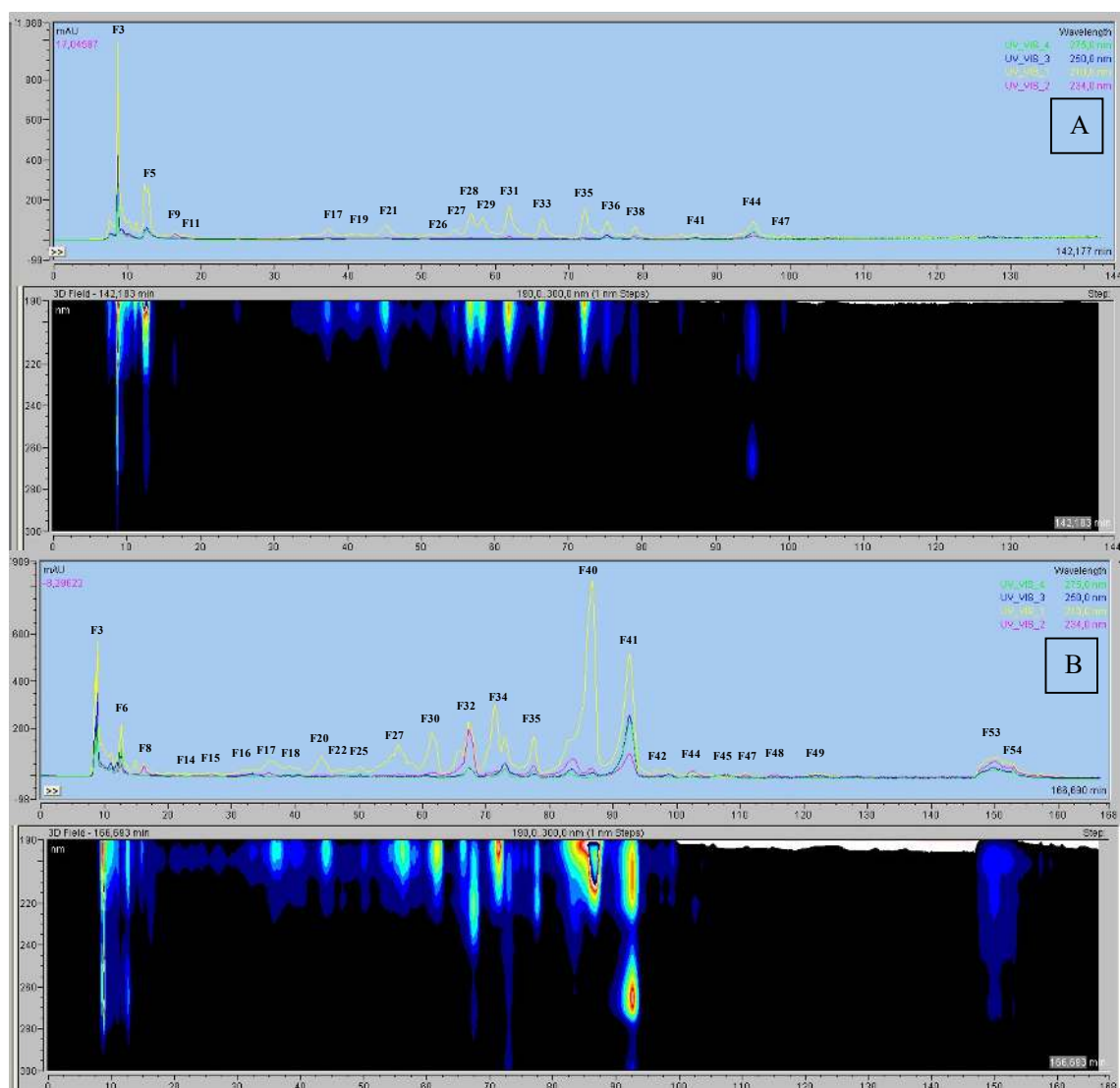


**Figure 3.4. Chromatogram with 3D field (190 – 300 nm) of the crude fraction F4-F7. A - fraction F4-F7 from a 7D culture; B - fraction F4-F7 from a 14D culture.**

For this fraction, the majority of the isolated compounds also presented a UV profile similar to that of the compounds of the above mentioned F2 fraction, indicating that they belong to the same family. Aside from those, other three compounds (F36, F41 and F44) presented very distinguishable UV spectra (Figure 3.5). The peak at 205.9 nm represents a region where many molecules can absorb.

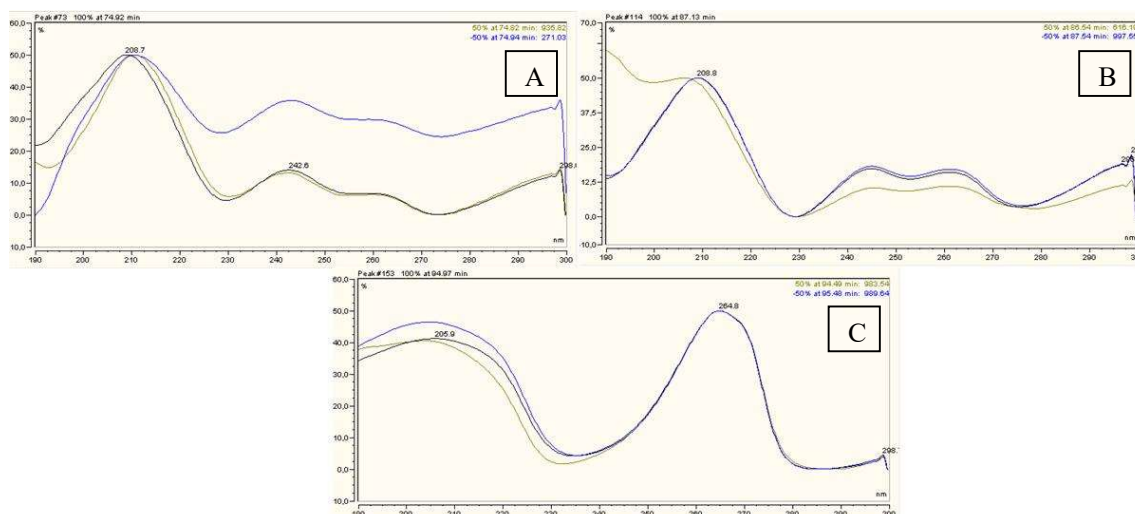


**Figure 3.5. UV profile of compounds isolated from fraction F4-F7.** The compounds A, B, and C correspond to the compounds F36, F41 and F44 of the 7D culture.

This fraction fared no better than the fraction F2 in the antimicrobial assay. No compound was found to present activity against both MRSA and VRE simultaneously. The compounds found to present some activity were F5 (MIC of 250  $\mu\text{g/ml}$  against VRE), F17 (MIC of 250  $\mu\text{g/ml}$  against MRSA), F38, F41 and F44 (all with MIC of 125  $\mu\text{g/ml}$  against VRE) (Table 3.3).

**Table 3.3. Yield and antimicrobial activity (MIC) of compounds isolated from fraction F4-F7, from a 7 days culture.**

Compound	R <sub>T</sub> (min)	Mass (mg)	MRSA COL ( $\mu\text{g/ml}$ )	VRE EF82 ( $\mu\text{g/ml}$ )
F3	8.6	6.55	n.a.	n.a.
F5	11.1	6.98	n.a.	250
F9	16.5	2.03	n.a.	n.a.
F11	17.7	0.62	n.a.	n.a.
F17	36.5	1.15	250	n.a.
F19	40.5	1.34	n.a.	n.a.
F21	44.3	2.24	n.a.	n.a.
F26	52	0.89	-	-
F27	53.4	1	-	-
F28	54.7	4.22	n.a.	n.a.
F29	58.4	1.55	-	-
F31	60.8	5.08	n.a.	n.a.
F33	66.1	1.27	n.a.	n.a.
F35	70.7	3.18	n.a.	n.a.
F36	74.6	1.81	n.a.	n.a.
F38	78.9	0.68	n.a.	125
F41	84.5	1.33	n.a.	125
F44	94.3	1.36	n.a.	125
F47	99.2	0.94	-	-

n.a. – not active; “-” – not tested

In a first approach to structural elucidation, the compounds presenting activity and/or enough mass were submitted to NMR experiments. Unfortunately, due to the overall negative results for the anti-fouling activity it was hypothesized that the samples were degraded. This degradation could be due to the fact that in some point the isolated compounds could have been exposed to light, which could have led to its degradation since the metabolites may be light sensitive, or the harsh treatment endured by the compounds during the phase of optimization of the HPLC program (evaporation, lyophilization) could be also responsible.

Nevertheless, samples were selected for structural elucidation since the fact of the studied strain a first time isolate from Portuguese waters, brings the prospect of discovering novel compounds. The compounds that proceeded to the structural elucidation were F20, F27, F30, F34 (=F35, 7D) and F41 from the 14D culture.



### 3.2.3. Fraction F8-F9

From the 7D culture, 18 compounds were isolated; and from the 14D culture, 26 compounds were isolated (Figure 3.6).

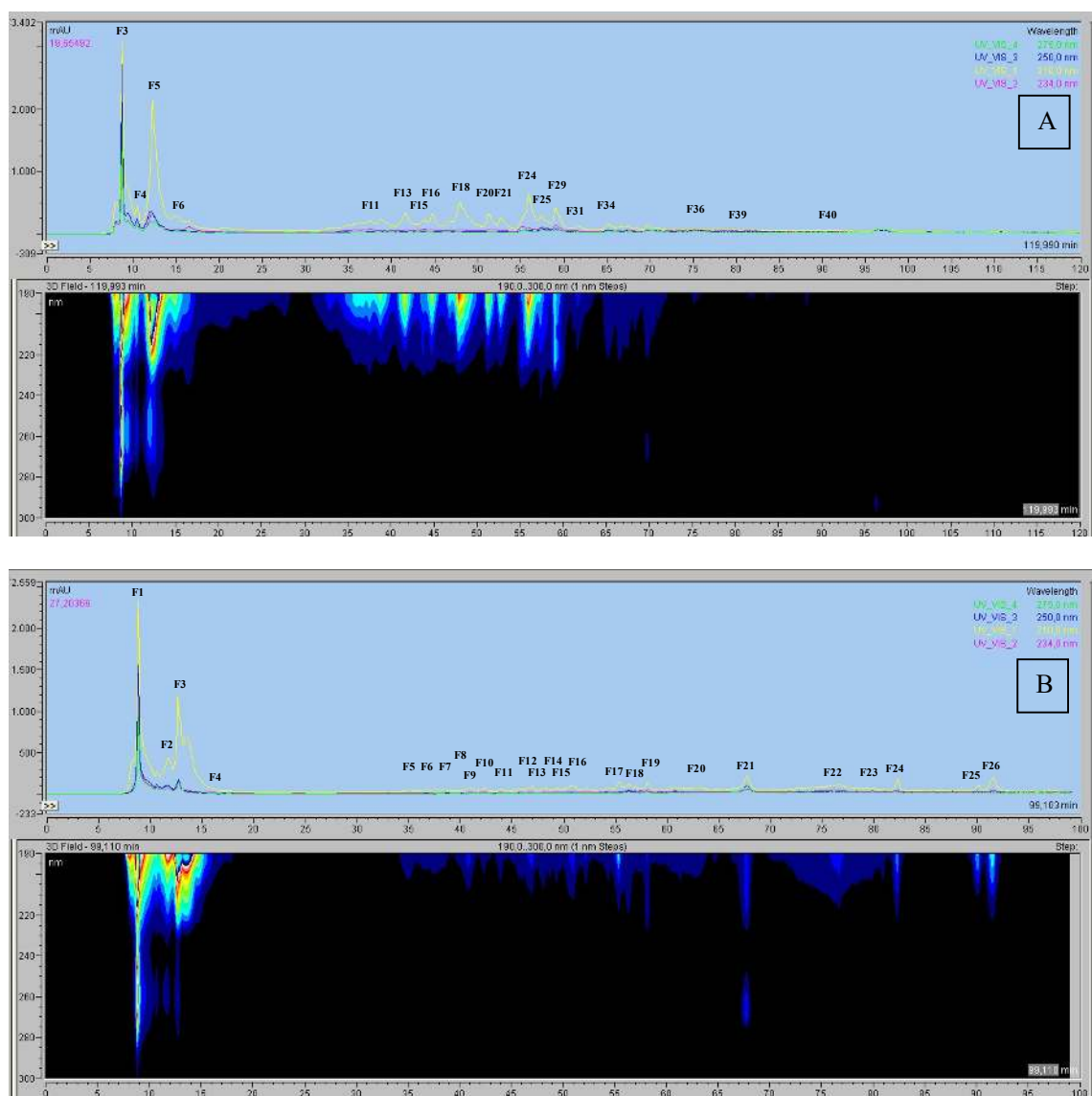


**Figure 3.6. Chromatogram with 3D field (190 – 300 nm) of the crude fraction F8-F9. A - fraction F8-F9 from a 7D culture; B - fraction F8-F9 from a 14D culture.**

The mass yield of this fraction for the 14D culture was so low for individual observable compounds in the 3D field that it was discarded after three HPLC runs. The peaks were discerned by analyzing the 3D field of the chromatogram. However, it was enough to obtain the overall picture of the UV profile of the compounds present in the sample. Once more, the family mentioned above persisted as the major component. For this fraction, to the similarity of fraction F4-F7, there were some interesting exceptions (Figure 3.7).

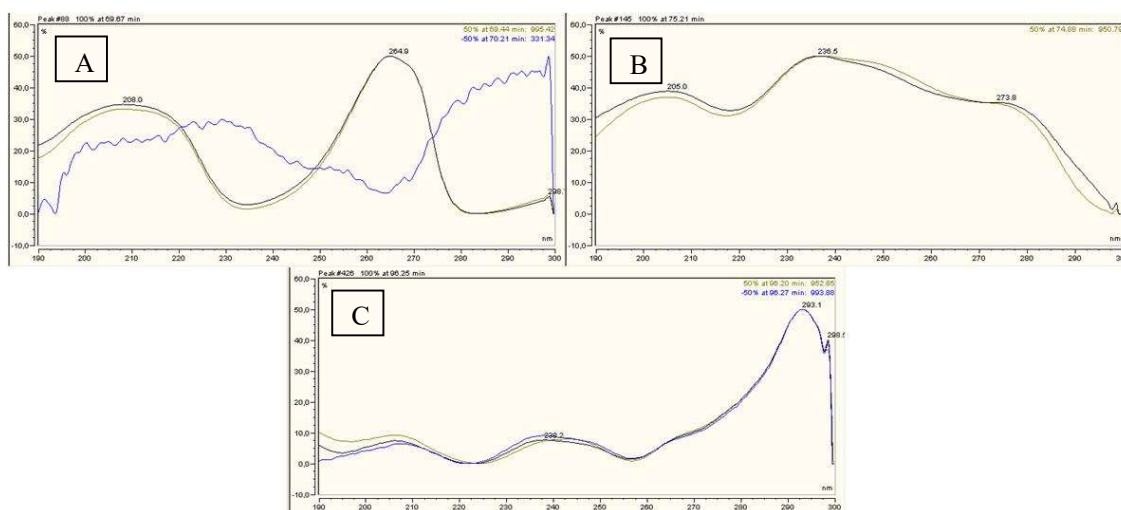


**Figure 3.7.** UV profile of compounds isolated from fraction F8-F9. The compounds A, B, and C correspond to the compounds F34, F36 and F40 of the 7D culture.

The similarity between the UV profile of compounds F34 of fraction F8-F9 and F44 of fraction F4-F7 suggest they belong to the same family. The compounds F36 and F40 also present absorbance in the region of peptides, but they clearly belong to different families than the ones referred so far.

Following the pattern of the activities of the compounds of the previous fractions, the fraction F8-F9 yielded bioactive compounds, but no remarkable activity was observed. Only one compound presented activity against both target pathogenic microbe – F39, with MIC of 125 µg/ml against MRSA and 250 µg/ml against VRE. The compounds F20, F21, F24 and F29 displayed activity against MRSA, with a MIC of 250 µg/ml, and the compound F3 inhibited VRE growth with a MIC of 250 µg/ml (Table 3.4). Once again, these results were not surprising, since the fraction F8 itself displayed no remarkable activity against the targeted strains.

**Table 3.4.** Yield and antimicrobial activity (MIC) of compounds isolated from fraction F8-F9, from a 7 days culture.

Fraction	R <sub>T</sub> (min)	Mass (mg)	MRSA COL (µg/ml)	VRE EF82 (µg/ml)
F3	8.5	31.85	n.a.	250
F4	10.4	1.98	n.a.	n.a.
F5	11	10.83	n.a.	n.a.
F6	14.6	2.76	n.a.	n.a.
F11	34.6	4.04	n.a.	n.a.
F13	40.9	3.59	n.a.	n.a.
F15	43.4	2.56	250	n.a.
F16	45.6	1.6	-	-
F18	47.4	5.22	n.a.	n.a.
F20	50.7	2.28	250	n.a.
F21	52.2	1.67	250	n.a.
F24	54.9	4.73	250	n.a.
F25	57.3	1.26	-	-
F29	59	1.05	250	n.a.

<b>F31</b>	60.1	1.24	-	-
<b>F34</b>	63.8	5.41	-	-
<b>F36</b>	75	1.51	-	-
<b>F39</b>	80.3	1.32	125	250
<b>F40</b>	93	2.01	-	-

n.a. – not active; “-” – not tested

### 3.2.3. Antifouling assay

Preliminary antifouling assays against the enzyme butyrylcholinesterase yielded an inhibition of 57.33% for the crude, and over 90% for fractions F4 to F7.

Unfortunately, the assays using pure compound samples from the fraction F4-F7 of the 7D culture yielded no inhibitory activity. This negative result may result from degraded samples or ill procedure during the assay. A new set of sample was prepared and sent for testing. As of the time of writing of this thesis, the results have not yet been received.

### 3.3. Structure elucidation

The structure of the isolated compounds was determined by combining a multitude of information from different spectroscopic and non-spectroscopic methods. At present time, NMR constitutes the go-to method for unraveling the structure of natural products. The method relies on the interaction between electromagnetic radiation in the radio frequency and a magnetic nucleus, and the chemical shift produced by it. In this present work we analyze the nucleus  $^1\text{H}$  (at 400 MHz) and  $^{13}\text{C}$  (at 101 MHz), in 1D and 2D experiments.

#### 3.3.1. PTM-99-(F2)-F27 and PTM-99-(F2)-F31

Due to the structural similarities between the compounds PTM-99-(F2)-F27 and PTM-99-(F2)-F31, the analysis of the spectroscopic data and subsequent structural elucidation will be performed in a parallel fashion. The narrative of the analysis will be relative to compound PTM-99-(F2)-F27, since it was the first to be worked with. The two compounds were identified primarily as macrolides due to the resemblance of the UV (Figure 3.8) and  $^1\text{H}$  NMR data with a macrolide previously identified by the lab (Paulino, 2016). The comparison of the  $^1\text{H}$  NMR and HMBC spectra indicated that the two compounds possessed a high degree of matching identity (Figure 3.9). However, the structural elucidation of compound PTM-99-(F2)-F31 proved particularly challenging due to the complexity of the data obtained by NMR.

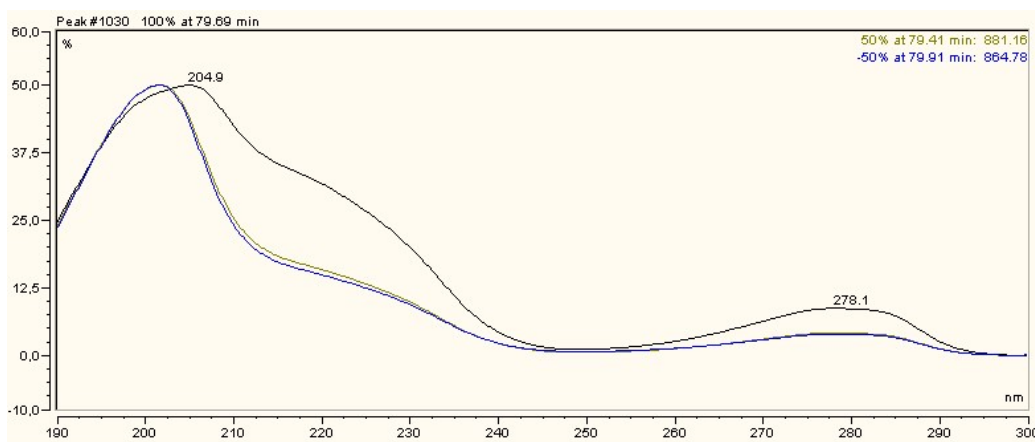
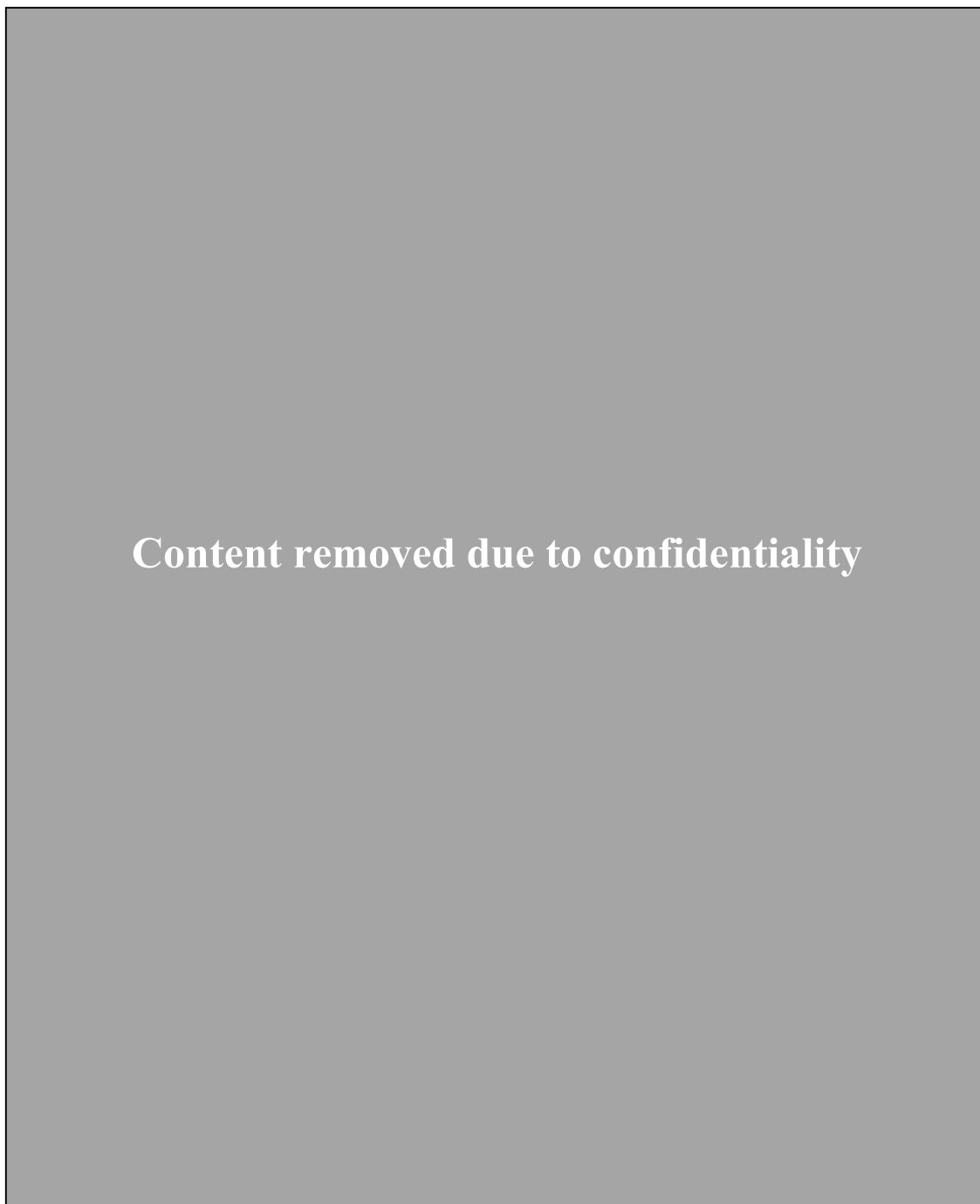


Figure 3.8. UV profile of compound PTM-99-(F2)-F27.

The analysis of the HSQC-DEPT (edited-HSQC) data of compound PTM-99-(F2)-F27, assigned the multiplet (distorted triplet) at 0.88 ppm to a carbon peak at 14.12 ppm; this analysis also revealed that this signal belongs to a methyl group. Adjacently, an intense multiplet signal in the region of 1.28 ppm, whose integral corresponding to 26 protons, was matched to several secondary methyl signals in the region of 22-31 ppm. These signals hinted at the existence of a long saturated chain, which is typical of macrolide molecules. However, the multiplet at 5.35 ppm (H26, H27) was linked to the carbon signals at 127-130 ppm, which were found to be CH carbon atoms. The correlation of these carbons to the protons attached to the carbons at 25.63 (C25), 27.2 ppm (C28) and the rest of the chain downfield in HMBC, led to the deduction of the existence of a double bond between the

carbons at 127-130 ppm Furthermore, the triplet at 2.77 (H25) does not couple or correlated with any other signal than those of H26, H27 and C26, C27 (Figure 3.10).



**Figure 3.9.**  $^1\text{H}$  NMR and HMBC spectra of compounds PTM-99-(F2)-F27 (A) and PTM-99-(F2)-F31 (B). The similarity are as follows in  $^1\text{H}$  NMR spectrum (order: A (B)): 0.88 (0.89), 1.28 (1.32), 1.61 (1.61), 2.03 (2.04), 2.30 (2.32), 4.14 (4.15), 4.29 (4.30), 5.26 (5.27), 5.35 (5.36) ppm. The signal present at 3.99 ppm in the spectrum of compound PTM-99-(F2)-F31 is absent in that of the compound PTM-99-(F2)-27. Moreover, the signal present at 6.98 ppm in the spectrum of compound PTM-99-(F2)-27 is absent in that of the compound PTM-99-(F2)-F31.

The proximity of the multiple carbon signals in the region of 127-130 ppm makes it tempting to hypothesize the existence of conjugated alkene groups, a common feature in macrolides, more so, with the value of proton integration indicating the existence of three of those.

Content removed due to confidentiality

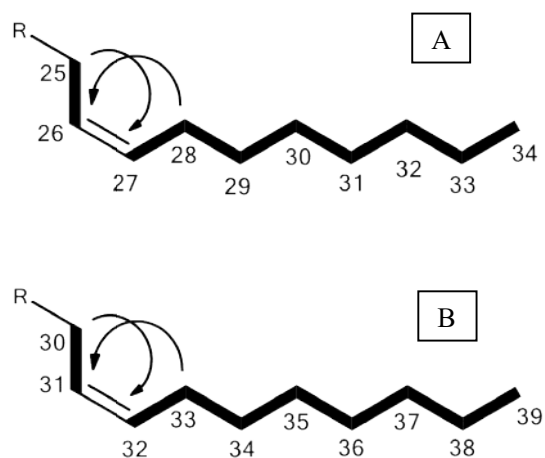


**Figure 3.10. NMR data and proposed alkene astructure for the corresponding section.**  $^{13}\text{C}$  NMR full spectrum. TOCSY (upper right) and HMBC (upper left). Inclosed  $^1\text{H}$  NMR chemical shifts at 0.88, 1.28, 2.03 and 2.77 ppm. Structures: A: PTM-99-(F2)-F27, B: PTM-99-(F2)-F31. Full black bars indicate COSY coupling, black arrows indicate HMBC correlation.

The proton corresponding to the multiplet at 1.61 ppm (H3, H14) is coupled with neighboring protons at 1.28 (H4-H6, H11-H13) and 2.30 (H2, H15) in COSY, and correlates in HMBC with the closely spatially related carbons at the regions of 29.13 to 29.77 (C4-C6, C11-C13), 34.04 to 34.2 (C2, C15) and to the quaternary carbon signals at 172.86 (C24) and 173.27 (C1, C16, qC1, qC2). Among the two sets of neighboring protons, the one at the chemical shift of 2.30 were the only ones presenting a (strong) correlation with the quaternary carbons. These observations allowed for the deduction of a second alkene chain being this one symmetrical with the double bond occupying the center of the chain (Figure 3.11).

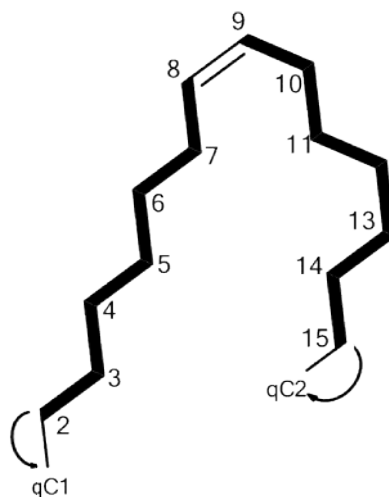


**Figure 3.11. Symmetrical alkene chain.** Full black bars indicate COSY coupling, black arrows indicate HMBC correlation.

The  $^{13}\text{C}$  NMR spectrum displayed signals of quaternary carbons with characteristics of amide's and ester's carbonyl group (172.86 and 173.27 ppm). The signal at 173.27 ppm displayed double the intensity of the signal at 172.86 ppm, leading to the deduction of the presence of two equivalent groups. The absence of labile proton indicates that the amide is most likely tertiary, in case the structure is found to be of such composition. To validate this observation in the proposed structure, the methine carbon at 125.52 ppm (C22, C23) was set as a bridge linking to the amide's carbonyl on both sides of the alkene chain. Despite the protons H22, H23 (6.98 ppm) showing no correlation in HMBC to the quaternary carbons, it was still considered as the best fit since it displayed HMB correlation to the C2, C15 carbons and to its own carbon, placing it both in the vicinity and indicating the existence of overlapping signals of equal chemical shift (Figure 3.12).

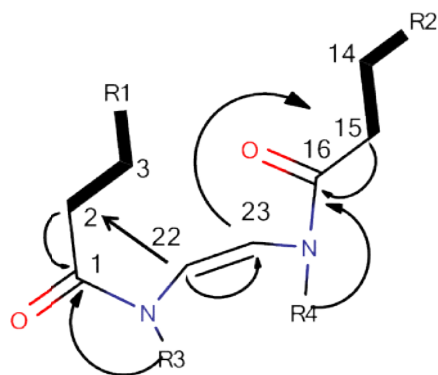


**Figure 3.12.** The carbon at 125.52 ppm closes the alkene chain forming a macrocyclic ring. Full black bars indicate COSY coupling, black arrows indicate HMBC correlation.

Finally, the analysis of the HSQC-DEPT and HMBC, attributed the duplet at 5.26 ppm to a CH group (C19, 68.88 ppm), that is coupled only with the two sets of double doublets H18, H20 (COSY), and correlates to the quaternary carbon at 172.86 ppm. On the other hand, the CH<sub>2</sub> protons only coupled with H19 and with each other, and correlated to the quaternary carbons. The interpretation of these results resulted in the deduction of a second, smaller, ring coupled to the macrocyclic ring (Figure 3.13).

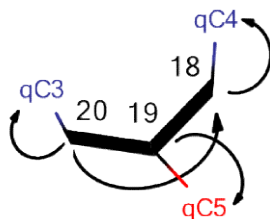


**Figure 3.13.** CH group at 68.88 ppm forms the bridge connecting two ends of a cyclic structure. Full black bars indicate COSY coupling, black arrows indicate HMBC correlation.



Content removed due to confidentiality

**Figure 3.14. Macrocyclic ring composed of quaternary carbons of ester and amide groups proposed for compound PTM-99-(F2)-F27.** Full black bars indicate COSY coupling, black arrows indicate HMBC correlation.

The similarities between the two compounds diminish as the analysis of the two compounds moves downfield in the spectra; however, there is still a punctual difference at the beginning of the spectra. The HSQC-DEPT spectra of compound PTM-99-(F2)-F31 links the proton signal at 0.89 ppm to three carbon signals (one isolated carbon at 10.98 ppm and three overlapped carbons in the region of 14.04 to 14.12 ppm), suggesting the existence of four methyl groups. The COSY spectra indicated the coupling of the methyl protons with the secondary methyl protons at 1.32 ppm; and the TOCSY revealed that the coupling was extended to three other secondary methyl protons at 1.61, 2.04 and 3.99 ppm. Probing of the full set of two-dimensional NMR experiments data indicated the existence of separations in the proton signals, which were designated left (*l*) and right (*r*). Figure 3.15 shows some examples.

Content removed due to confidentiality

**Figure 3.15. Two-dimensional NMR data for proton signal 1.32 illustrating the partitioning of the signal into left (*l*) and right (*r*) side.** The sides couple and correlate with similar signals in different parts of the compound.

The methyl protons correlated in HMBC to the right (*r*) with the carbon signals at 22.58 to 22.97 (C37, C38) and at 30.41 to 31.92 ppm (C34-C36). The proton signal at 2.04 ppm couples, in COSY, with both the secondary methyl proton H34 and the olefinic proton at 5.36 ppm, and in HMBC correlates to the left (*l*) with the olefinic carbons at 127.9 and 128.07 (C8, C9, C31, C32), and to the right (*r*) with those at 129.69 to 130.24 ppm (C8, C9, C31, C32). Similarly to the compound PTM-99-(F2)-F27, the lack of correlation between the proton signal at 1.61 ppm and the olefinic carbons (C31, C32), and the lack of any other correlation between the signal at 2.78 (H30) aside from those with the olefinic carbons, allowed for the deduction of the alkene chain presented in Figure 3.10, B.

An alkene chain similar to that presented in Figure 3.11 was also deduced for compound PTM-99-(F2)-F31, with the length of the chain possibly differing due to the difference in the number of carbons to be assigned (the integration of the peak at 1.32 ppm suggests 33 protons).

The proton singlet at 1.61 ppm was found to interact with neighboring protons at 2.32 ppm and 3.99 (H21, H25) ppm in COSY, and correlating in HMBC with the carbons at 34.2 (C28, C30) and 66.81 ppm (C26). The protons at 3.99 and 1.6 ppm correlate with the carbon signal at 23.79 ppm (C23, C23', C27 and C27'), providing a link for a new chain, which culminates in a methyl group probably the chemical shift of 10.98 ppm (C24, C24', C28, C28'). This observation allowed the deduction of a 2-ethyl-1-butyl group (Figure 3.16). The HMBC spectrum suggests this group was linked to a quaternary carbon by the carbon qC3.

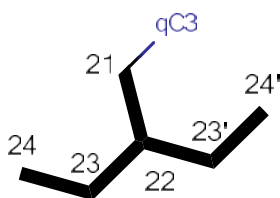


**Figure 3.16. 2-Ethyl-1-butyl substituent.** Full black bars indicate COSY coupling, black arrows indicate HMBC correlation.

Finally, at the similarity of compound F27, the  $^{13}\text{C}$  NMR spectrum displayed signals of quaternary carbons that showed characteristics of amide's and ester's carbonyl (172.84, 173.25, 173.54 ppm). The absence of labile proton indicates that the amide is most likely tertiary, in case the structure is found to be of such composition. The analysis of the HSQC-DEPT and HMBC, attributed the multiplet at 5.27 ppm to a CH group (C19, 68.88 ppm) and correlated it to the three, neighboring, quaternary carbons, revealing it to be the center piece giving form to the ring structure (Figure 3.17).

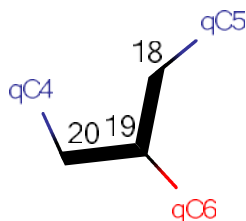


**Figure 3.17. CH group at 68.88 ppm forms the bridge connecting two ends of a cyclic structure.** Full black bars indicate COSY coupling, black arrows indicate HMBC correlation.

The carbons at 34.02 to 34.2 (C2, C15), 62.11 (C18, C20) and 68.88 ppm (C19), and respective protons, were correlated in HMBC and TOCSY with the quaternary carbons to form the ring (Figure 3.18). Whether the macrocyclic motif is a lactam or a lactone, or possesses elements of both, remains to be unraveled.



**Figure 3.18. Macrocyclic ring composed of quaternary carbons of ester and amide groups proposed for compound PTM-99-(F2)-F31.**

At the present moment, we believe the two major structural pieces proposed for both structures (the alkene chain in Figure 3-10 and the macrocyclic ring in Figure 3.14/ Figure 3.18) should connect. The evidence for this comes from the observable TOCSY correlation between the proton signals at 2.77 and 2.30 ppm. However, we were not able to draw forth this link at the light of data currently in our possession. Therefore, structures have not yet been fully elucidated. Another compound isolated in the lab, presented a similar NMR spectra and analysis by mass spectrometry revealed the presence of Cl or Br atoms. The full NMR data for both compounds is shown on Tables 3.5 and 3.6.

The nule values obtained from the measurement of optical rotation for both compounds suggest that the molecules either possess a plane of symmetry or are present as a racemic mixture. Given that the latter case is of extremely low occurrence among natural products, it is supposed that the latter case is more probable. If the case is so – and it does make sense due to the overall high density of CH<sub>2</sub> groups in the NMR spectral data, then it is within reason to deduce the existence of CH<sub>2</sub> chains linked in such fashion that the molecule is rendered symmetrical. The nule result for optical rotation was obtained for all measured compounds of fraction F2 (data not shown), and also obtained for the other macrolide isolated in the lab, mentioned above.

The proposed structures are also supported by IR data. The data for the compound F27 shows an intense signal at  $2928.48\text{ cm}^{-1}$  characteristic of  $\text{sp}^3$  and  $\text{sp}^2$  C-H stretching. The stretching of the C-O in the ester showed at  $1158.14$ , and the carbonyl of the amide group at  $1745.14\text{ cm}^{-1}$ . The signal at  $724.87\text{ cm}^{-1}$  is characteristic of the Cl atom, which could be part of the structure (Figure 3.19).

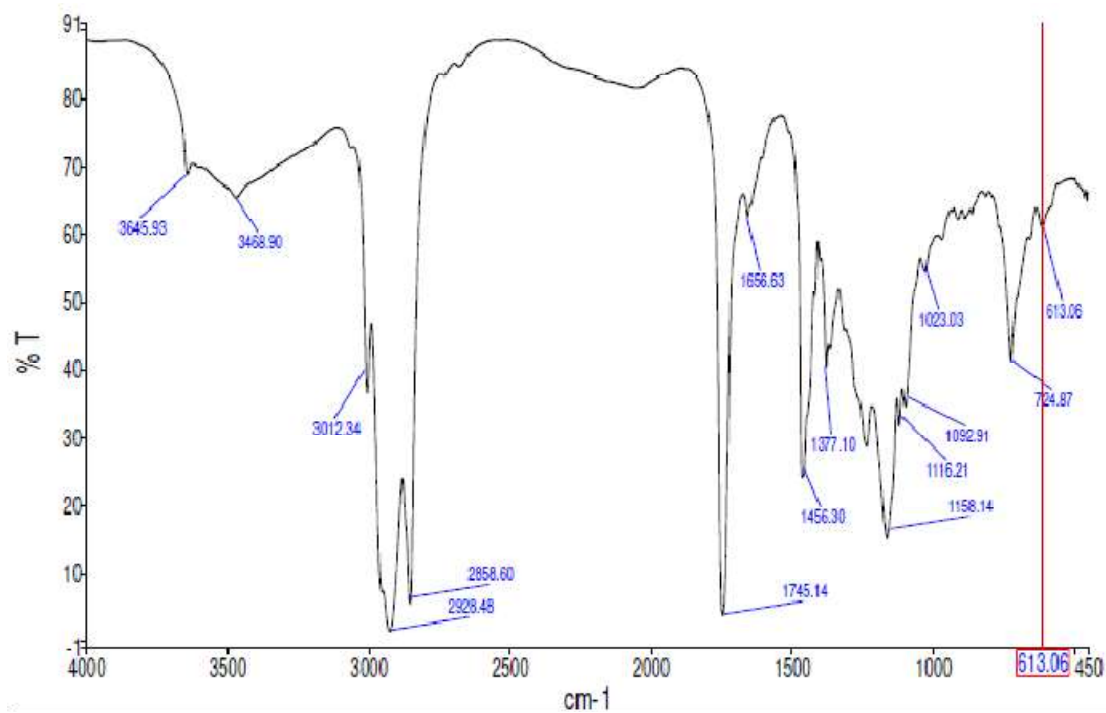


Figure 3.19. IR spectrum of compound PTM-99-(F2)-F27.

**Table 3.5. NMR data for compound PTM-99-(F2)-F27.**

**Content removed due to confidentiality**

NOTE: given that the macrocyclic structure is symmetrical, only the carbon or proton designation from one side of the molecule was considered in order to provide a table which is easy to be read. This applies to both compounds (F27 and F31).

**Table 3.6. NMR data for compound PTM-99-(F2)-F31.**

**Content removed due to confidentiality**

A final remark concerning the structural elucidation of these compounds. The low overlapping of the signals in the NMR spectra produced a certain degree of ambiguity as the signals of members in different spatial and chemical environment could be correlated, yields the prospect of mobility of certain substitute group either by total displacement or a sort of bending. Such case applies to the 2-Ethyl-1-butyl whose HMBC and TOCSY correlations hinted at a circular structure involving the alkene chain. The proposed structure was found to fit best with the data, after several drafts.

### 3.3.2. PTM-99-(F4-F7)-F30

Although UV profiling is usually a reliable method for purposes of dereplication, unfortunately in this study it did little to help differentiating diketopiperazines and macrolides.

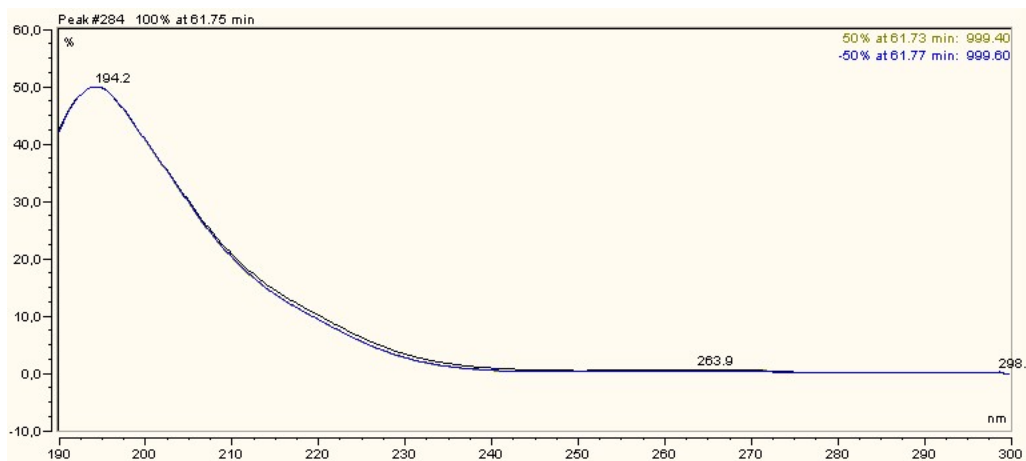


Figure 3.20. UV profile of compound PTM-99-(F4-F7)-F30.

The  $^1\text{H}$  NMR spectrum indicated the presence of two distinct methyl groups at the shifts 0.96 and 1.01 ppm, two CH groups at 4.02 and 4.13 ppm, and a broad singlet at 6.01 ppm, consistent with a labile proton. The analysis of the HSQC-DEPT gave the carbon signals corresponding to the protons indicated above: 21.17, 23.27, 53.38 and 58.96 ppm, respectively, where the two first signals belong to an isobutyl group. Furthermore,  $^{13}\text{C}$  spectra showed signals characteristic of the carbonyl of the amide groups at the shifts 166.13 and 170.23 ppm. The analysis of the HMBC correlations of 4.02 and 6.01 to 166.13, 4.13 ppm to 170.23, and 1.53-2.04 to 166.13 ppm confirmed the diketopiperazine unity. The characteristic methylene multiplets in the shift range of 1.76 to 3.57 ppm (H7, H8, H9, H10 and H11) in the  $^1\text{H}$  NMR spectrum, along with HMBC correlations indicated the presence of a proline alike moiety (Figures 3.21 and 3.22).

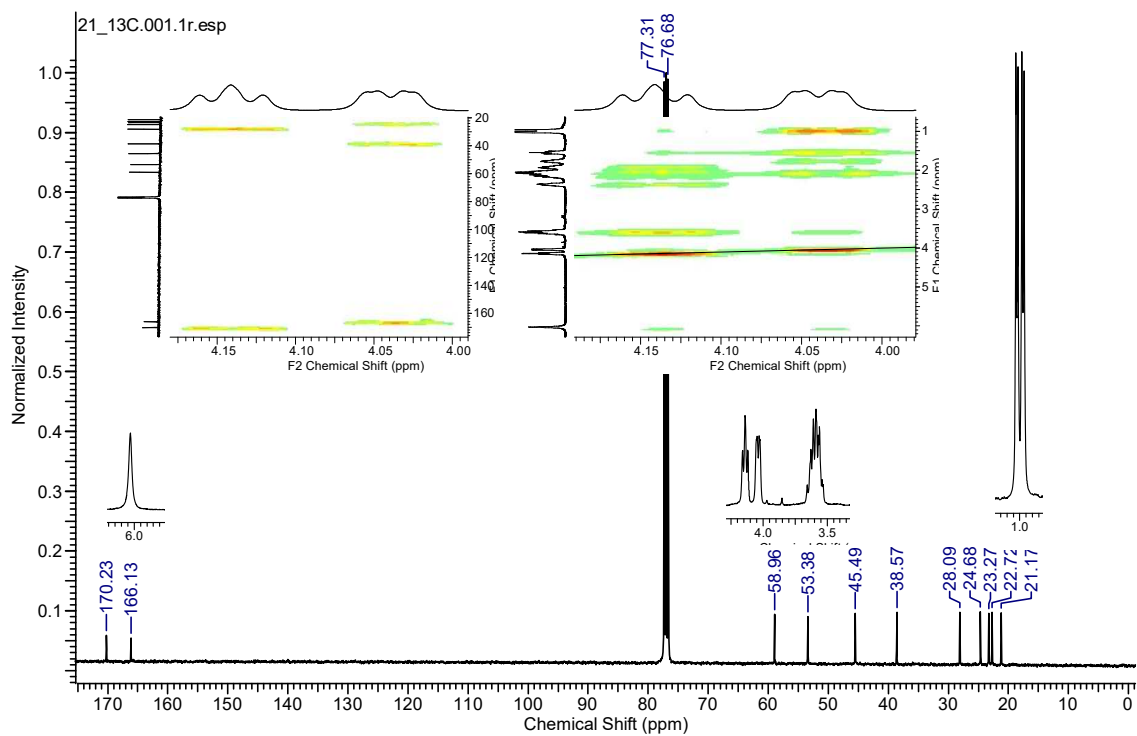


Figure 3.21. NMR data highlighting the lactam core of the diketopiperazine.  $^{13}\text{C}$ ,  $^1\text{H}$ , HMBC (upper left) and TOCSY (upper right).

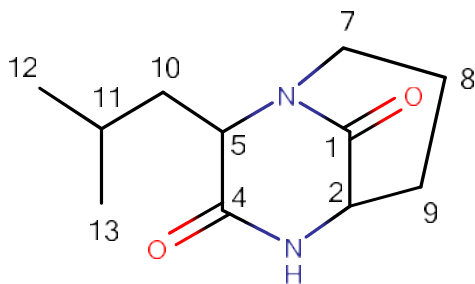


Figure 3.22. Proposed structure for the compound PTM-99-(F4-F7)-F30.



**Table 3.7. NMR data for compound PTM-99-(F4-F7)-F30.**

Position	$\delta_C$ , Type	$\delta_H$ , multiplicity, (J in Hz)	COSY	HMBC	TOCSY
1	170.23, q	-	-	-	-
2	58.96, CH	4.13, t, 8.01	H9	C9, C13	H3, H7, H8, H9, H10, H12, H13
3	-	6.01, s	-	C1	H2, H5
4	166.13, q	-	-	-	-
5	53.38, CH	4.02, dd, 9.17, 2.45	H10	C11, C10, C4	H2, H3, H8, H10, H11, H12, H13
6	-	-	-	-	-
7	45.49, CH <sub>2</sub>	3.57, m	H8	C8, C9, C2	H2, H5, H8, H9
8	22.72, CH <sub>2</sub>	1.91, m; 2.04, m	H7, H11	C2, C7, C9	H2, H7, H9
9	28.09, CH <sub>2</sub>	2.13, m; 2.36, dtd, 12.90, 6.69, 2.93	H2, H8	C2, C8	H2, H7, H8, H2, H5, H11, H12, H13
10	38.57, CH <sub>2</sub>	1.53, ddd, 14.43, 9.48, 4.95; 2.04	H5, H7, H11	C4, C5, C12, C13	H5, H10, H12
11	24.68, CH	1.76, m	H12, H13, H10	C12, C13	, H5, H10, H11, H13
12	23.27, CH <sub>3</sub>	1.01, d, 6.60	H11	C5, C10 C11, C13	H5, H10, H11, H13
13	21.17, CH <sub>3</sub>	0.96, d, 6.60	H11	C10, C12	H5, H10, H11, H12

During the analysis, three structures were proposed, being all of them diketopiperazines (Figures 3.22 and 3.23). The structure A, a 2,6-DKP, was the first excluded as it did not meet a couple of information in the data obtained in the NMR experiments, to know: the <sup>13</sup>C NMR data in D<sub>2</sub>O shows a shift on the carbonyl group at 166.13 ppm (shifts to 166.18 ppm), while the carbon of the carbonyl group at 170.23 ppm shows no shift whatsoever. This is the major point on our final choice as it indicates the vicinity, or distance, of these groups to the labile proton at 6.01 ppm with which they interact; another reason for discarding this structure concerns the double doublet at 4.02 ppm and the triplet at 4.13 ppm. The TOCSY data shows that both these protons interact with the labile proton, but at different extent, with the 4.13 ppm proton having a greater intensity. This suggests that the 4.13 ppm proton is closer to the labile proton compared to the 4.02 ppm proton. This observation was further confirmed by <sup>1</sup>H NMR using D<sub>2</sub>O; the 4.13 shifted to 4.11 ppm and 4.02 shifted to 4.01 ppm. These two sets of NMR also exclude the structure B.

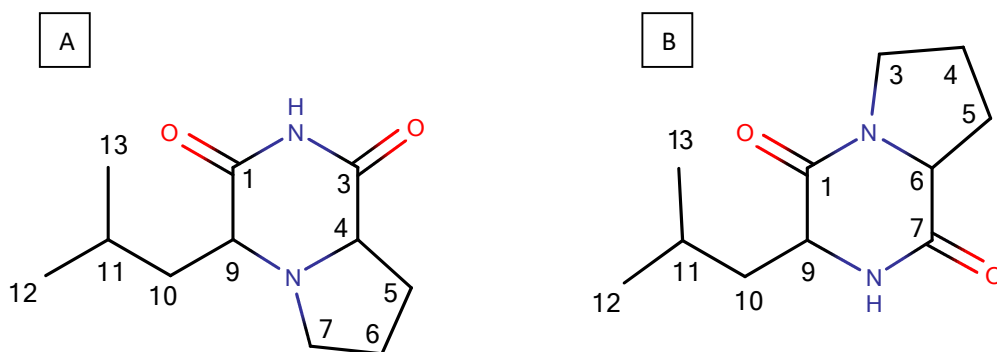


Figure 3.23. Initially proposed structures for the compound PTM-99-(F4-F7)-F30.

This structure was not immediately excluded, as structure A, since the protons and carbonyl groups above mentioned presented an interaction fitting the data obtained initially. To meet the new data obtained, the structure would have to have its carbonyl groups exchanging place, with the same being necessary for the two CH groups. Finally, the only structure left, and the best guess, is the structure on the Figure 3.22. Firstly, it fits with the data, and, secondly, the placement of the carbonyl at 166.13 ppm, right next to the labile proton, suggests a possible formation of hydrogen bond between the oxygen and the proton, whose disruption could account for the shift observed in the NMR under the D<sub>2</sub>O.

The IR spectrum yielded a peak characteristic of the amide NH bending at 1637, stretching at 1675.26 and alkyl CH stretch at 2956.43 cm<sup>-1</sup>.

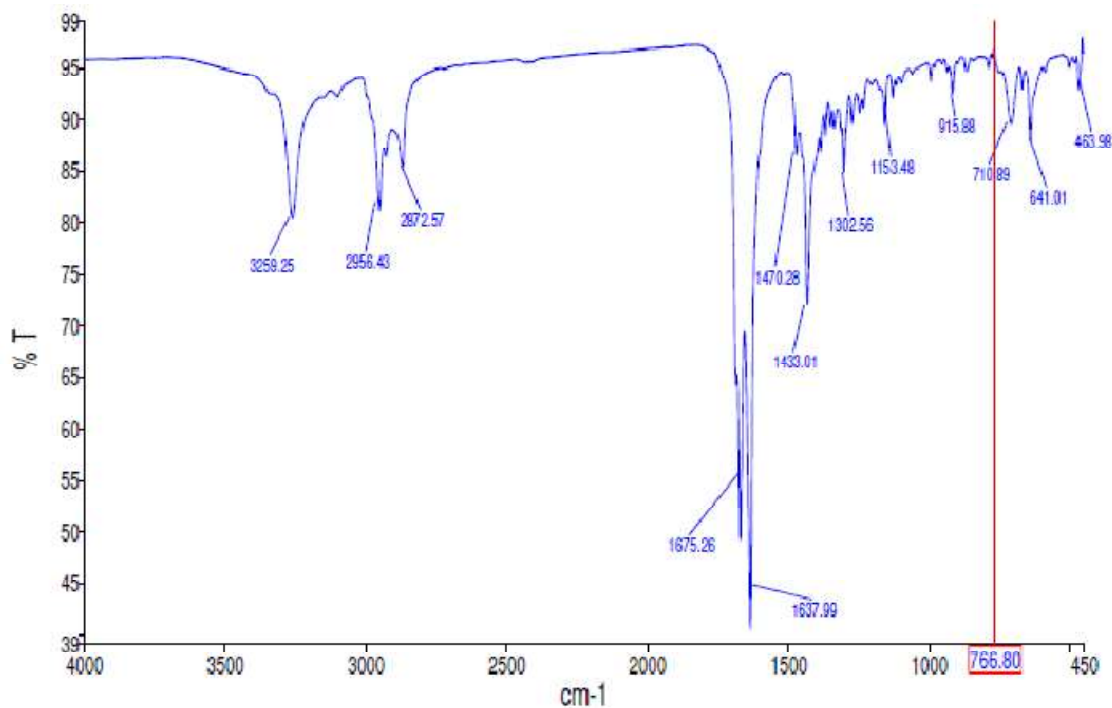


Figure 3.24. IR spectrum of compound PTM-99-(F4-F7)-F30.

### 3.3.3. PTM-99-(F4-F7)-F34

The structural elucidation of this compound spawns from that of the compound PTM-99-(F4-F7)-F30, therefore its description will skip the diketopiperazine core.

The aromatic protons were readily identified due to their characteristic signals, with shifts at 7.24, 7.30 and 7.35 ppm. The corresponding carbons were attributed using the HSQC-DEPT data: 129.1, 127.55 and 129.26 ppm, respectively. Lastly, the formation of the aromatic ring was given by the HMBC correlations of 7.35 to 129.1 and 135.87, 7.24 to 127.55, and 7.30 to 129.1 ppm. Likewise, the identification of the diketopiperazine was upright with the characteristic carbonyl of the amide groups spotted at the shifts 165.05 and 169.44 ppm in the  $^{13}\text{C}$  NMR spectrum, and confirmed by HSQC-DEPT and HMBC correlations. The proline unity was obtained by analyzing the HMBC correlations H3 to C5, H4 to C3, C5, C6 and H6 to C7 (Figure 3.25; Table 3.8).

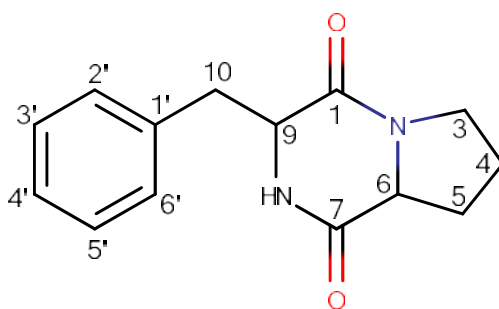


Figure 3.25. Proposed structure for the compound PTM-99-(F4-F7)-F34.

Table 3.8. NMR data for compound PTM-99-(F4-F7)-F34.

Position	$\delta_{\text{C}}$ , Type	$\delta_{\text{H}}$ , multiplicity, (J in Hz)	COSY	HMBC	TOCSY
1	165.05, qC	-	-	-	-
2	-	-	-	-	-
3	28.33, CH <sub>2</sub>	2.02, m; 2.34, m	H4, H6	C5, C7	H5, H6
4	22.52, CH <sub>2</sub>	1.93, dd, 16.87, 7.34; 2.02, m	H3, H5, H6	C7	H3, H5, H6
5	45.45, CH <sub>2</sub>	3.57, m; 3.66, m	H4, H9, H10	C3, C4, C9, C1', C3', C5'	H3, H4, H6, H9, H10
6	59.12, CH	4.09, t, 7.27	H3, H4	C3, C7	H3, H4, H5, H8, H9, H10
7	169.44, qC	-	-	-	-
8	-	5.72, s	-	C1	H6, H9
9	56.18, CH	4.28, dd, 10.96, 9.28	H5, H10	C1, C10	H5, H6, H10
10	36.77, CH <sub>2</sub>	2.80, dd, 14.31, 10.64; 3.57, m	H4, H9	C1, C3, C4, C9, C1', C3', C5'	H9
1'	135.87, qC	-	-	-	-
2'	129.26, CH <sub>2</sub>	7.35, d, 7.46	H3', H4'	C1', C3', C5'	-
3'	129.10, CH <sub>2</sub>	7.24, d, 6.97	H2', H4'	C10, C4'	H5, H10

<b>4'</b>	127.55, CH	7.30, d, 7.09	H2', H3'	C3'	-
<b>5'</b>	129.10, CH <sub>2</sub>	7.24, d, 6.97	H2', H4'	C10, C4'	H5, H10
<b>6'</b>	129.26, CH <sub>2</sub>	7.35, d, 7.46	H3', H4'	C1', C3', C5'	-

The proposed structure for PTM-99-(F4-F7)-F34 is the known metabolite *Cyclo-(L-Ph-L-Pro)* and the structure proposed for PTM-99-(F4-F7)-F30 is most likely *Cyclo-(L-Leu-L-Pro)* (Martínez-Luis *et al.*, 2011). However, to the best of our knowledge, this is the first time these compounds are being reported as isolated from the *Salinispora* genus.



**Conclusions**  
**and future work 4**



#### 4. CONCLUSIONS AND FUTURE WORK

The difference in the number of compounds produced by the *S. arenicola* strain PTM-99 for a 7 days culture and a 14 days culture, suggest the existence of time dependence in the production of secondary metabolites, which is consistent with what is known about their production pattern. However, the considerable increase in the number of metabolites produced is a point still in need of clarification. Furthermore, there seems to be a massive production of what appears to be compounds of a family containing a lactam core, piperazine core and/or aromatic backbone. However, these compounds have not displayed any remarkable activity against the pathogenic bacteria vancomycin-resistant *Enterococcus faecium* VRE EF82 and methicillin-resistant *Staphylococcus aureus* MRSA COL, as per results of tests of the 7D culture. From the total of 52 compounds isolated from the 7 days culture, 20 displayed activity. From the 14 days culture, 71 compounds were isolated, but were not tested for antimicrobial activity. The most potent compounds were found to be PTM-99-(F2)-F2 and PTM-99-(F2)-F15 with the lowest MIC of 62.5 µg/ml. The structure proposed for the F15 equivalent F27 appears to belong to the macrolide class of natural compounds. The compound PTM-99-(F2)-F31 also appears to belong to the same class.

As of the moment the two structures proposed (F27 and F31) are amid elucidation. More data are needed to have a final structure. Future work should pass by the employment of techniques such as high-resolution mass spectrometry and x-ray crystallography to discern the structure of the compounds mentioned above. Furthermore, these compounds should be tested against the targets used in this thesis, and also some that were not used such cancer cell lines and antibiofil, since similar compounds tested at the lab have shown promising bioactivity.

The overall of compounds should be isolated again to retrieve enough mass for structure elucidation. This procedure should be performed for both 7 days and 14 days culture, since there is a remarkable discrepancy in the production of metabolites. Finally, the 14 days culture should be tested against a broad range of bioassay targets, including cancer cell lines, since they have not yet been tested.





## *References 5*



## 5. REFERENCES

1. Abarzua, S., & Jakubowski, S. (1995). Biotechnological investigation for the prevention of biofouling. I. Biological and biochemical principles for the prevention of biofouling. *Marine Ecology Progress Series Mar. Ecol. Prog. Ser.*, 123, 301-312. doi:10.3354/meps123301
2. Abdelmohsen, U. R., Bayer, K., & Hentschel, U. (2014). Diversity, abundance and natural products of marine sponge-associated actinomycetes. *Natural product reports*, 31(3), 381-399.
3. Ahmed, L., Jensen, P. R., Freel, K. C., Brown, R., Jones, A. L., Kim, B. Y., & Goodfellow, M. (2013). *Salinispora pacifica* sp. nov., an actinomycete from marine sediments. *Antonie Van Leeuwenhoek*, 103(5), 1069-1078.
4. Almeida, J., Freitas, M., Cruz, S., Leão, P., Vasconcelos, V., & Cunha, I. (2015). Acetylcholinesterase in Biofouling Species: Characterization and Mode of Action of Cyanobacteria-Derived Antifouling Agents. *Toxins*, 7(8), 2739-2756. doi:10.3390/toxins7082739
5. Alzieu, C. (2000). Impact of Tributyltin on Marine Invertebrates. *Ecotoxicology*, 9: 71. doi:10.1023/A:1008968229409
6. Artuso, Anthony. (2000). Bioprospecting, Benefit Sharing, and Biotechnological Capacity Building. *World Development*, 30(8), 1355-368
7. Asolkar, R. N., Freel, K. C., Jensen, P. R., Fenical, W., Kondratyuk, T. P., Park, E. J., & Pezzuto, J. M. (2010). Arenamides A– C, Cytotoxic NFκB Inhibitors from the Marine Actinomycete *Salinispora arenicola*. *Journal of Natural Products*, 73(4), 796-796.
8. Assmann, M., E. Lichte, Jr Pawlik, and M. Köck. (2000). Chemical Defenses of the Caribbean Sponges *Agelas Wiedenmayeri* and *Agelas Conifera*. *Marine Ecology Progress Series Mar. Ecol. Prog. Ser.* 207: 255-62.
9. Beer, D. D., Stoodley, P., Roe, F., & Lewandowski, Z. (1994). Effects of biofilm structures on oxygen distribution and mass transport. *Biotechnol. Bioeng. Biotechnology and Bioengineering*, 43(11), 1131-1138. doi:10.1002/bit.260431118
10. Bérdy, J. (2012). Thoughts and facts about antibiotics: where we are now and where we are heading. *The Journal of antibiotics*, 65(8), 385-395.
11. Bertrand, S., N. Bohni, S. Schnee, O. Schumpp, *et al.* (2014). Metabolite induction via microorganism co-culture: a potential way to enhance chemical diversity for drug discovery. *Biotechnol Adv.* 32 p.1180-1204.
12. Bladt, T. T., Frisvad, J. C., Knudsen, P. B., & Larsen, T. O. (2013). Anti-cancer and antifungal compounds from *Aspergillus*, *Penicillium* and other filamentous fungi. *Molecules*, 18(9), 11338-11376.
13. Boobathy S, Kumar T and Katherisan K. (2009). Isolation of symbiotic bacteria and bioactive proteins from the marine sponge *Callyspongia diffusa*. *Indian J Biotechnol.*, 8: 272-275.
14. Bose, U., Hewavitharana, A. K., Ng, Y. K., Shaw, P. N., Fuerst, J. A., & Hodson, M. P. (2015). LC-MS-based metabolomics study of marine bacterial secondary metabolite and antibiotic production in *Salinispora arenicola*. *Marine drugs*, 13(1), 249-266.
15. Bowling, J. J., Kochanowska, A. J., Kasanah, N., and Hamann, M. T. (2007) Nature's bounty – drug discovery from the sea. *Expert Opin. Drug Discovery*, 2, 1505
16. Brautaset, T., Sekurova, O. N., Sletta, H., Ellingsen, T. E., Strøm, A. R., Valla, S., & Zotchev, S. B. (2000). Biosynthesis of the polyene antifungal antibiotic nystatin in *Streptomyces noursei* ATCC 11455: analysis of the gene cluster and deduction of the biosynthetic pathway. *Chemistry & biology*, 7(6), 395-403.
17. Bredholdt, H., Galatenko, O. A., Engelhardt, K., Fjærvik, E., Terekhova, L. P., & Zotchev, S. B. (2007). Rare actinomycete bacteria from the shallow water sediments of the Trondheim fjord, Norway: isolation, diversity and biological activity. *Environmental microbiology*, 9(11), 2756-2764.
18. Burns, E., Ifrach, I., Carmeli, S., Pawlik, J., & Ilan, M. (2003). Comparison of anti-predatory defenses of Red Sea and Caribbean sponges. I. Chemical defense. *Marine Ecology Progress Series Mar. Ecol. Prog. Ser.*, 252, 105-114. doi:10.3354/meps252105

19. Burns, E., Ifrach, I., Carmeli, S., Pawlik, J., & Ilan, M. (2003). Comparison of anti-predatory defenses of Red Sea and Caribbean sponges. I. Chemical defense. *Marine Ecology Progress Series Mar. Ecol. Prog. Ser.*, 252, 105-114. doi:10.3354/meps252105
20. Cannell, Richard J. P. (1998). How to Approach the Isolation of a Natural Product. *Natural Products Isolation Methods in Biotechnology.*, 1-51.
21. Carla C. C. R. De Carvalho, & Fernandes, P. (2010). Production of Metabolites as Bacterial Responses to the Marine Environment. *Marine Drugs*, 8(3), 705-727. doi:10.3390/md8030705
22. Carter, G. T. (2011). Natural products and Pharma 2011: Strategic changes spur new opportunities. *Nat. Prod. Rep. Natural Product Reports*, 28(11), 1783. doi:10.1039/c1np00033k
23. Challis, G. L. (2008). Mining microbial genomes for new natural products and biosynthetic pathways. *Microbiology*, 154(6), 1555-1569. doi:10.1099/mic.0.2008/018523-0
24. Challis, G. L. (2014). Exploitation of the *Streptomyces coelicolor* A3 (2) genome sequence for discovery of new natural products and biosynthetic pathways. *Journal of industrial microbiology & biotechnology*, 41(2), 219-232.
25. Cragg, G. M., and David J. Newman. (2013) Natural Products: A Continuing Source of Novel Drug Leads. *Biochimica Et Biophysica Acta (BBA) - General Subjects* 1830.6, 3670-695.
26. Cragg, G. M., Grothaus, P. G., & Newman, D. J. (2009). Impact of Natural Products on Developing New Anti-Cancer Agents †. *Chemical Reviews Chem. Rev.*, 109(7), 3012-3043. doi:10.1021/cr900019j
27. Cragg, G. M., Katz, F., Newman, D. J., & Rosenthal, J. (2012). Legal and Ethical Issues Involving Marine Biodiscovery and Development. *Handbook of Marine Natural Products*, 1314-1342. doi:10.1007/978-90-481-3834-0\_27
28. Cunha, I., Mangas-Ramirez, E., & Guilhermino, L. (2007). Effects of copper and cadmium on cholinesterase and glutathione S-transferase activities of two marine gastropods (*Monodonta lineata* and *Nucella lapillus*). *Comparative Biochemistry and Physiology Part C: Toxicology & Pharmacology*, 145(4), 648-657. doi:10.1016/j.cbpc.2007.02.014
29. Dafforn, K. A., Lewis, J. A., & Johnston, E. L. (2011). Antifouling strategies: History and regulation, ecological impacts and mitigation. *Marine Pollution Bulletin*, 62(3), 453-465. doi:10.1016/j.marpolbul.2011.01.012
30. Das, S., Lyla, P. S., & Khan, S. A. (2006). Marine microbial diversity and ecology: importance and future perspectives. *Current Science*, 90(10), 1325-1335.
31. Davey, M. E., & O'toole, G. A. (2000). Microbial Biofilms: From Ecology to Molecular Genetics. *Microbiology and Molecular Biology Reviews*, 64(4), 847-867. doi:10.1128/mmbr.64.4.847-867.2000
32. Davidson, B. (1995). New dimensions in natural products research: Cultured marine microorganisms. *Current Opinion in Biotechnology*, 6(3), 284-291. doi:10.1016/0958-1669(95)80049-2
33. Deepa, I., Kumar, S. N., Sreerag, R. S., Nath, V. S., & Mohandas, C. (2015). Purification and synergistic antibacterial activity of arginine derived cyclic dipeptides, from *Achromobacter* sp. associated with a rhabditid entomopathogenic nematode against major clinically relevant biofilm forming wound bacteria. *Frontiers in microbiology*, 6.
34. Demain, Arnold L., and Sergio Sanchez. (2009) ChemInform Abstract: Microbial Drug Discovery: 80 Years of Progress. *ChemInform* 40.19
35. Dewick, P. M. (2001). Secondary Metabolism: The Building Blocks and Construction Mechanisms, in Medicinal Natural Products: A Biosynthetic Approach, *Second Edition*, John Wiley & Sons, Ltd, Chichester, UK. doi: 10.1002/0470846275.ch2
36. Dias, D. A., Urban, S., & Roessner, U. (2012). A Historical Overview of Natural Products in Drug Discovery. *Metabolites*, 2(4), 303-336. doi:10.3390/metabo2020303
37. Dinsmore, C. J., & Beshore, D. C. (2002). Recent advances in the synthesis of diketopiperazines. *Tetrahedron*, 58(17), 3297-3312. doi:10.1016/s0040-4020(02)00239-9
38. Dionisi, H. M., Lozada, M., & Olivera, N. L. (2012). Bioprospection of marine microorganisms: biotechnological applications and methods. *Revista argentina de microbiología*. 44: p. 49-60.

39. Dobretsov, S. V., & Qian, P. (2003). Pharmacological Induction of Larval Settlement and Metamorphosis in the Blue Mussel *Mytilus edulis* L. *Biofouling*, 19(1), 57-63. doi:10.1080/0892701021000060860
40. Dobretsov, S., Dahms, H., & Qian, P. (2006). Inhibition of biofouling by marine microorganisms and their metabolites. *Biofouling*, 22(1), 43-54. doi:10.1080/08927010500504784
41. Dobretsov, S., Teplitski, M., & Paul, V. (2009). Mini-review: Quorum sensing in the marine environment and its relationship to biofouling. *Biofouling*, 25(5), 413-427. doi:10.1080/08927010902853516
42. Donia, M., & Hamann, M. T. (2003). Marine natural products and their potential applications as anti-infective agents. *The Lancet Infectious Diseases*, 3(6), 338-348. doi:10.1016/s1473-3099(03)00655-8
43. Du, H., Jiao, N., Hu, Y., & Zeng, Y. (2006). Diversity and distribution of pigmented heterotrophic bacteria in marine environments. *FEMS Microbiology Ecology*, 57(1), 92-105. doi:10.1111/j.1574-6941.2006.00090.x
44. Faimali, M., Falugi, C., Gallus, L., Piazza, V., & Tagliafierro, G. (2003). Involvement of Acetyl Choline in Settlement of *Balanus amphitrite*. *Biofouling*, 19(Sup1), 213-220. doi:10.1080/0892701021000044228
45. Faulkner DJ. (2001). Marine natural products. *Nat. Prod. Rep. Natural Product Reports*, 19(1), 1-48. doi:10.1039/b009029h
46. Feling, R. H., Buchanan, G. O., Mincer, T. J., Kauffman, C. A., Jensen, P. R., & Fenical, W. (2003). Salinosporamide A: a highly cytotoxic proteasome inhibitor from a novel microbial source, a marine bacterium of the new genus *Salinospora*. *Angewandte Chemie International Edition*, 42(3), 355-357.
47. Fenical, W., & Jensen, P. R. (1993). Marine Microorganisms: A New Biomedical Resource. *Pharmaceutical and Bioactive Natural Products*, 419-457. doi:10.1007/978-1-4899-2391-2\_12
48. Fenical, W., & Jensen, P. R. (2006). Developing a new resource for drug discovery: marine actinomycete bacteria. *Nature chemical biology*, 2(12), 666-673.
49. Fenical, W., & Jensen, P. R. (2006). Developing a new resource for drug discovery: marine actinomycete bacteria. *Nature chemical biology*, 2(12), 666-673.
50. Fenical, W., Jensen, P. R., Palladino, M. A., Lam, K. S., Lloyd, G. K., & Potts, B. C. (2009). Discovery and development of the anti-cancer agent salinosporamide A (NPI-0052). *Bioorganic & Medicinal Chemistry*, 17(6), 2175-2180. doi:10.1016/j.bmc.2008.10.075
51. Ferrari, Simone. (2010). Biological Elicitors of Plant Secondary Metabolites: Mode of Action and Use in the Production of Nutraceuticals. *Advances in Experimental Medicine and Biology Bio-Farms for Nutraceuticals*: 152-66.
52. Firn, R. D., & Jones, C. G. (2003). Natural products ? a simple model to explain chemical diversity. *Nat. Prod. Rep. Natural Product Reports*, 20(4), 382. doi:10.1039/b208815k
53. Fischbach, M. A., & Clardy, J. (2007). One pathway, many products. *Nature Chemical Biology Nat Chem Biol*, 3(7), 353-355. doi:10.1038/nchembio0707-353
54. Folmer, F., Houssen, W.E., Scott, R.H., Jaspars, M. (2007) Biomedical research tools from the seabed. *Curr. Opin. Drug Discov. Dev.* 10, 145-152.
55. Freel, K. C., Edlund, A., & Jensen, P. R. (2012). Microdiversity and evidence for high dispersal rates in the marine actinomycete 'Salinispora pacifica'. *Environmental microbiology*, 14(2), 480-493.
56. Gerwick, W., & Moore, B. (2012). Lessons from the Past and Charting the Future of Marine Natural Products Drug Discovery and Chemical Biology. *Chemistry & Biology*, 19(12), 1631. doi:10.1016/j.chembiol.2012.12.004
57. Gill, S. R. *et al.* (2005). Insights on Evolution of Virulence and Resistance from the Complete Genome Analysis of an Early Methicillin-Resistant *Staphylococcus aureus* Strain and a Biofilm-Producing Methicillin-Resistant *Staphylococcus epidermidis* Strain. *J. Bacteriol.* 187, 2426-2438
58. Girard, E., Bernard, V., Minic, J., Chatonnet, A., Krejci, E., & Molgó, J. (2007). Butyrylcholinesterase and the control of synaptic responses in acetylcholinesterase knockout mice. *Life Sciences*, 80(24-25), 2380-2385. doi:10.1016/j.lfs.2007.03.011

59. Gomez-Escribano, J. P., & Bibb, M. J. (2013). Heterologous expression of natural product biosynthetic gene clusters in *Streptomyces coelicolor*: From genome mining to manipulation of biosynthetic pathways. *Journal of Industrial Microbiology & Biotechnology J Ind Microbiol Biotechnol*, 41(2), 425-431. doi:10.1007/s10295-013-1348-5
60. Gomez-Escribano, J. P., Alt, S., & Bibb, M. J. (2016). Next Generation Sequencing of Actinobacteria for the Discovery of Novel Natural Products. *Marine drugs*, 14(4), 78.
61. Gram, L., Melchiorson, J. & Bruhn, J. (2010). Antibacterial activity of marine culturable bacteria collected from a global sampling of ocean surface waters and surface swabs of marine organisms. *Mar Biotechnol.*, 12:439–451.
62. Guidi, L., & Landi, M. (2014). Aromatic Plants: Use and Nutraceutical Properties. *Applications in Food, Medicine and Cosmetics Novel Plant Bioresources*, 303-345. doi:10.1002/9781118460566.ch23
63. Gul, W., & Hamann, M. T. (2005). Indole alkaloid marine natural products: An established source of cancer drug leads with considerable promise for the control of parasitic, neurological and other diseases. *Life Sciences*, 78(5), 442-453. doi:10.1016/j.lfs.2005.09.007
64. Habbu, P., Warad, V., Shastri, R., Madagundi, S., & Kulkarni, V. H. (2016). Antimicrobial metabolites from marine microorganisms. *Chinese Journal of Natural Medicines*, 14(2), 101-116. doi:10.1016/s1875-5364(16)60003-1
65. Habbu, P., Warad, V., Shastri, R., Madagundi, S., & Kulkarni, V. H. (2016). Antimicrobial metabolites from marine microorganisms. *Chinese Journal of Natural Medicines*, 14(2), 101-116. doi:10.1016/s1875-5364(16)60003-1
66. Han, J. L. (2012). Potential of Marine Bacteria as a Source of New Biofilm Formation Inhibiting Compounds. *UNF Undergraduate Honors Theses*. Paper 1.
67. He, H., Ding, W. D., Bernan, *et al.* (2001). Lomaiviticins A and B, Potent Antitumor Antibiotics from *Micromonospora lomaivitiensis*. *Journal of the American Chemical Society*, 123(22), 5362-5363.
68. <http://digitalcommons.unf.edu/honors/1>
69. Hu, G., Yuan, J., Sun, L., She, Z., *et al.* (2011). Statistical Research on Marine Natural Products Based on Data Obtained between 1985 and 2008. *Marine Drugs*, 9(12), 514-525. doi:10.3390/md9040514
70. Huang, R. M., Yi, X. X., Zhou, Y., Su, X., Peng, Y., & Gao, C. H. (2014). An update on 2, 5-diketopiperazines from marine organisms. *Marine drugs*, 12(12), 6213-6235.
71. Huang, R., Zhou, X., Xu, T., Yang, X., & Liu, Y. (2010). Diketopiperazines from Marine Organisms. *Chemistry & Biodiversity*, 7(12), 2809-2829. doi:10.1002/cbdv.200900211
72. Huggett, M. J., Nedved, B. T., & Hadfield, M. G. (2009). Effects of initial surface wettability on biofilm formation and subsequent settlement of *Hydroides elegans*. *Biofouling*, 25(5), 387-399. doi:10.1080/08927010902823238
73. Imhoff, J. F., Labes, A., & Wiese, J. (2011). Bio-mining the microbial treasures of the ocean: New natural products. *Biotechnology Advances*, 29(5), 468-482. doi:10.1016/j.biotechadv.2011.03.001
74. Jayanth K, Jeyasekaran G and Jeya Shakila, R. (2002). Isolation of marine bacteria, antagonistic to human pathogens. *Ind J Mar Sci.*, 31: 39-44.
75. Jensen, P. R., Gontang, E., Mafnas, C., Mincer, T. J., & Fenical, W. (2005). Culturable marine actinomycete diversity from tropical Pacific Ocean sediments. *Environmental microbiology*, 7(7), 1039-1048.
76. Jensen, P. R., Moore, B. S., & Fenical, W. (2015). The marine actinomycete genus *Salinispora*: A model organism for secondary metabolite discovery. *Nat. Prod. Rep.*, 32(5), 738-751. doi:10.1039/c4np00167b
77. Jensen, P. R., Williams, P. G., Oh, D. C., Zeigler, L., & Fenical, W. (2007). Species-specific secondary metabolite production in marine actinomycetes of the genus *Salinispora*. *Applied and environmental microbiology*, 73(4), 1146-1152.
78. Jensen, Paul R., Bradley S. Moore, and William Fenical. (2015). The Marine Actinomycete Genus *Salinispora*: A Model Organism for Secondary Metabolite Discovery. *Nat. Prod. Rep.* 32.5: 738-51. Web.

79. Johnson, G., & Moore, S. W. (2012a). Why has butyrylcholinesterase been retained? Structural and functional diversification in a duplicated gene. *Neurochemistry International*, 61(5), 783-797. doi:10.1016/j.neuint.2012.06.016
80. Johnson, G., & Moore, S. W. (2012b). The carboxylesterase/cholinesterase gene family in invertebrate deuterostomes. *Comparative Biochemistry and Physiology Part D: Genomics and Proteomics*, 7(2), 83-93. doi:10.1016/j.cbd.2011.11.003
81. Kanoh, K., Kohno, S., Katada, J., Takahashi, J., & Uno, I. (1999). (-)-Phenylahistin Arrests Cells in Mitosis by Inhibiting Tubulin Polymerization. *The Journal of antibiotics*, 52(2), 134-141.
82. Kim, T. K., Garson, M. J., & Fuerst, J. A. (2005). Marine actinomycetes related to the 'Salinispora' group from the Great Barrier Reef sponge *Pseudoceratina clavata*. *Environmental microbiology*, 7(4), 509-518.
83. Kim, T. K., Hewavitharana, A. K., Shaw, P. N., & Fuerst, J. A. (2006). Discovery of a new source of rifamycin antibiotics in marine sponge actinobacteria by phylogenetic prediction. *Applied and environmental microbiology*, 72(3), 2118-2125.
84. Kirschner, C. M., & Brennan, A. B. (2012). Bio-Inspired Antifouling Strategies. *Annu. Rev. Mater. Res. Annual Review of Materials Research*, 42(1), 211-229. doi:10.1146/annurev-matsci-070511-155012
85. Kotake, Y. (2012). Molecular Mechanisms of Environmental Organotin Toxicity in Mammals. *Biol. Pharm. Bull. Biological and Pharmaceutical Bulletin Biological and Pharmaceutical Bulletin*, 35(11), 1876-1880. doi:10.1248/bpb.b212017
86. Kuehn, Christian, Karolin Graf, Wieland Heuer, Andres Hilfiker, Iris F. Chaberny, Meike Stiesch, and Axel Haverich. "Economic Implications of Infections of Implantable Cardiac Devices in a Single Institution." *European Journal of Cardio-Thoracic Surgery* 37.4 (2010): 875-79. Web.
87. Lam, K. S. (2007). New aspects of natural products in drug discovery. *Trends in Microbiology*, 15(6), 279-289. doi:10.1016/j.tim.2007.04.001
88. Lane, R. M., Potkin, S. G., & Enz, A. (2005). Targeting acetylcholinesterase and butyrylcholinesterase in dementia. *The International Journal of Neuropsychopharmacology Int. J. Neuropsychopharm.*, 9(01), 101. doi:10.1017/s1461145705005833
89. Lebar, M. D., Heimbegner J. L., and Baker, B. J. (2007) Cold-water marine natural products. *Nat. Prod. Rep.*, 24, 774-797 DOI: 10.1039/B516240H
90. Lee, J., Orlikova, B., & Diederich, M. (2015). Signal Transducers and Activators of Transcription (STAT) Regulatory Networks in Marine Organisms: From Physiological Observations towards Marine Drug Discovery. *Marine Drugs*, 13(8), 4967-4984. doi:10.3390/md13084967
91. Liao, S., Xu, Y., Tang, Y., Wang, J., Zhou, X., Xu, L. and Liu, Y. (2015) Design, Synthesis And Biological Evaluation of Soluble 2,5-Diketopiperazines Derivatives As Potential Antifouling Agents. *RSC Adv.*, DOI: 10.1039/C5RA06210A.
92. Liu, K. and L. Jiang (2012) Bio-inspired self-cleaning surfaces. *Annu Rev Mater Res.* 42 p.231-263.
93. Long, R. A., & Azam, F. (2001). Antagonistic Interactions among Marine Pelagic Bacteria. *Applied and Environmental Microbiology*, 67(11), 4975-4983. doi:10.1128/aem.67.11.4975-4983.2001
94. Slattery, M., Rajbhandari, I., Wesson, K. (2001). Competition-mediated antibiotic induction in the marine bacterium *Streptomyces tenjimariensis*. *Microbial Ecology*, 41(2): 90-96
95. Magin, C. M., Cooper, S. P., & Brennan, A. B. (2010). Non-toxic antifouling strategies. *Materials Today*, 13(4), 36-44. doi:10.1016/s1369-7021(10)70058-4
96. Maldonado, L. A., et al. (2005). *Salinispora arenicola* gen. nov., sp. nov. and *Salinispora tropica* sp. nov., obligate marine actinomycetes belonging to the family Micromonosporaceae. *International Journal of Systematic and Evolutionary Microbiology*, 55(5), 1759-1766.
97. Manzo, Emiliano, M. Letizia Ciavatta, Guido Villani, Mario Varcamonti, S. M. Abu Sayem, Rob Van Soest, and Margherita Gavagnin. (2011). Bioactive Terpenes from *Spongia officinalis*. *J. Nat. Prod. Journal of Natural Products* 74.5: 1241-247. Web.



98. Mato, R. *et al.* (2009). Assessment of high-level gentamicin and glycopeptide-resistant *Enterococcus faecalis* and *E. faecium* clonal structure in a Portuguese hospital over a 3-year period. *Eur. J. Clin. Microbiol. Infect. Dis.* 28, 855–859
99. Margulis, L. & M.J. Chapman (2009) *Kingdoms and domains: an illustrated guide to the phyla of life on Earth*. Elsevier Science.
100. Marine Pharmacology: Clinical Development. (n.d.). Retrieved August 30, 2016, from <http://marinepharmacology.midwestern.edu/clinPipeline.htm>
101. Marit Hallvardsdotter Stafsnes (2013). Characterization and exploitation of a marine microbial culture collection – a special focus on carotenoid producing heterotrophic bacteria. Norwegian University of Science and Technology Faculty of Natural Sciences and Technology Department of Biotechnology
102. Marrie, T. J., J. Nelligan, & J. W. Costerton. (1982). A Scanning and Transmission Electron Microscopic Study of an Infected Endocardial Pacemaker Lead. *Circulation* 66.6: 1339-341.
103. Martins, A., Vieira, H., Gaspar, H., & Santos, S. (2014). Marketed Marine Natural Products in the Pharmaceutical and Cosmeceutical Industries: Tips for Success. *Marine Drugs* 12.2: 1066-101. Web.
104. Martins, M. B., & Carvalho, I. (2007). Diketopiperazines: biological activity and synthesis. *Tetrahedron*, 63(40), 9923-9932.
105. Masson, P., & Lockridge, O. (2010). Butyrylcholinesterase for protection from organophosphorus poisons: Catalytic complexities and hysteretic behavior. *Archives of Biochemistry and Biophysics*, 494(2), 107-120. doi:10.1016/j.abb.2009.12.005
106. Mayer, A. M., & Hamann, M. T. (2005). Marine pharmacology in 2001–2002: Marine compounds with anthelmintic, antibacterial, anticoagulant, antidiabetic, antifungal, anti-inflammatory, antimalarial, antiplatelet, antiprotozoal, antituberculosis, and antiviral activities; affecting the cardiovascular, immune and nervous systems and other miscellaneous mechanisms of action. *Comparative Biochemistry and Physiology Part C: Toxicology & Pharmacology*, 140(3-4), 265-286. doi:10.1016/j.cca.2005.04.004
107. Mayer, A. M., Glaser, K. B., Cuevas, C., Jacobs, R. S., Kem, W., Little, R. D., McIntosh, J. M., Newman, D. J., Potts, B. C., and Shuster, D. E. (2010). The odyssey of marine pharmaceuticals: A current pipeline perspective. *Trends in Pharmacological Sciences*, 31(6), 255-265. doi:10.1016/j.tips.2010.02.005
108. Mayer, A. M., Nguyen, M., Newman, D. J., and Glaser, K. B. [http://www.fasebj.org/content/30/1\\_Supplement/932.7?related\\_urls=yes&legid=fasebj:30/1\\_Supplement/932.7-aff-3](http://www.fasebj.org/content/30/1_Supplement/932.7?related_urls=yes&legid=fasebj:30/1_Supplement/932.7-aff-3) (2016). The Marine Pharmacology and Pharmaceuticals Pipeline in 2015. *The FASEB Journal* vol. 30 no. 1 Supplement 932.7
109. Mayer, A., Rodríguez, A., Tagliatalata-Scafati, O., & Fusetani, N. (2013). Marine Pharmacology in 2009–2011: Marine Compounds with Antibacterial, Antidiabetic, Antifungal, Anti-Inflammatory, Antiprotozoal, Antituberculosis, and Antiviral Activities; Affecting the Immune and Nervous Systems, and other Miscellaneous Mechanisms of Action. *Marine Drugs*, 11(7), 2510-2573. doi:10.3390/md11072510
110. McGlinchey, R. P., Nett, M., Eustáquio, A. S., Asolkar, R. N., Fenical, W., & Moore, B. S. (2008). Engineered biosynthesis of antiprotealide and other unnatural salinosporamide proteasome inhibitors. *Journal of the American Chemical Society*, 130(25), 7822-7823.
111. Mearns-Spragg, A., Bregu, M., Boyd, K. G., & Burgess, J. G. (1998). Cross-species induction and enhancement of antimicrobial activity produced by epibiotic bacteria from marine algae and invertebrates, after exposure to terrestrial bacteria. *Letters in Applied Microbiology Lett Appl Microbiol*, 27(3), 142-146. doi:10.1046/j.1472-765x.1998.00416.x
112. Millero, F.J. (2013) *Chemical oceanography*. CRC press.
113. Mincer, T. J., Fenical, W., & Jensen, P. R. (2005). Culture-dependent and culture-independent diversity within the obligate marine actinomycete genus *Salinispora*. *Applied and environmental microbiology*, 71(11), 7019-7028.
114. Molinski, T.F., Dalisay, D.S., Lievens, S.L., and Saludes, J.P. (2009) Drug development from marine natural products. *Nat Rev Drug Discov* 8: 69–85.
115. Mollica, A., *et al.* (2014). Synthesis and anti-cancer activity of naturally occurring 2, 5-diketopiperazines. *Fitoterapia*, 98, 91-97.

116. Motlagh, A. M., Bhattacharjee, A. S., & Goel, R. (2016). Biofilm control with natural and genetically-modified phages. *World Journal of Microbiology and Biotechnology World J Microbiol Biotechnol*, 32(4). doi:10.1007/s11274-016-2009-4
117. Murphy, B. T., Narender, T., Kauffman, C. A., Woolery, M., Jensen, P. R., & Fenical, W. (2010). Saliniquinones A–F, new members of the highly cytotoxic anthraquinone- $\gamma$ -pyrones from the marine actinomycete *Salinispora arenicola*. *Australian journal of chemistry*, 63(6), 929-934.
118. Nett, M., Ikeda, H., & Moore, B. S. (2009). Genomic basis for natural product biosynthetic diversity in the actinomycetes. *Nat. Prod. Rep. Natural Product Reports*, 26(11), 1362. doi:10.1039/b817069j
119. Newman, D. J., & Giddings, L. (2013). Natural products as leads to antitumor drugs. *Phytochem Rev Phytochemistry Reviews*, 13(1), 123-137. doi:10.1007/s11101-013-9292-6
120. Newman, D. J., Cragg, G. M., and Snader, K. M. (2000) "The Influence of Natural Products upon Drug Discovery (Antiquity to Late 1999)". *Nat. Prod. Rep. Natural Product Reports* 17.3, 215-34
121. Newman, D., & Cragg, G. (2014). Marine-Sourced Anti-Cancer and Cancer Pain Control Agents in Clinical and Late Preclinical Development. *Marine Drugs*, 12(1), 255-278. doi:10.3390/md12010255
122. Nir, S., & Reches, M. (2016). Bio-inspired antifouling approaches: The quest towards non-toxic and non-biocidal materials. *Current Opinion in Biotechnology*, 39, 48-55. doi:10.1016/j.copbio.2015.12.012
123. Pagning, A. N., *et al.* (2016). Antimicrobial, antioxidant and butyrylcholinesterase inhibition activities of extracts and isolated compounds from *Scadoxus pseudocaulus* and semi-synthetic farrerol derivatives. *South African Journal of Botany*, 102, 166-174. doi:10.1016/j.sajb.2015.06.009
124. Palumbi, S.R. and Palumbi, A.R. (2015) *The extreme life of the sea*. Princeton University Press.
125. Patridge, E., Gareiss, P., Kinch, M. S., & Hoyer, D. (2016). An analysis of FDA-approved drugs: Natural products and their derivatives. *Drug Discovery Today*, 21(2), 204-207. doi:10.1016/j.drudis.2015.01.009
126. Paulino, M. A. C. (2016). Isolamento e identificação de isoprenóides híbridos e macrólidos bioativos de *Strpetomyces aculeolatus* obtidas de sedimentos oceânicos provenientes do Arquipélago da Madeira. *Faculty of Science and Technology of New University of Lisbon*
127. Russo, P., Del Bufalo, A. & Fini, M. (2015) Deep sea as a source of novel-anti-cancer drugs: update on discovery and preclinical/clinical evaluation in a systems medicine perspective. *EXCLI Journal*.14:228-236 – ISSN 1611-2156
128. Penesyan, Anahit, Jan Tebben, Matthew Lee, Torsten Thomas, Staffan Kjelleberg, Tilmann Harder, & Suhelen Egan. (2011). Identification of the Antibacterial Compound Produced by the Marine Epiphytic Bacterium *Pseudovibrio* Sp. D323 and Related Sponge-Associated Bacteria. *Marine Drugs* 9(12), 1391-402.
129. Penn, K., *et al.* (2009). Genomic islands link secondary metabolism to functional adaptation in marine Actinobacteria. *The ISME journal*, 3(10), 1193-1203.
130. Pettit, G. R., Herald, C. L., Doubek, D. L., Herald, D. L., Arnold, E., & Clardy, J. (1982). Isolation and structure of bryostatin 1. *J. Am. Chem. Soc. Journal of the American Chemical Society*, 104(24), 6846-6848. doi:10.1021/ja00388a092
131. Pezzementi, L., Nachon, F., & Chatonnet, A. (2011). Evolution of Acetylcholinesterase and Butyrylcholinesterase in the Vertebrates: An Atypical Butyrylcholinesterase from the Medaka *Oryzias latipes*. *PLoS ONE*, 6(2). doi:10.1371/journal.pone.0017396
132. Prieto-Davó *et al.*, (2013). Targeted search for actinomycetes from nearshore and deep-sea marine sediments. *FEMS microbiology ecology*, 84(3), 510-518.
133. Prieto-Davó *et al.*, (2016). The Madeira Archipelago As a Significant Source of Marine-Derived Actinomycete Diversity with Anti-cancer and Antimicrobial Potential. *Frontiers in Microbiology*, 7. doi:10.3389/fmicb.2016.01594
134. Qian, P., & Xu, S. Y. (2012). Antifouling Activity of Marine Natural Products. *Handbook of Marine Natural Products*, 749-821. doi:10.1007/978-90-481-3834-0\_14

135. Qian, P., Lau, S. C., Dahms, H., Dobretsov, S., & Harder, T. (2007). Marine Biofilms as Mediators of Colonization by Marine Macroorganisms: Implications for Antifouling and Aquaculture. *Marine Biotechnology Mar Biotechnol*, 9(4), 399-410. doi:10.1007/s10126-007-9001-9
136. Rahimi, R., Khosravi, M., Tehrani, M. H., Rabbani, M., & Safavi, E. (2016). Solid-Phase Peptide Synthesis of Dipeptide (Histidine- $\beta$ -Alanine) as a Chelating Agent by Using Trityl Chloride Resin, for Removal of Al<sup>3+</sup>, Cu<sup>2+</sup>, Hg<sup>2+</sup> and Pb<sup>2+</sup>: Experimental and Theoretical Study. *Journal of the Brazilian Chemical Society*. doi:10.5935/0103-5053.20160064
137. Rao, S. R., & Ravishankar, G. (2002). Plant Cell Cultures: Chemical Factories of Secondary Metabolites." *Biotechnology Advances* 20(2), 101-53.
138. Ray, GC, ed. Ecological diversity in coastal zones and oceans. Biodiversity, ed. EO Wilson. 1988, National Academy Press: Washington, D. C.. 36-50.
139. Reading, N. C., & Sperandio, V. (2006). Quorum sensing: The many languages of bacteria. *FEMS Microbiology Letters*, 254(1), 1-11. doi:10.1111/j.1574-6968.2005.00001.x
140. Recommended methods for the Identification and Analysis of Piperazines in Seized Materials (2013). Laboratory and Scientific Section United Nations Office on Drugs and Crime (UNODC). New York.
141. Richter, T. K., Hughes, C. C., & Moore, B. S. (2015). Sioxanthin, a novel glycosylated carotenoid, reveals an unusual subclustered biosynthetic pathway. *Environmental microbiology*, 17(6), 2158-2171.
142. Ruiz, B., Chávez, A., Forero, A., *et al.* (2010). Production of Microbial Secondary Metabolites: Regulation by the Carbon Source." *Critical Reviews in Microbiology* 36(2), 146-67.
143. Russo, P., Nastrucci, C., & Cesario, A. (2011). From the Sea to Anti-cancer Therapy. *CMC Current Medicinal Chemistry*, 18(23), 3551-3562. doi:10.2174/092986711796642652
144. Rypien, K. L., Ward, J. R., & Azam, F. (2010). Antagonistic interactions among coral-associated bacteria. *Environmental Microbiology*, 12(1), 28-39. doi:10.1111/j.1462-2920.2009.02027.x
145. Salta, M. (2012) Method development for enhanced antifouling testing using novel natural products against marine biofilms, University of Southampton, PhD Thesis
146. Santos, A. P. A., Watanabe, E., Andrade, D. (2011). Biofilm on artificial pacemaker: fiction or reality?. *Arq. Bras. Cardiol.*, São Paulo, 97(5), 113-120,
147. Sawadogo, W.R., M. Schumacher, M.H. Teiten, C. Cerella, *et al.* (2013). A survey of marine natural compounds and their derivatives with anti-cancer activity reported in 2011. *Molecules*. 18 p.3641-3673.
148. Schultz, A. W., *et al.* (2008). Biosynthesis and structures of cyclomarins and cyclomarazines, prenylated cyclic peptides of marine actinobacterial origin. *Journal of the American Chemical Society*, 130(13), 4507-4516.
149. Schultz, M. P., Bendick, J. A., Holm, E. R., & Hertel, W. M. (2011). Economic impact of biofouling on a naval surface ship. *Biofouling*, 27(1), 87-98. doi:10.1080/08927014.2010.542809
150. Shen, B., L. Du, C. Sanchez, D. J. Edwards, M. Chen, and J. M. Murrell. "The Biosynthetic Gene Cluster for the Anti-cancer Drug Bleomycin from *Streptomyces Verticillus* ATCC15003 as a Model for Hybrid Peptide-polyketide Natural Product Biosynthesis." *Journal of Industrial Microbiology and Biotechnology* 27.6 (2001): 378-85. Web.
151. Simister, R. L., Deines, P., Botté, E. S., Webster, N. S., & Taylor, M. W. (2012). Sponge-specific clusters revisited: a comprehensive phylogeny of sponge-associated microorganisms. *Environmental Microbiology*, 14(2), 517-524.
152. Singh, R., Nadhe, S., Wadhvani, S., Shedbalkar, U., & Chopade, B. (2016). Nanoparticles for Control of Biofilms of *Acinetobacter* Species. *Materials*, 9(5), 383. doi:10.3390/ma9050383
153. Sivakumar, K., Sahu, M. K., Thangaradjou, T., & Kannan, L. (2007). Research on marine actinobacteria in India. *Indian journal of Microbiology*, 47(3), 186-196.

154. Sonak, S., Pangam, P., Giriyan, A., & Hawaldar, K. (2009). Implications of the ban on organotins for protection of global coastal and marine ecology. *Journal of Environmental Management*, 90. doi:10.1016/j.jenvman.2008.08.017
155. Staniek, Agata, Harro Bouwmeester, Paul D. Fraser, Oliver Kayser, Stefan Martens, Alain Tissier, Sander Van Der Krol, Ludger Wessjohann, and Heribert Warzecha. "Natural Products - Modifying Metabolite Pathways in Plants." *Biotechnology Journal* 8.10 (2013): 1159-171. Web.
156. Stoodley P, de Beer D, Lewandowski, Z. (1994) Liquid flow in biofilm systems. *Applied and Environmental Microbiology*, 60: 2711
157. Subramani, R., & Aalbersberg, W. (2012). Marine actinomycetes: an ongoing source of novel bioactive metabolites. *Microbiological research*, 167(10), 571-580.
158. Sudek, S., Lopanik, N. B., Waggoner, L. E., Hildebrand, M., Anderson, C., Liu, H., . . . Haygood, M. G. (2007). Identification of the Putative Bryostatin Polyketide Synthase Gene Cluster from " Candidatus Endobugula sertula", the Uncultivated Microbial Symbiont of the Marine Bryozoan Bugula neritina. *J. Nat. Prod. Journal of Natural Products*, 70(1), 67-74. doi:10.1021/np060361d
159. Symeon, Metallidis, and Pilalas Dimitris. "Infections of Permanent Pacemakers and Implantable Cardioverter-Defibrillators." *Modern Pacemakers - Present and Future* (2011): n. pag. Web.
160. Taylor, M.W., R. Radax, D. Steger, and M. Wagner (2007) Spongeassociated microorganisms: evolution, ecology, and biotechnological potential. *Microbiol Mol Biol R.* 71 p.295-347.
161. Trautner, Barbara W., and Rabih O. Darouiche. "Role of Biofilm in Catheter-associated Urinary Tract Infection." *American Journal of Infection Control* 32.3 (2004): 177-83. Web.
162. Tsueng, G., & Lam, K. S. (2008). Growth of *Salinispora tropica* strains CNB440, CNB476, and NPS21184 in nonsaline, low-sodium media. *Applied microbiology and biotechnology*, 80(5), 873-880.
163. Tsueng, G., & Lam, K. S. (2010). A preliminary investigation on the growth requirement for monovalent cations, divalent cations and medium ionic strength of marine actinomycete *Salinispora*. *Applied microbiology and biotechnology*, 86(5), 1525-1534.
164. Tsueng, G., Teisan, S., & Lam, K. S. (2008). Defined salt formulations for the growth of *Salinispora tropica* strain NPS21184 and the production of salinosporamide A (NPI-0052) and related analogs. *Applied microbiology and biotechnology*, 78(5), 827-832.
165. Udvary, D. W., Zeigler, L., Asolkar, R. N., Singan, V., Lapidus, A., Fenical, W., ... & Moore, B. S. (2007). Genome sequencing reveals complex secondary metabolome in the marine actinomycete *Salinispora tropica*. *Proceedings of the National Academy of Sciences*, 104(25), 10376-10381.
166. Vidgen, M. E., Hooper, J. N. A., & Fuerst, J. A. (2012). Diversity and distribution of the bioactive actinobacterial genus *Salinispora* from sponges along the Great Barrier Reef. *Antonie Van Leeuwenhoek*, 101(3), 603-618.
167. Vimala, R. (2016) Marine organisms: A potential source of natural antifouling metabolites. *Int.J. ChemTech Res.* 9(1),pp 208-217
168. Webster, N.S. and Taylor, M.W. (2012). Marine sponges and their microbial symbionts: love and other relationships. *Environ Microbiol.* 14 p.335-346.
169. Whitehead R. (1999). Natural product chemistry. *Annu Rep Prog Chem Sec B.*, 95: 183-205.
170. Williams, P. G., Miller, E. D., Asolkar, R. N., Jensen, P. R., & Fenical, W. (2007). Arenicolides AC, 26-membered ring macrolides from the marine actinomycete *Salinispora arenicola*. *The Journal of organic chemistry*, 72(14), 5025-5034.
171. Worm, B., H.K. Lotze, & R.A. Myers (2003) Predator diversity hotspots in the blue ocean. *P Natl Acad Sci USA.* 100 (17) 9884-9888. doi: 10.1073/pnas.1333941100
172. Ziemert, N., Lechner, A., Wietz, M., Millán-Aguíñaga, N., Chavarria, K. L., & Jensen, P. R. (2014). Diversity and evolution of secondary metabolism in the marine actinomycete genus *Salinispora*. *Proceedings of the National Academy of Sciences*, 111(12), E1130-E1139.

# ***Annex 6***



## 6. ANNEX

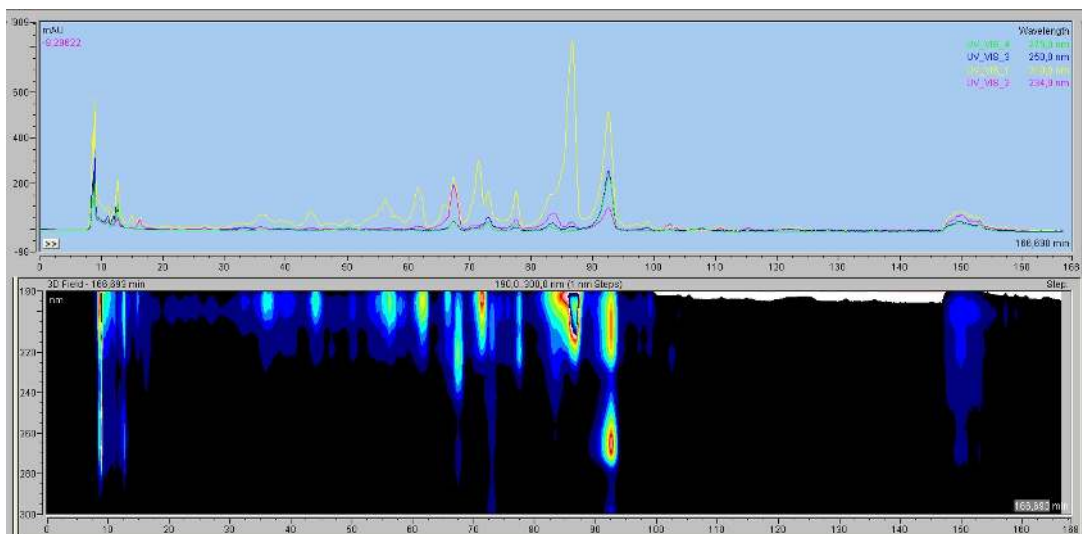


Figure 6.1. Chromatogram profile of F2 from 14D culture, with 3D field.

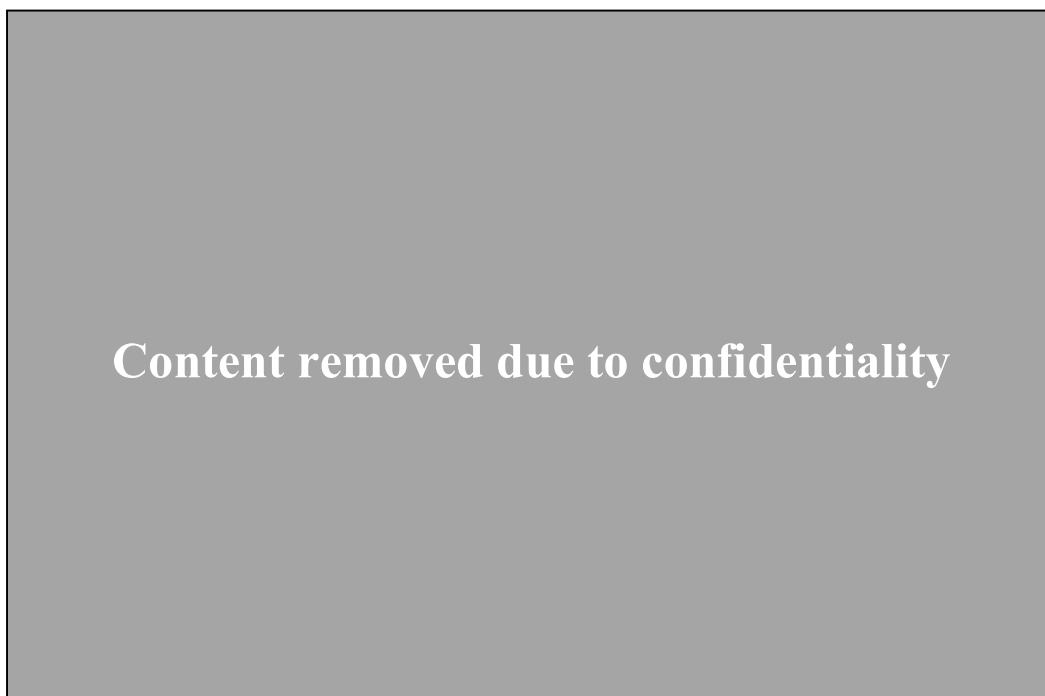


Figure 6.2.  $^1\text{H}$  NMR of the compound PTM-99-(F2)-F27.

Content removed due to confidentiality

**Figure 6.3.**  $^{13}\text{C}$  NMR of the compound PTM-99-(F2)-F27.

Content removed due to confidentiality

**Figure 6.4.** COSY of the compound PTM-99-(F2)-F27.



Content removed due to confidentiality

**Figure 6.5 HSQC-DEPT of the compound PTM-99-(F2)-F27.**

Content removed due to confidentiality

**Figure 6.6 HMBC of the compound PTM-99-(F2)-F27.**

Content removed due to confidentiality

**Figure 6.7. TOCSY of the compound PTM-99-(F2)-F27.**

Content removed due to confidentiality

**Figure 6.8.**  $^1\text{H}$  NMR of the compound PTM-99-(F2)-F31.

Content removed due to confidentiality

**Figure 6.9.**  $^{13}\text{C}$  NMR of the compound PTM-99-(F2)-F31.

Content removed due to confidentiality

**Figure 6.10. COSY of the compound PTM-99-(F2)-F31.**

Content removed due to confidentiality

**Figure 6.11. HSQC-DEPT of the compound PTM-99-(F2)-F31.**

Content removed due to confidentiality

**Figure 6.12. HMBC of the compound PTM-99-(F2)-F31.**

Content removed due to confidentiality

**Figure 6.13. TOCSY of the compound PTM-99-(F2)-F31.**

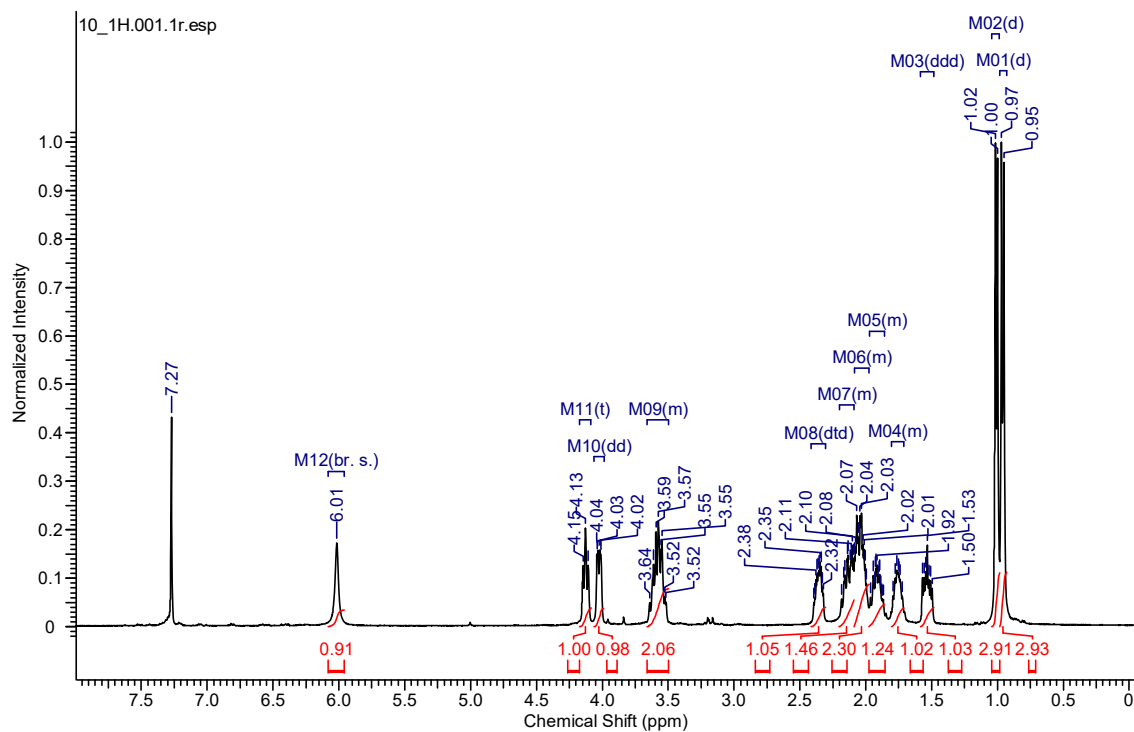


Figure 6.14.  $^1\text{H}$  NMR of the compound PTM-99-(F4-F7)-F30.

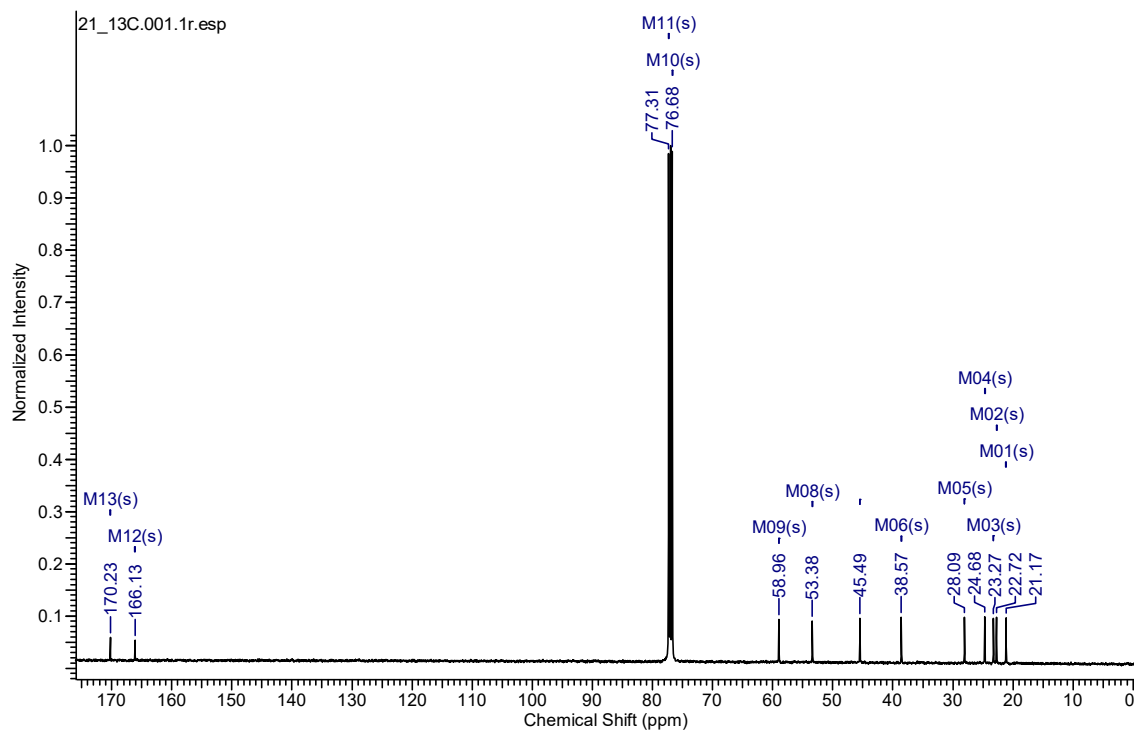
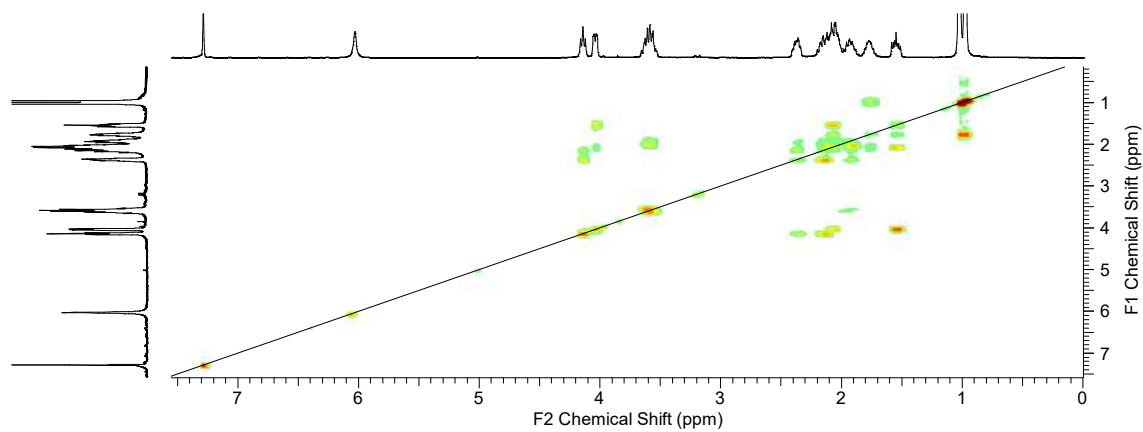
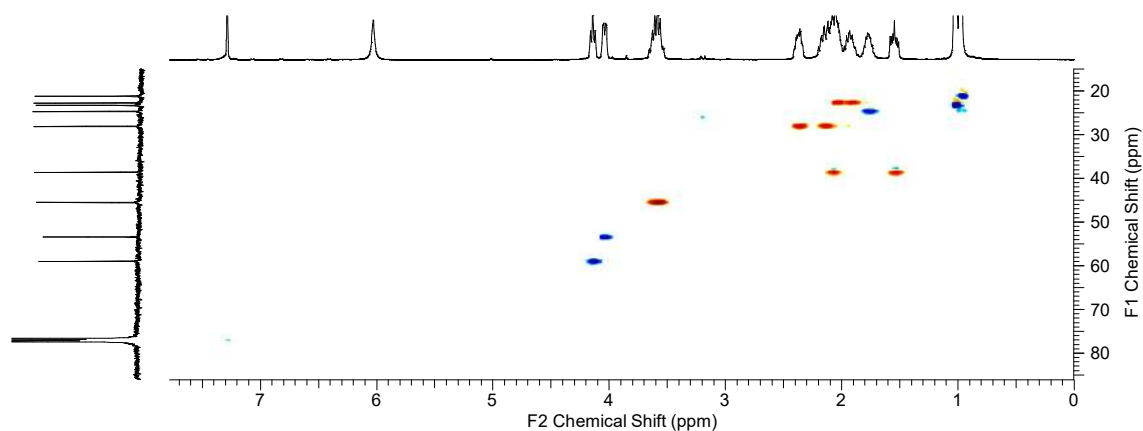


Figure 6.15.  $^{13}\text{C}$  NMR of the compound PTM-99-(F4-F7)-F30.



**Figure 6.16. COSY of the compound PTM-99-(F4-F7)-F30.**



**Figure 6.17. HSQC-DEPT of the compound PTM-99-(F4-F7)-F30.**

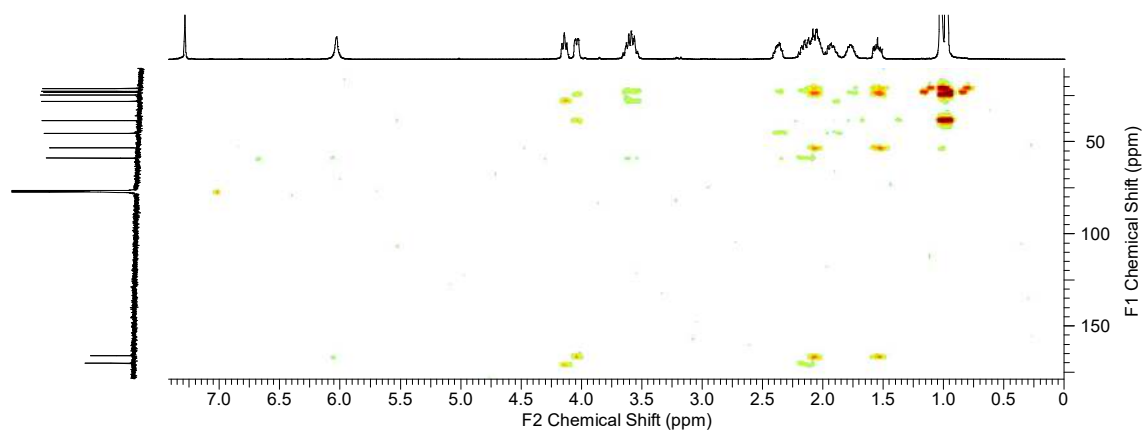


**Figure 6.18. HMBC of the compound PTM-99-(F4-F7)-F30.**

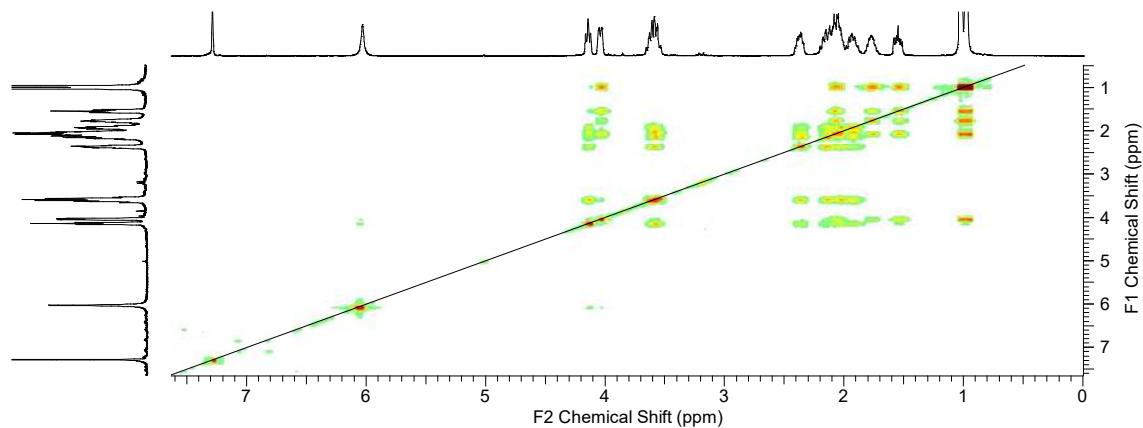


Figure 6.19. TOCSY of the compound PTM-99-(F4-F7)-F30.

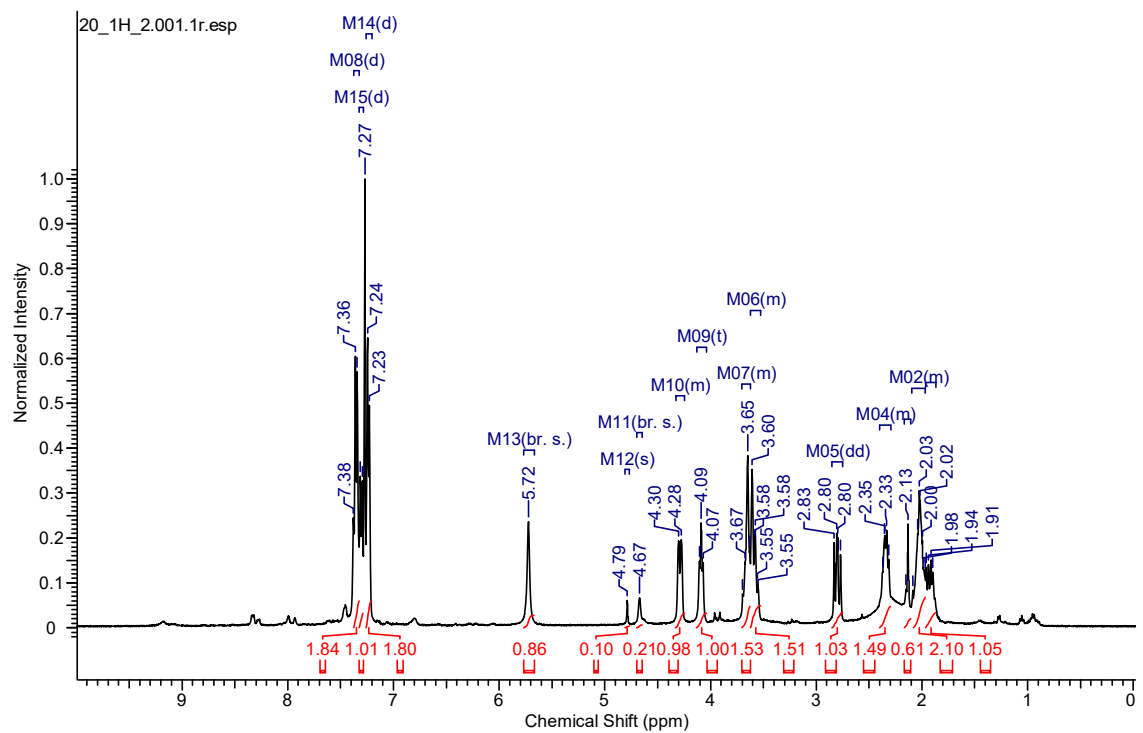


Figure 6.20.  $^1\text{H}$  NMR of the compound PTM-99-(F4-F7)-F34.

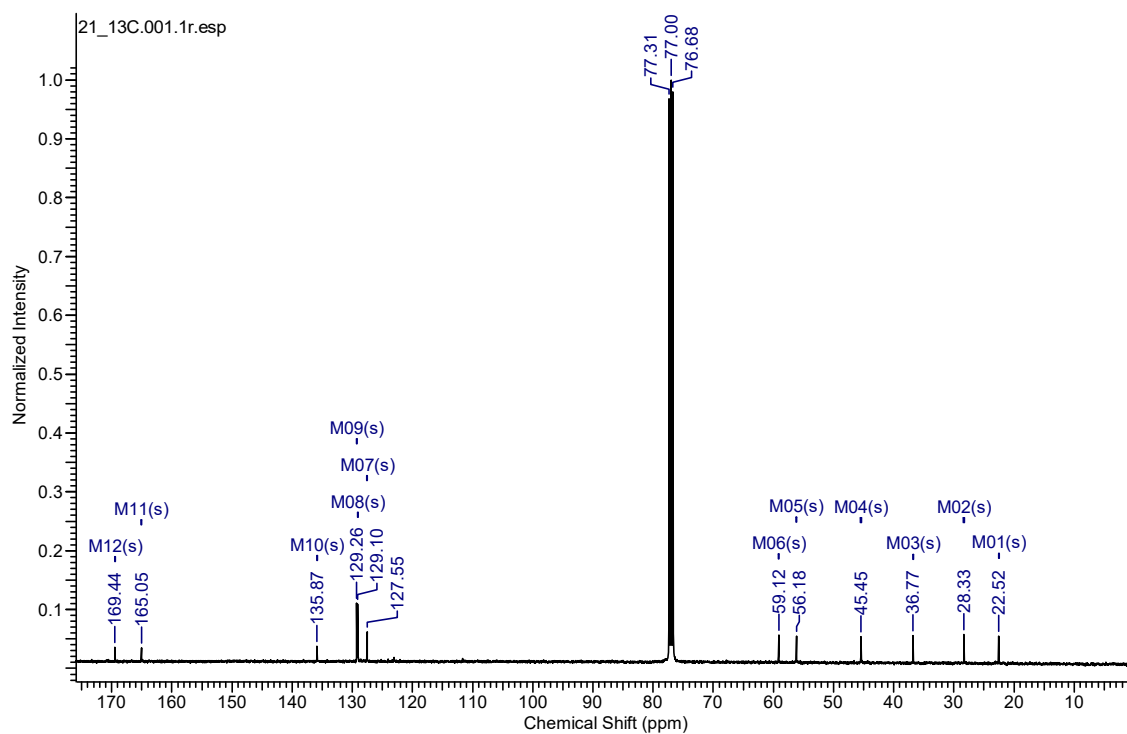


Figure 6.21.  $^{13}\text{C}$  NMR of the compound PTM-99-(F4-F7)-F34.

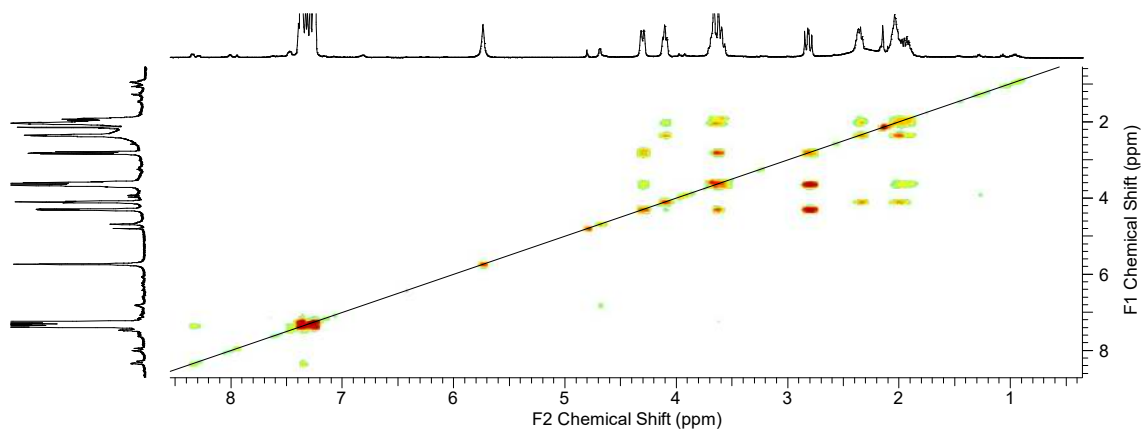
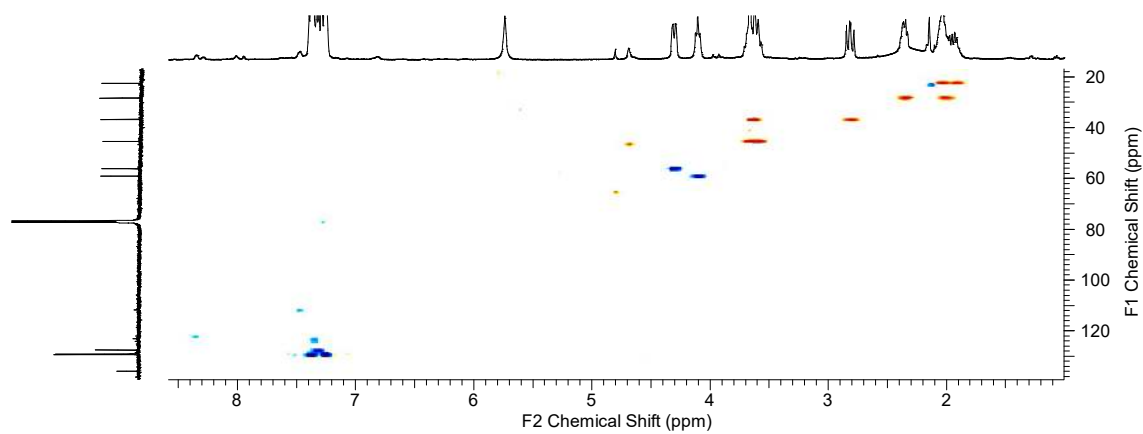
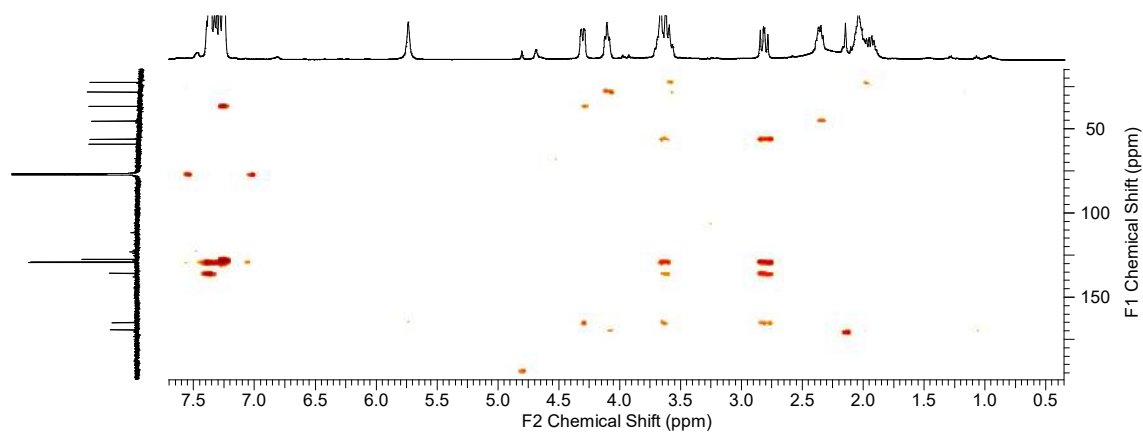


Figure 6.22. COSY of the compound PTM-99-(F4-F7)-F34.





**Figure 6.23. HSQC-DEPT of the compound PTM-99-(F4-F7)-F34.**



**Figure 6.24. HMBC of the compound PTM-99-(F4-F7)-F34.**

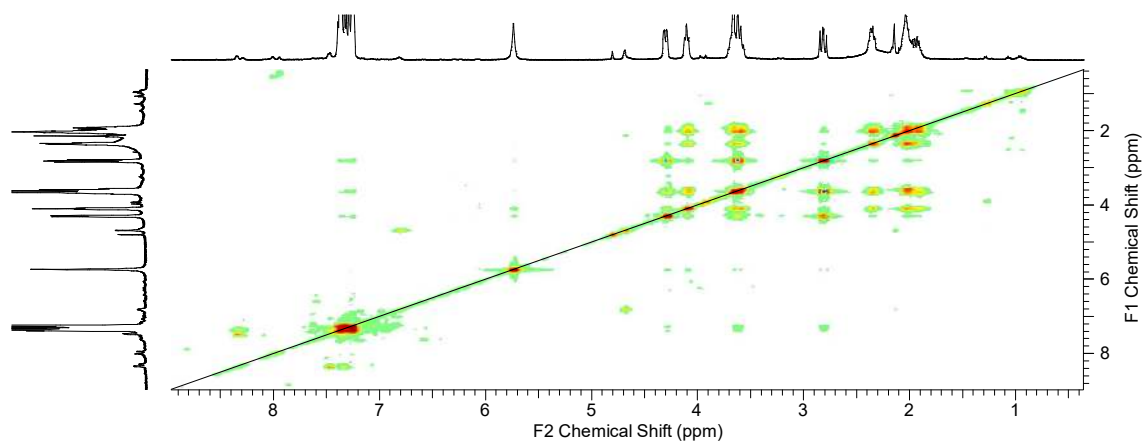


**Figure 6.25. TOCSY of the compound PTM-99-(F4-F7)-F34.**